/
Article / Book Information

( )	
Title(English)	Synthesis and Microstructure Control in Cubic Boron Nitride Sintered Composite by the High Pressure and High Temperature Method
( )	AKHMADIEKOWARDOYO
Author(English)	Wardoyo Akhmadi Eko
( )	: ( ), : , : 9450 , :2014 3 26 , : , : , , S. , ,
Citation(English)	Degree:Doctor (Engineering), Conferring organization: Tokyo Institute of Technology, Report number: 9450 , Conferred date:2014/3/26, Degree Type:Course doctor, Examiner:,,,,
( )	
Type(English)	Doctoral Thesis

Synthesis and Microstructure Control in Cubic Boron Nitride Sintered Composite by the High Pressure and High Temperature Method

AKHMADI EKO WARDOYO

Contents

Chapter 1   Introduction

1.1 Cubic boron nitride: properties and applications

Cubic boron nitride (cBN) was first produced in 1957 by Robert H. Wentorf, a physical chemist for the General Electric Company [1], just two years after the first artificial diamonds were synthesized [2]. In analogy to the fabrication of diamond crystals, cBN was produced from hexagonal boron nitride (hBN) under high pressure and high-temperature (HPHT) conditions. It is not only the synthesis process that is similar for cBN and diamond: cBN is sometimes referred to as "the better diamond", which is mainly related to the fact that both materials share many extreme properties, but cBN is superior to diamond in some cases (see table 1 for a comparison of selected properties of single-crystalline diamond and cBN).

Table 1.1 Comparison of selected physical properties of single-crystalline diamond and cBN [3]

	Diamond	cBN
lattice constant [nm]	0.3567	0.3615
bond length [nm]	0.1545	0.1565
atomic density [nm^{-3}]	176	170
mass density [g/cm^3]	3.51	3.48
Vickers hardness [GPa]	80-100	50-70
thermal conductivity at RT [W/cm/K]	20-22	2-13
thermal expansion coefficient [$10^{-6}\,K^{-1}$]	0.8	4.8
band gap [eV]	5.45	6.4

After diamond, it is one of the hardest materials known, with roughly 50-70 GPa Vickers hardness vs. 70+ GPa for diamond. However, cBN exhibits a much better chemical inertness and thermal stability. Diamond readily reacts with iron, cobalt, and nickel at temperatures above 1000 °C or is subject to oxidation at T > 800 °C, which results into a disintegration of the diamond surface into gaseous CO_2. In contrast, cBN is chemically inert against iron group metals for temperatures of up to 1800 °C [4] and its high stability against oxidation is a consequence of the formation of liquid or solid B_2O_3, which protects the surface against further oxidation [5]. Thus, cBN is a promising material for corrosion- and wear resistant coatings for machinery and cutting tools, particularly in those cases where the reactivity of diamond makes this unsuitable.

Cubic boron nitride also has the potential to outclass diamond in view of electronic applications. It not only has a high band-gap ($E_g = 6.4$ eV) and the second highest room temperature thermal conductivity after diamond (2-13 W/cm/K), but, in contrast to diamond, it can be easily doped to obtain both *n*- and *p*-type conductivities [6, 7].

1.2. BN phase system.

1.2.1. BN crystal structures.

Analogous to carbon, boron nitride forms both hard, diamond-like sp^3-bonded phases and softer, graphite-like sp^2-bonded phases. In contrast to the carbon phases, which can be found in nature, all BN modifications are only synthetic materials. cBN crystallizes like diamond in a zinc-blende structure, in which the atoms are bonded to four nearest neighbors of the alternate species through sp^3-hybridization in a three-dimensional tetrahedral framework.
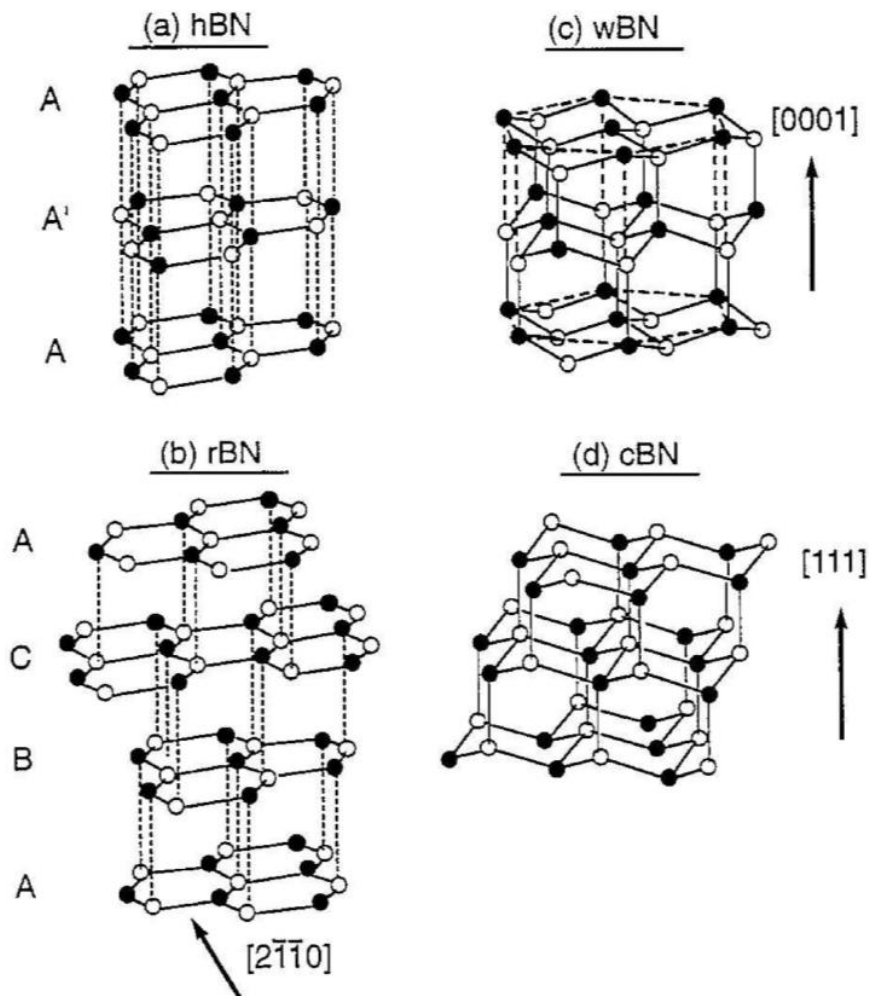

Fig. 1.1. Structures of the sp^3-bonded phases cBN and wBN and the sp^2-bonded phases hBN and rBN with respective stacking sequences [8].

In hBN and rhombohedral Boron nitride (rBN), the atoms within the basal planes are bonded to three nearest neighbors through strong in-plane sp^2-hybridization, but the hexagonal planes are bonded to each other through weak van der Waals interaction only. This bonding anisotropy leads to different physical properties depending on the crystal direction.

For example, the compressibility is much higher along the c-axis than along the a-axis. Both BN polymorphs exhibit a density comparable to graphite (hBN $=2.25$ g/cm^3, graphite $= 2.26$ g/cm^3,), and they generally share many properties with graphite. In fact, hBN is sometimes referred to as "white graphite", which accounts for both the similarities and differences between these two materials: graphite is a soft, black, and conducting material whereas hBN is soft, white, and insulating.

1.2.2. Equilibrium (P-T) phase diagram.

Up to date, the only technique available to produce c-BN under equilibrium conditions is the HPHT synthesis. The use of HPHT methods to establish a phase diagram for boron nitride has proven to be difficult because of several reasons: First, the experimentally accessible Pressure-Temperature (P-T) values are restricted to a narrow region characteristic for each individual experimental setup. The respective hBN/cBN equilibrium line then has to be extrapolated based on previous experimental results or on thermodynamical calculations. Second, the cBN to hBN transformation (and vice-versa) depends strongly on parameters like grain size, crystalline defect concentration, and purity of the starting material [13]. Therefore, the equilibrium (P-T) phase diagram for boron nitride, especially the equilibrium line between hBN and cBN, are controversially discussed in the literature.

Immediately after the first successful synthesis of cBN in 1957 by Wentorf [1], attempts to establish a pressure-temperature phase diagram for boron nitride were initiated. A first version of a (P-T) phase diagram was introduced by Bundy and Wentorf in 1963 [14] based on Wentorf's experimental data on conversion of graphite-like hexagonal BN into the cubic form [1, 15, 16] and data on hBN melting under high pressures [17]. Interestingly, cubic BN was found to be the stable phase at ambient conditions, which, however, was changed a few years later in an ensuing publication. In 1975, Corrigan and Bundy [10] modified the phase diagram of 1963 by extrapolating the measured hBN/cBN boundary line to the low-temperature region by analogy to the graphite/diamond equilibrium curve [18]. This way, they found that hBN was the thermodynamically stable phase under standard conditions, while cBN was metastable. This version of the phase diagram was generally accepted up to the late 80s.

Figure 2 shows the equilibrium lines as suggested by Corrigan and Bundy (dashed line) together with some of the experimentally observed regions for cBN formation. In 1988, Solozhenko suggested a revised version of the phase diagram based on new experimental data on thermodynamic properties of all BN modifications [10]. The hBN/cBN equilibrium line as calculated by Solozhenko is also shown in Fig. 1.2 (solid line). Its position differs drastically from the one proposed by Corrigan and Bundy, since the new equilibrium line intersects the temperature axis at around 1500 K (1227 °C), so that the thermodynamically stable BN modification at ambient pressure is the cubic and not the hexagonal one.

Various experiments have been performed after Solozhenko published the revised version of the phase diagram that supports his calculations. For example, Singh et al. [19], Sachdev et al. [20] and Will et al. [13] synthesized cBN at pressures and temperatures far from the equilibrium line proposed by Corrigan and Bundy. Furthermore, Solozhenko was able to show that the threshold pressure for spontaneous cBN crystallization can be lowered even down to atmospheric pressure in the presence of diamond seed crystals [12]. Finally, various theoretical calculations were carried out as well [21, 22] and were found to be in good agreement with the phase diagram published by Solozhenko.

Both wBN and rBN have no thermodynamically stable region in the equilibrium (P-T) phase diagram of boron nitride over the whole range of pressures and temperatures. However, wBN can be synthesized by a transformation of hBN or rBN under high pressure. A transition from hBN to wBN and rBN to cBN, respectively, involves two deformation processes: a lattice compression along the c axis and splitting of flat basal layers [23]. These changes result in an increase of density from 2.2 up to 3.5 g/cm^3 and in a formation of sp^3 hybridized tetrahedral bonds [24]. On the other hand, a direct transition from hBN to cBN and from rBN to wBN is unlikely, since it would require both breaking and changing the nature of chemical bonds [4]. Thus, the direct transformation from hBN to cBN requires the simultaneous application of very high temperatures and pressures in order to overcome the activation barrier for the conversion.
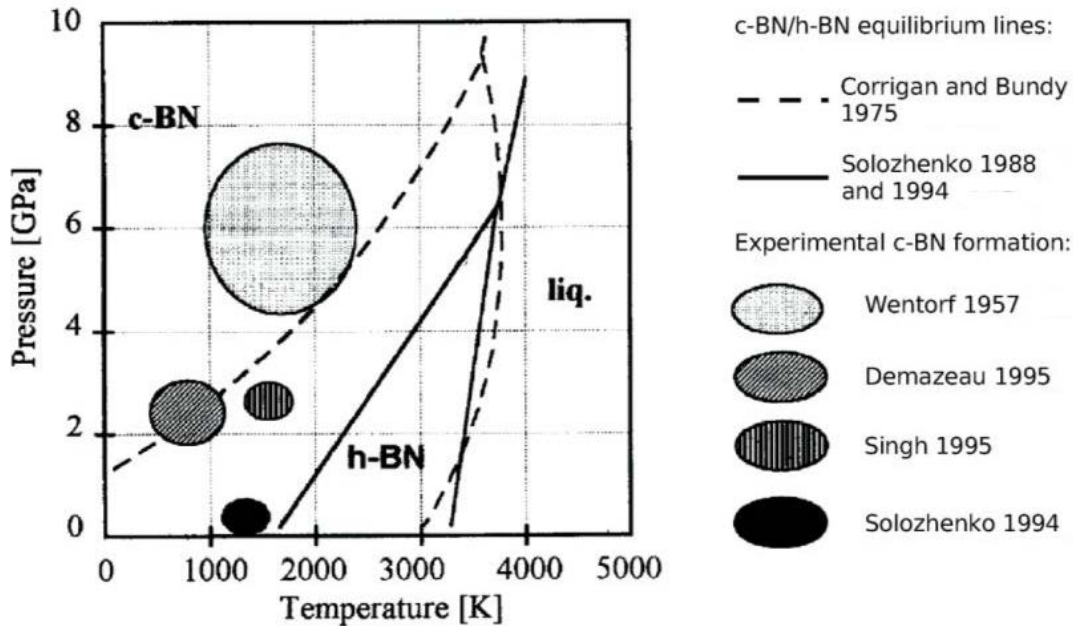
Fig. 1.2. Equilibrium (P-T) phase diagram of boron nitride showing the equilibrium lines as proposed by Corrigan and Bundy [9] and more recently by Solozhenko [10, 11, 12]. Additionally some experimentally observed regions for cBN formation are displayed. This compilation was taken from ref. [5].

1.3. Boron nitride synthesis techniques.

The sp^2 type hBN and the sp^3 type cBN are both strong bonding type. To rearrange such bonding, high energy are required and the phase transformation are not easily occurred. To directly transform hBN to cBN, at least 6-8 GPa, 1400 °C of high pressure and temperature is needed. By pressurizing, a transformation from hBN to the wBN phase will occur first and under high temperature condition, a solid phase diffusion reaction transform it into cBN. The direct phase transformation from hBN to cBN was originally performed by Bundy and Wentorf in 1963 [14]. After that, it was found that the initial condition of the starting material strongly affect the hBN-cBN transformation process [25, 26] and by strictly controlled the pressure and temperature, a translucent cBN compacted body was successfully developed [27, 28].

The use of the catalyst or solvent in the cBN synthesis was introduced as the same analogy with the catalyst or solvent in the graphite-diamond synthesis process. The introduction of synthesis catalyst in the hBN-cBN transformation process was able to lower its pressure and temperature condition around 4-5 GPa and 1300-1500 °C. In 1955, research group from General Electric Co. successfully synthetized the diamond.

The key of this success are, first is the development of the high pressure high temperature apparatus and second is the use of metal catalyst [2]. They use the group VIII transition metal such as Fe, Co, Ni and Cr, Mn, Ta along with its alloy to synthetize diamond from graphite. They demonstrated that under certain high pressure and high temperature where diamond is thermodynamically stable, the graphite dissolves into the molten metal catalyst and then precipitate and recrystallize as the diamond [29]. In 1957 or two years after the introduction of first man made diamond, Wentorf a member of above GE research group predicted and showed that as the same with carbon, boron nitride has a cubic phase. Wentorf, in his second paper on cBN synthesis wrote that even by using diamond synthesis catalyst of Fe, Co, Ni, cBN could not be synthetized [1]. But, by using alkali, alkali-earth metals such as Li or Mg, cBN was successfully synthesized. The cBN synthesis using Sb, Sn, Pb was also reported [15].

From the BN saturation perspective, comparing with the alkali metals [15], alkali-earth metals [15, 30] or their nitride [15, 31-33], boron nitrogen compounds of alkali and alkali-earth elements such as Li_3BN_2 [34], Mg_3BN_3 [35, 36], $Ca_3B_2N_4$ [37, 38], SrB_2N_4 [39], Ba-BN [40] are better suited for synthesizing high-quality cBN single crystals. Such catalysts are commonly used in industry and/or laboratories as conventional solvents for growing cBN crystals. However, care must be taken with these solvents, because the alkali and alkali-earth compounds are not chemically stable in the ambient atmosphere, and air and humidity can easily affect the purity of the compounds. When controlling the quality of a resultant product by using a solvent, controlling the purity of the solvent is essential. Development of effective solvents for cBN formation with chemical stability is an important subject. On the other hand, the diamond synthesis solvent of transition metal such as Ni is easy to handle in the air. It could be said that synthesizing cBN is more complicated comparing with diamond synthesis process.

Metal and metallic alloys were reported to be effective solvents for use in the preparation of cBN at HPHT. Saito et al. reported that cBN can be synthesized using Fe-Al solvent at temperatures in excess of 1550 °C and pressures greater than 4.5 GPa [41]. After that, GE research group submitted some cBN synthesis related patent by adding Al into the transition metals [42-44]. The alloys in the above patents became the base of the nowadays cBN sintering agent to produce polycrystalline cBN compact cutting tools for machining hardened steel and cast iron for automotive industry. On the other reports, Si [45] and Co [46] showed as the cBN catalyst too. Taniguchi reported that cBN could be synthesized using Co, Co-Al, and Ni-Al solvents at pressures of approximately 5.5 GPa. Taniguchi obtained yellowish facetted single crystals through

spontaneous nucleation followed by long-duration growth [47].

The above mentioned metals of the cBN synthesis solvents are thought to be analogous with the diamond synthesis solvent, in which cBN will precipitate from the supersaturated boron and nitrogen in the molten solvent. Essentially the lower limit of the temperature will be the eutectic of BN and its solvent. The diamond synthesis region is showed as the V shape area between the solvent-carbon eutectic line and graphite-diamond equilibrium line. cBN synthesis region was thought to be different from the diamond synthesis area, where in the cBN synthesis region there is a lower limit of the pressure. Fukunaga et al. successfully synthesized cBN at the area where it was thought to be impossible to synthesize at around 3.0-3.5 GPa by extending the reaction time for certain period. They studied the hBN-cBN equilibrium line experimentally [48].

If cBN could be easily synthetized at such relatively low pressure region, it will lighten the burden imposed on the HPHT moulds and dies. The scale up of the apparatus and the life time of the moulds and dies will increase significantly, means the synthesis cost could be reduced. But, such above extra long reaction time is inefficient on an industrial scale so that the development of the effective solvent is needed.

In accordance with the experience gained with diamond synthesis, we can think of two solvent methods: the so-called high-pressure film method [49] and the temperature difference (or temperature gradient) method [50, 51]. Both methods provide supersaturation of B and N atoms in a solvent from which BN crystals are precipitated.

As shown in Fig. 1.3, the high-pressure film method may be regarded as a solvent-mediated phase transition in which hBN dissolves in a solvent and cBN crystals precipitate from it. Because hBN is metastable and cBN is stable at high pressures, hBN should dissolve more in a high-pressure solvent than cBN. Therefore, B and N atoms supersaturate for cBN; as a result, deposition of cBN crystals occurs.
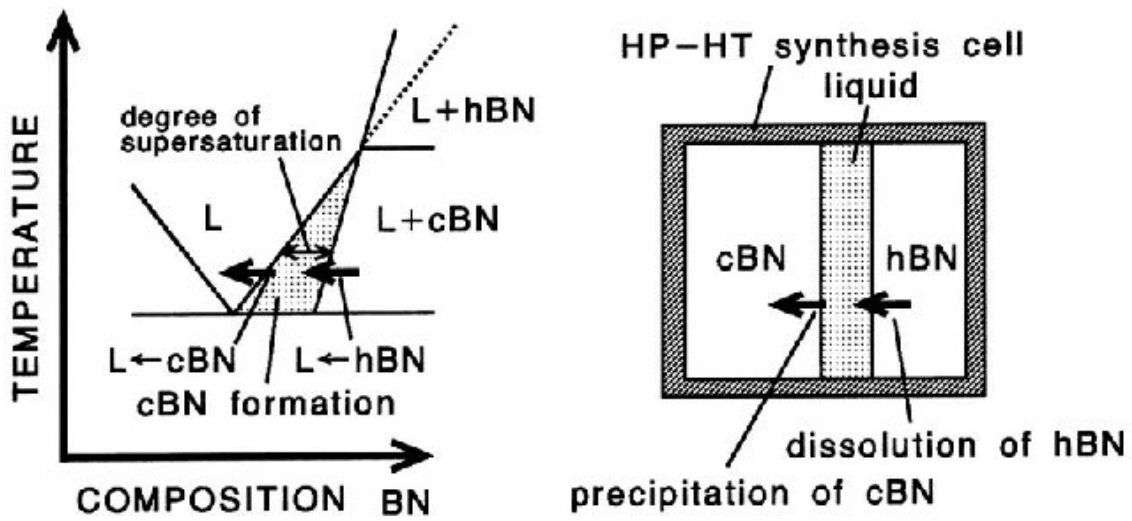
Fig. 1.3. Cubic BN formation by the high-pressure film method [52].

For diamond synthesis by the high-pressure film method, a thin solvent film always exists between the graphite source material and the diamond crystal produced. The formation mechanism of cBN powders is believed to be the same as that for the synthesis of diamond by the high pressure film method, although a solvent film between the hBN source material and the cBN crystal produced has not been observed as clearly as it has been for diamond [56].
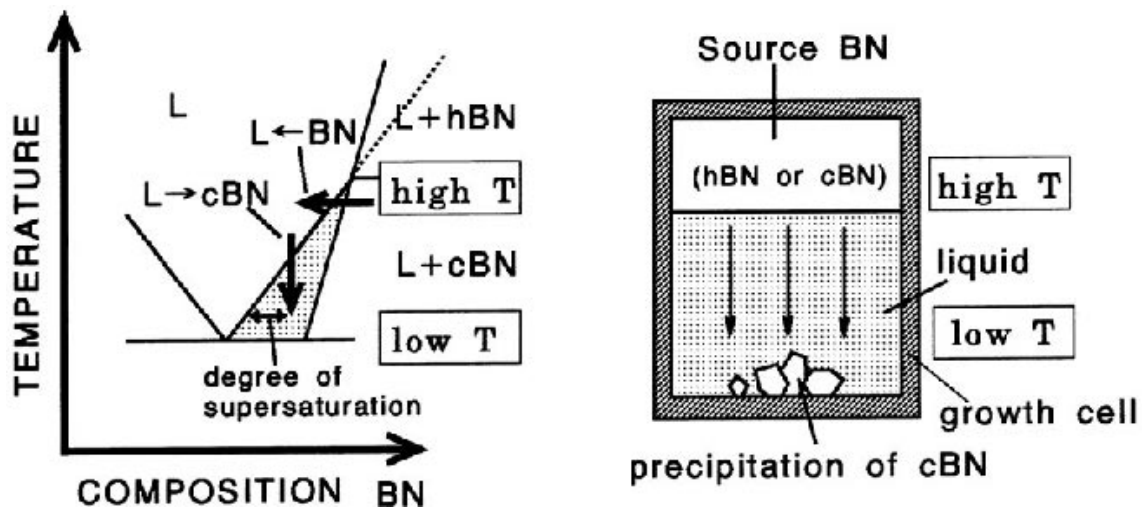
Fig. 1.4. Cubic BN formation by the temperature difference method [52].

The temperature difference method as in Fig. 1.4. utilizes the difference in solubility at different temperatures. Consider a solvent with high- and low-temperature regions.

Generally, a material dissolves more easily in a higher temperature region than in a lower temperature region. Then, in the low-temperature region, the material becomes supersaturated in the solvent and precipitates. When this general method is applied for cBN growth at high pressures, the BN source material dissolves in the high-temperature region and cBN crystals precipitate in the low-temperature region.

When the temperature difference is small and thus the degree of supersaturation of B and N atoms is small, spontaneous nucleation is suppressed and cBN crystals grow slowly on seed crystals. High temperatures induce rapid growth of the crystals, providing relatively large but low-quality crystals with cracks and solvent inclusions. At low temperatures, the crystals grow very slowly. Under appropriate growth conditions, cBN crystals up to 3 mm in size grow in several tens of hours [34, 53]. Naturally, the size of the crystals produced is ultimately limited by the size of high-pressure apparatuses, which is restricted to be smaller than the size of synthesis apparatuses at normal pressure.

Recently, Kubota et al. has investigated Co, Ni, Ni-Cr, Ni-Mo and Ni_3Al as the growth solvents of cBN crystal. They successfully reduced the minimum temperature for the cBN growth down to 1350 °C at the pressure range of 5-5.5 GPa [54-56]. Fukunaga et al. concluded in their report that Fe-Mo and Co-Mo work as solvent of B and N atoms and Al acts as a nucleation agent of cubic BN. By using the Co57.6-Mo38.4-Al4 wt% ternary alloy, they successfully synthesized the cubic BN at minimum pressure of about 4.4 GPa and temperature of about 1250 °C. The addition of Mo in the Ni solvent improves the extremely low solubility of nitrogen in molten Ni. Moreover, the addition of Cr to Ni solvent, which can better enhance the nitrogen solubility in molten Ni than Mo, resulted in further increasing the crystal size [57].

The previous reports on the synthesis solvent of metal alloys including transition metals (Fe, Ni, Co, Mn), nitrogen solvents (Mo, Cr, V) and Al suggested as a candidate to realize homogeneous cBN-metal composite for cutting tool applications. However, few experimental studies on cBN-metal composite such as controlling the grain growth were available in the literatures. From a view point of industrial scale production, lowering production cost while keeping the quality of the cBN crystal is one of the most important issues. The ability to keep the cBN synthesis condition at relatively low pressure and temperature will be huge benefit for the cBN synthesis industry.

1.4. Polycrystalline cubic boron nitride sintering techniques.

As the size of the cBN that can be grown in the high pressure and high temperature system is limited up to several millimeters and since they do not have the required fracture toughness as the grinding or cutting tool [27], the cBN crystals are usually compacted into a conglomerate mass of sufficient size, toughness, hardness and chemical stability under high pressure and high temperature similar with its synthesis's condition. The compacting methods could be a direct conversion of hBN to cBN along with simultaneous sintering [7, 9, 58, 59] or direct sintering of cBN powder at the pressure around 7.7 GPa and temperature between 2000-2500 °C [60].

Polycrystalline cBN compact (PCBN) can also be manufactured at relatively lower pressures and temperatures than those required without using any additives by the use of some binding or catalyst materials. Generally these binders are selected from the carbides, carbonitrides, borides, and silicides of Group IVa, Va, and VIa of the periodic table. The pioneer work by Wentorf and Rocco [44] disclosed polycrystalline mass of greater than 70 vol% cBN and metallic bonding agents (metallic binder PCBN). The metallic bonding agents were selected containing Al and at least one alloying element selecting Ni, Co, Mn, Fe, V and Cr. The technique to produce laminated PCBN and the carbide substrate was also disclosed. The laminated PCBN compact was suitable to braze larger carbide tools. Since then, a number of papers regarding the cBN compacting process have been published. The cBN content varies depending on application; "low content cBN material" with ~50 vol% cBN can be used for turning case hardened steels and ball bearing steels, while "high content cBN material" with ~80-90 vol% cBN can be used in high speed machining of cast iron [61].

Rong et al. reported the cBN-Al sintered compact with the Knoop hardness value of 3700 kgf/mm^2. They premixed 90 mol% 1-4 μm fine-grained cBN powders along with Al powder and sintered it at 5.75 GPa and 1400 °C for 20 min. From their observation, cBN reacted with Al and formed AlN and AlB$_2$ [62]. Lv et al. sintered the cBN compacts from 7-12 μm cBN powders, using 15 wt% Al and 20 wt% AlN respectively as additives, in the temperature range of 1300–1700 °C for 20 min under high pressure of 5.0 GPa. The highest Vickers hardness of 32.1 GPa was achieved. While in the cBN-AlN system, highest cBN-AlN composite hardness of 29 GPa was achieved at 1600 °C [63].

Rong et al. also used the cBN powders of 1-3 μm with TiN-Al as a sintering agent to produced the cBN-TiN-Al composite for cutting tool under the condition of 5.8 GPa and at temperatures of 1200 and 1400 °C for 30 min and showed that the highest micro hardness of 30.7 GPa was achieved for the 75 vol% cBN-13vol%TiN-12vol%Al

composition specimen sintered at both 1200 and 1400 °C [64]. Sintering cBN disk from the 6-9 μm cBN powders using TiN and TiC as the binder at 5.8 GPa and 1450 °C was also reported by Agarwala et al. resulting the cBN compact with Knoop hardness of 3400 kgf/mm^2 at the highest [65]. In different report, the varies values of Knoop hardness between 2400 to 3600 kgf/mm^2 could be achieved by sintering cBN from the 6-9 μm cBN powders with TiC$_x$N$_{1-x}$, (0<x<1) and Al at 5.8 GPa and 1450 °C [66].

There are several reports on the cBN sintering process with metal and Al as a sintering agents. Li et al. sintered the 10 μm cBN-Al mixtures on the WC-16 wt% Co substrates under static high pressure of 5.0 GPa and at temperatures of 800-1400 °C for 30 min. Vickers hardness of the sintered samples increased with increasing cBN content, and the highest hardness of 32.7 GPa was achieved for the cBN-5 wt%Al specimens sintered at 1400 °C. The cBN composite sintered at 1200 °C from a cBN-15 wt%Al mixture showed the best cutting performance [67].

In contrast, the cBN sintering process using an infiltration method of the molten solvent or catalyst is not yet being well studied due to the difficulties in controlling the microstructure homogeneity as a result of cBN abnormal grain growth.

Jia et al. reported the preparation of polycrystalline cBN compact from 10-14 μm cBN powders by high-pressure infiltration using cemented carbide at 5.2 GPa, 1450 °C for 6 min. The experimental results show that the WC and Co from WC–Co substrate spread into cBN layer through melting permeability under HPHT. The binder phases of WC, MoCoB and Co$_3$W$_3$C realized the interface compound of PCBN compact, and the PCBN layer formed a dense concrete microstructure with the Vickers hardness of 29.3 GPa [68]. Similar achievement of this kind of infiltration method of cBN-WC/Co sintering method experiments was performed by Tan et al [69]. The highest Vickers hardness from the sample using the cBN powder with the grain size of 8-12 μm was 34.5 GPa.

As shown above, while there are many literatures on cBN with ceramics binder, very few literatures studied the sintering process of cBN compact using metal catalyst, especially cBN powders with relatively fine grain size less than 2 μm.

1.5. Polycrystalline cBN compact cutting tools and their application.

In the majority of machining operations today the tool material is in the form of what are referred to as indexable inserts, about 1-2 cm across and some 0.5 cm thick, which are mechanically clamped to a tool holder, so that when one edge of the insert is worn it can be indexed to bring another edge into operation.

During machining the workpiece material is removed as chips. The terminology of

metal cutting, (see Fig. 1.5), refers to the machining speed, at which workpiece material moves over the cutting edge; this can be simply related to the length of chip which is produced in a given time; to the feed, which is the distance that the tool moves along the workpiece with each rotation and this is related to the thickness of the chip; and to the depth of cut, which is the width of chip which is removed during machining.

With today's machine tools and cutting tool materials, speeds of up to a 1000 m/min are possible with feeds of up to 1 m/min. Depths of cut vary from 0.1 mm for fine finishing operations up to as much as several mm for heavy roughing cuts [70].
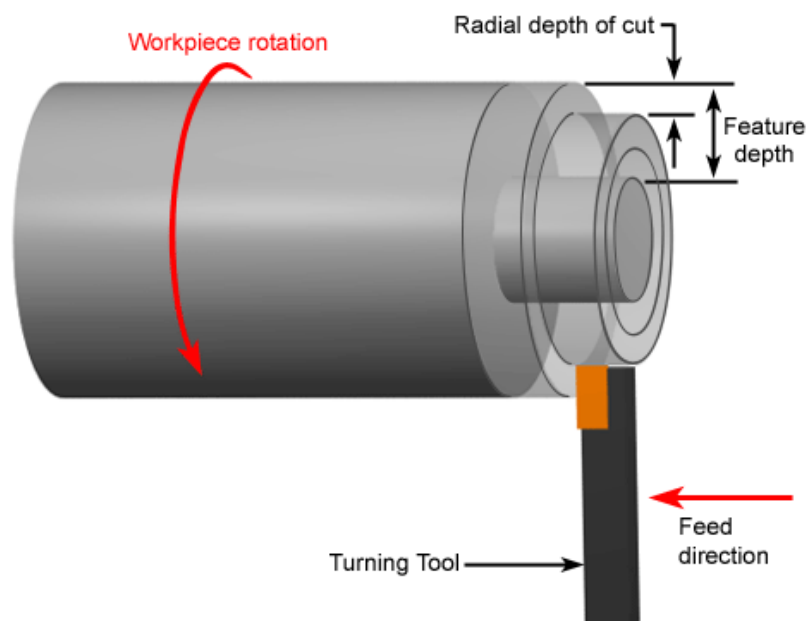
Fig. 1.5. Definition of speed, feed, and depth of cut, in metal cutting

Machining efficiency can be continuously improved by increasing the material volume removal rate by high-speed or high-performance cutting (HSC or HPC); by lowering downtime and/or time and the number of tool changes by using complex tools. Improvements can also be made by replacing several machining processes with a single one.

This trend towards greater efficiency results in not only a growing demand for wear-resistant tools and a two-digit growth rate of consumption of PCBN, but also in a steady improvement of hard metal and ceramic tools. cBN has proven to be well suited to machining grey cast iron at high cutting speeds, as well as chilled cast iron, hardened steels (HRC 57) and super alloys [71].

Hardened steel rolls (60-68 HRC) can be machined at speeds of 45 to 60 m/min (150 to 200 ft/min) and feeds of 0.2 to 0.4 mm/rev. Chilled cast iron rolls are reported as

being machined in the same range of speed and feed. The rate of metal removal is several times greater than that possible with cemented carbide tools [72].

An example of the comparison between cBN tool and K10 tungsten carbide-cobalt alloy in the cutting (turning) of martensitic cast iron was shown in fig. 1.6.
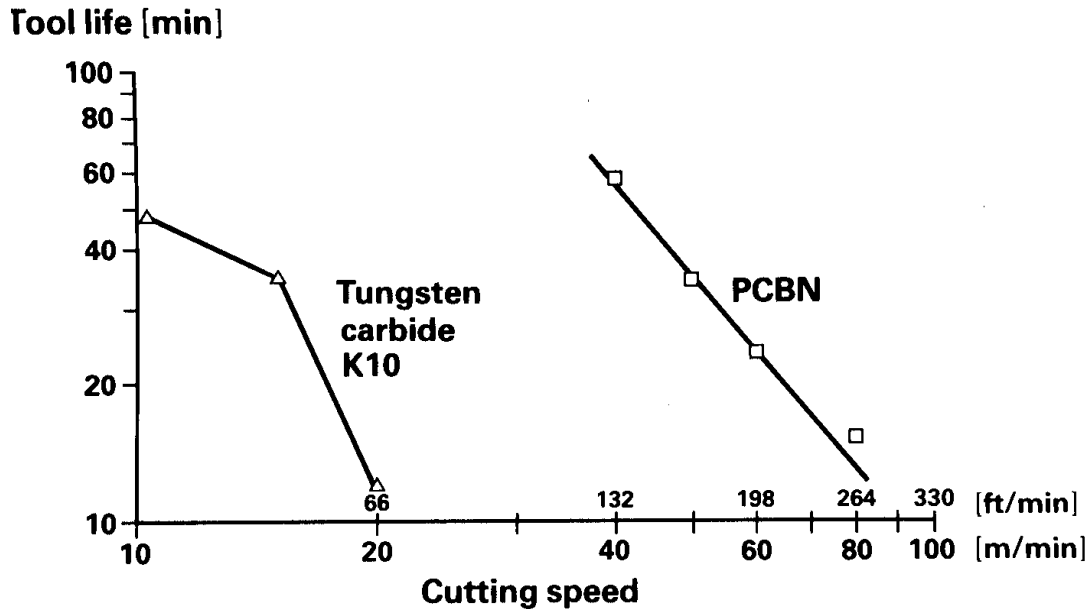
Tool life [min]

Fig. 1.6. Tool life vs cutting speed for PCBN tools compare with K10 tungsten carbide-cobalt alloy, at a feed of 0.3 mm/rev with no coolant, when machining hard, martensitic cast iron [72].

Tool life is long so that rolls may often be machined to a dimensional tolerance and surface finish which avoid the necessity for a grinding operation. Hardened tool steels, including high speed steel, can be machined in this same speed and feed range [73].

The ability of PCBN to cut such hard materials at high speeds is due to the retention of strength to higher temperatures than other tool materials, combined with excellent abrasion resistance and resistance to reaction with the ferrous work materials. Table 1.2 showed the mechanical properties of some commonly used cutting tools. The data relate to sintered polycrystalline materials. The properties of these polycrystalline materials are not absolute figures but depend on grain size and the amount of binder phase used. PCBN refers to commercial PCBN with low binder content. As seen in Table 1.2 cBN is the second hardest material after diamond and conducts heat extremely well [71].

Table 1.2. Properties of polycrystalline hard phases

Properties		PcBN	WC	β-Si3N4	α-β Sialon	α-Sialon	Al2O3	Al2O3-TiC
Density	g/cm	3,5	15,7	3,3	3,25	3,4	3,9	4,3
Grain size	μm	2-5	0.15	-	-	2-3	< 1	< 1
Hardness HV0.1		≤ 4000	3500	-	-			
Hardness HV0.5				1800	1900			2250
Hardness HV10			2900	1650	1750	~ 2000	2200	1900
Hardness HV10 at 1000ºC			~ 1200	900	-		600	
KIC (from crack length)	MPam1/2		6	~ 7	6	5-7	3-4	4-5,5
Fracture strength	MPa		≤ 1000	1100	~ 1000	~ 1000	600-700	600-700
Elastic modulus	GPa	680	700	320	320	320	380	400
Thermal conductivity	W/(mK)	1300	~ 100	15-20	5-15	5-15	25-30	33

With the automotive industry currently more competitive now than at anytime in its history, there is a consistent drive to reduce manufacturing costs and improve efficiency in both component manufacture and component performance in use. This has lead to a desire to employ the most advanced component materials and machining technologies. Generally the new component materials are more complex, as well as harder and more wear resistant than those they replace. They are also required to be machined to more exacting tolerances and surface finishes. These drivers have led to the exponential growth in the use of PCBN cutting tools in the automotive industry.

When the engine, transmission and power train units are broken down into their parts, a significant number of the machining operations are now carried out with PCBN tooling. The typical components currently machined with PCBN tooling are shown in Table 1.3. Over 50% of all PCBN tooling sold globally is consumed in the automotive industry [74].

The growing PCBN market allows enlarging the number of grades produced. By changing grain size and different kinds and amounts of binder the properties of PCBN tools can be changed to meet the requirements of the cutting application [75].

Each of these PCBN tools has unique mechanical properties to meet the requirement in cutting the above workpeaces in Table 1.3.

The PCBN tools manufacturers also have their own recommendation of the cutting condition of their products [76]. As described before, "low content cBN material" with ~50 vol% cBN can be used for turning case hardened steels, while "high content cBN material" with ~80-90 vol% cBN can be used in high speed machining of cast iron [61].

Table 1.3. Typical components currently machined with PCBN tooling [74].

Grey cast iron	Hard steels / irons	Sintered irons
Engine blocks	Synchromesh gears/ shafts	Valve seats
Cylinder liners	Pinion gears	Valve guides
Brake drums	CV joints	
Brake discs	Clutch sleeves	
Flywheels	Bearings	
Cam followers	Axial drive bevel wheels	
Crankshafts	Ring gears	
Gearbox casings	Fuel pump barrels	
Axle casings	Fuel injector nozzles	
Clutch plates	Timing gears	
Brake cylinder		

1.6. Research purpose and approach

Table 1.4. Conventional and proposed cubic BN synthesis and sintering method

	Synthesis method	Solvent type	Example of Solvent system	Minimum P-T condition	Technical issues/features	Application as cutting tool (sintering P-T)
Previous researches	Direct conversion	none	none	6 GPa, 1500 °C	High cost (short die life)	Yes. (7 GPa, 2000 °C)
	Solvent method (main method in industrial scale practices)	Alkali-alkali earth metals, nitrides, boron-nitrides	Li, Mg, Li_3N, Mg_3N_2 Li_3BN_2, Mg_3BN_3	4.5 GPa 1400 °C	hygroscopic and easily oxidized in the ambient atmosphere	No.
		Transition metals-Al alloy	Fe-Al, Co-Al, Co-W-Al Ni-Cr-Al Co-Mo-Al	4.4 GPa, 1250 °C	Low cBN yield	Yes. (6 GPa, 1600 °C)
This study	Solvent method	Transition metals-(nitrogen dissolver element)-Al	(Fe, Co, Ni)-(Cr, Mo, V)-Al	To be determined	• Easy handling • Low P-T (lower cost) • High cBN yield	To be checked

15

As described earlier, the needs of the cBN weather as the grits or as the polycrystalline sintered compact in the metal working industry are increasing steadily. Cost reduction by means of lowering the pressure and the temperature in the cBN synthesis and the use of easy handling synthesis catalyst to simplify the preparation process is highly demanded [74]. Table 1.4 summarized the well known and already described cBN synthesis methods along with their minimum Pressure-Temperature (P-T) conditions and also their application in cBN sintering technology.

While some previous studies explained the methods and suggested some choices of the relatively easy handling metal catalyst that effective in lowering the cBN synthesis condition [58-61], there is no study that focuses in the controlling of the microstructure of the cBN grains by changing its synthesis catalyst. As seen in Fig. 1.7, the common and widely known method to control the grains size in cBN synthesis is by changing the pressure and temperature conditions [52]. Under the same temperature, the number of spontaneously nucleated cBN crystals increased rapidly with the increasing pressure. The nucleation of cBN crystals was very sensitive against the excess pressure above equilibrium line between hBN and cBN. The nucleation of cBN was also changed with change of the temperature at any constant pressure. The spontaneous nucleation of cBN was maximum at the lowest temperature and number of euhedral crystals was increased with increasing temperature.
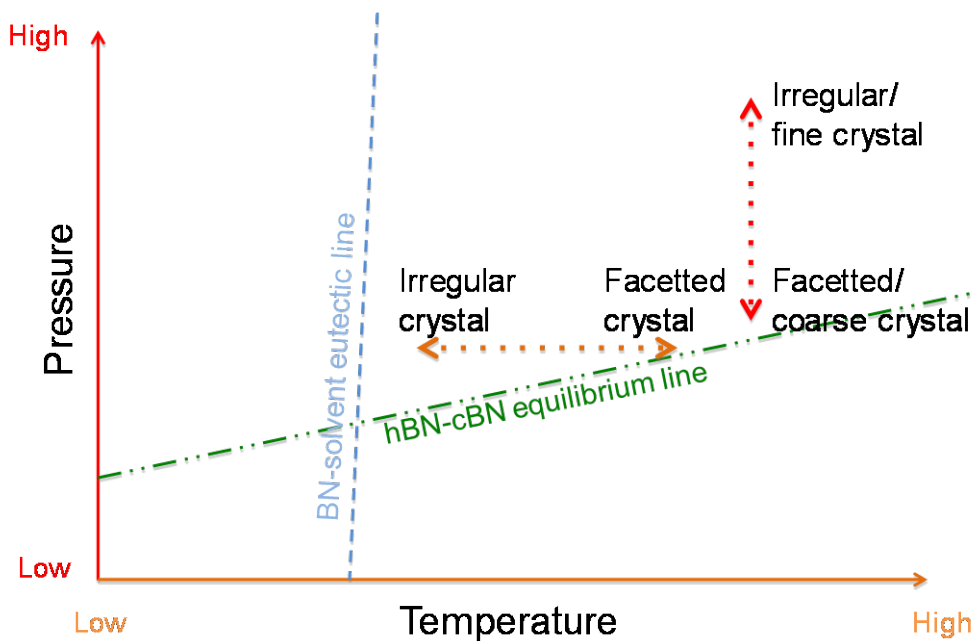

Fig. 1.7 Conventional method of grain size and morphology control in cubic BN synthesis process

As shown in Table 1.4, previous reports showed that Fe–Mo and Co–Mo work as solvent of B and N atoms and Al acts as a nucleation agent of cubic BN. The cubic BN could be synthesized at minimum pressure of about 4.4 GPa and temperature of about 1250 °C. The addition of Mo in the Ni solvent improves the extremely low solubility of nitrogen in molten Ni. Moreover, the addition of Cr to Ni solvent, which can better enhance the nitrogen solubility in molten Ni than Mo, resulted in further increasing the crystal size [57]. The same as Mo, vanadium as shown in Fig. 1.8 was also reported to be effective in increasing the solubility of the nitrogen in the Fe–V, Fe–Cr–Ni–V and Co-V system [77-79].
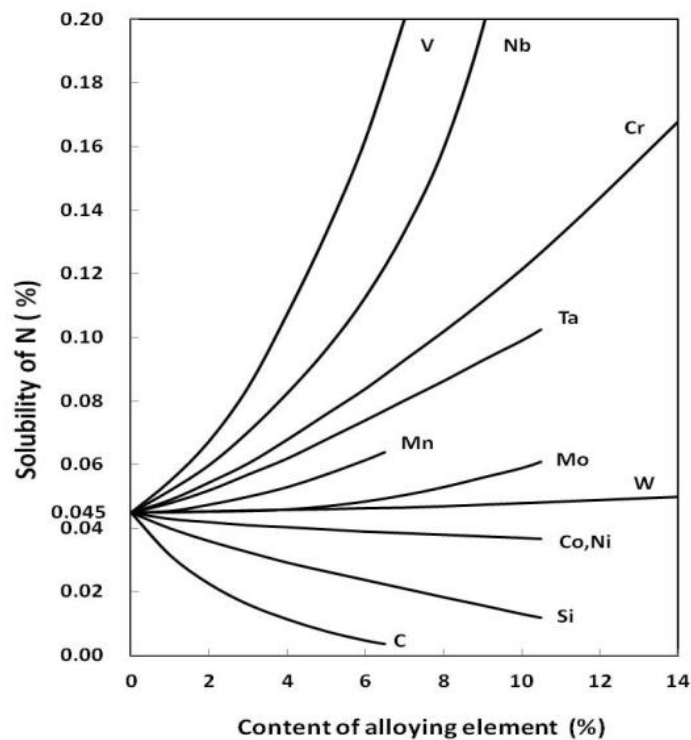

Fig. 1.8. Nitrogen solubility in Fe Alloy [77]

This research will be focused in controlling the cBN grain size during synthesis process using the transition metal as the catalyst. Co–Cr–Al base solvent was employed and Cr with Mo or V was exchanged in the solvent to control the grain size of cBN crystals. The effect of V addition into the Co–Al and Co–Cr–Al in comparison with Co–Cr–Mo–Al metal solvent during cBN synthetic process was studied. The P-T region of the cBN growth was determined by both Co–(Cr, Mo)–Al and Co–(Cr, V)–Al alloys as the synthetic solvent. The ratio of Cr and V under Co–Cr–V–Al solvent system was also changed to compare the cBN growth rate and its morphology between Co–V–Al and Co–Cr–Al solvent system.

As shown in Fig. 1.9, it was suggested that controlling the nitrogen solubility in the metal solvent by changing the solvent composition might be used as the method to control the grain size and the morphology of the cBN crystal under certain P-T condition instead by changing the P-T condition itself. By keeping the synthesis condition at relatively low P-T region, the cost of the synthesis will be hugely reduced as the lifetime of the HPHT die is longer and bigger reaction chamber could be used.
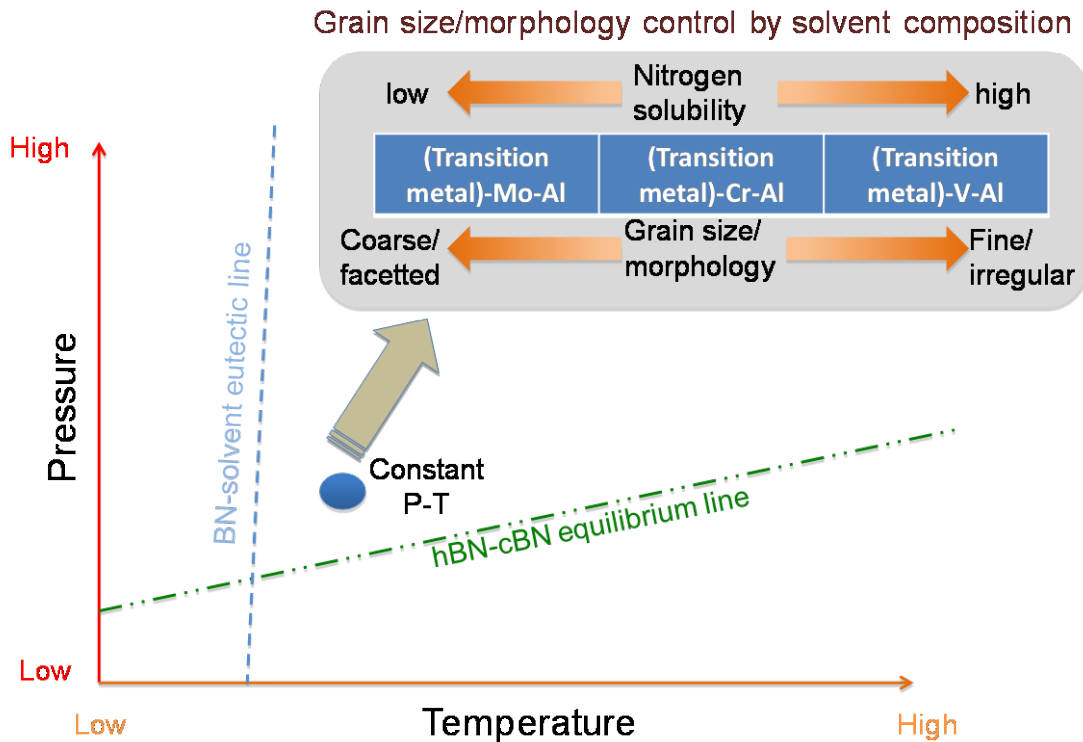

Fig. 1.9. Proposed method of grain size and morphology control in cubic BN synthesis process

As the metal solvent for cBN synthesis and the metal solvent (catalyst) for cBN sintering are in general the same, It was suggested that metal alloy solvent or catalysts which are able to suppress the cBN grain growth during cBN synthesis, should also be useful in order to produce the cBN compact with a homogenous microstructure during the infiltration sintering method. Therefore, it was deduced that adding an element that would act as a grain growth inhibitor into the already well studied metal solvent during the cBN synthesis process and observing the morphology of its cBN crystal, could be a starting point in investigating the metal catalyst for sintering cBN with infiltration method.

High content polycrystalline cBN compact with Co-V-Al metal catalyst was also

sintered. It was predicted that as the nitrogen solubility in the metal catalyst increased by the addition of vanadium or chrome, the dissolution–precipitation process of the cBN grains in the molten metal catalyst during sintering process would be more active. Hence, enhancing the cBN-cBN direct bonding and resulting the increasement of the hardness in PCBN compacts sintered compacts. The change behavior in the hardness of the PCBN compacts sintered with Co-V-Al metal catalyst was compared with the already reported cBN-Al sintered compacts in the function of Al/(Al + BN) and the microstructure of the compact will be discussed. Finally, high volume content cBN cutting tools with Co-V-Al as a sintering media was made and its cutting performance was evaluated on the ductile cast iron as a work material.

This thesis is comprised of 8 chapters.

Chapter 2 presents the methods used to generate high pressures and measure the synthesized samples.

Chapter 3 showed the various morphology of cubic boron nitride crystals synthesized from hBN disk source using (Fe, Co, Ni)-(Cr, Mo)-Al alloy solvents. Effect of the metal alloy combination along with the HPHT synthesis conditions on the morphology of the cBN crystal and its grain size was studied.

In Chapter 4 the synthesis and grain size control of cubic BN using Co-Cr -Al base alloy solvents under high pressure was studied. The P–T region of the cBN growth was determined by both Co–(Cr, Mo)–Al and Co–(Cr, V)–Al alloys. The ratio of Cr and V under Co–Cr–V–Al solvent system was changed to study the cBN growth behavior under such alloys systems.

In Chapter 5 the details of the microstructure of cBN-metal composites synthesized from hBN using Co–Cr–Al, Co–V–Al and Co–Cr–V–Al as infiltration solvents under fix (certain) high pressure and high temperature conditions (5.6 GPa and 1700 °C for 30 min) was studied.

Chapter 6 discussed the polycrystalline cBN compact sintering process using cBN powders as the starting materials with Co-V-Al as a sintering agent. The hardness of the compact was measured and

Chapter 7 showed the cutting performance of the PCBN compact sintered with Co-V-Al sintering media on the gray cast iron and the ductile cast iron.

The results presented in the above chapters along with the possibilities of future works were all summarized in Chapter 8.

References

[1] H. Wentorf, J. Chem. Phys. 26, (1957) 956.

[2] P. Bundy, H. T. Hall, H. M. Strong, and R. H. Wentorf, Nature 176, (1955) 51.

[3] Hofs¨ass and C. Ronning, in 2nd Internat. Conf. Beam Processing of Advanced Materials, J. Singh, S. M. Copley, and J. Mazumder (eds.), ASM Int., Materials Park (1996) 29.

[4] L. Vel, G. Demazeau, and J. Etourneau, Mater. Sci. Eng. B 10, (1991) 149.

[5] A. Bartl, S. Bohr, R. Haubner, and B. Lux, Int. J. of Refractory Metals and Hard Materials 14, (1996) 145.

[6] R. H. Wentorf, J. Chem. Phys. 36, (1962) 1990.

[7] O. Mishima, in: Synthesis and Properties of Boron Nitride, J. J. Pouch, S. A. Alterovitz (eds.), Materials Science Forum, Vol. 54/55, Trans Tech Publications, Brookfield (1990) 313.

[8] P. B. Mirkarimi, K. F. McCarty, and D. L. Medlin, Mater. Sci. Eng. R 21, (1997) 47.

[9] F. R. Corrigan and F. P. Bundy, J. Chem. Phys. 63, (1975) 3812.

[10] V. L. Solozhenko, Dok. Phys. Chem. 301, (1988) 592.

[11] V. L. Solozhenko, Thermochim. Acta 218, (1993) 221.

[12] V. L. Solozhenko, Diamond Relat. Mater. 4, (1994) 1.

[13] G. Will, G. Nover, and J. von der G¨onna, J. Solid State Chem. 154, (2000) 280.

[14] F. P. Bundy and R. H. Wentorf, J. Chem. Phys. 38, (1963) 1144.

[15] R. H. Wentorf, J. Chem. Phys. 34, (1961) 809.

[16] R. H. Wentorf, Chem. Eng. 68, (1961) 177.

[17] R. H. Wentorf, J. Phys. Chem. 63, (1959) 1934.

[18] K. Nassau and J. Nassau, J. Cryst. Growth 46, (1979) 157.

[19] B. P. Singh, G. Nover, and G. Will, J. Cryst. Growth 152, (1995) 143.

[20] H. Sachdev, R. Haubner, H. N¨oth, and B. Lux, Diamond Relat. Mater. 6, (1997) 286.

[21] K. Albe, Phys. Rev. B 55, (1997) 6203.

[22] G. Kern, G. Kresse, and J. Hafner, Phys. Rev. B 59, (1999) 8551.

[23] A. V. Kurdyumov, V. F. Britun, and I. A. Petrusha, Diamond Relat. Mater. 5, (1996) 1229.

[24] J. Furthm¨uller, J. Hafner, and G. Kresse, Phys. Rev. B 50, (1994) 15606.

[25] M. Wakatsuki, K. Ichinose and T. Aoki, Mater. Res. Bull. 7 (1972) 999.

[26] H. Sumiya, T. Iseki and A. Onodera, Mater. Res. Bull. 18 (1983) 1203.

[27] M. Akaishi, T. Sato, M. Ishii, T. Taniguchi and S. Yamaoka, J. mater. Sci. Lett. 12 (1993) 1883.

[28] H. Sumiya, The Rev. of High Press. Sci. and Tech. 13 (2003) 24.

[29] H. P. Bovenkerk, P. Bundy, H. T. Hall, H. M. Strong, and R. H. Wentorf, Nature 184 (1959) 1094.

[30] T. Endo, O. Fukunaga and M. Iwata, J. Mater. Sci. 14 (1979) 1375.

[31] R. C. DeVries, J. F. Fleischer, J. Cryst. Growth 13 (14) (1972) 88.

[32] H. Lorenz, B. Lorenz, U. Kuhne and C. Hohlfeld. J. Mater. Sci. 23 (1988) 3254.

[33] G. Bocquillon, C. Loriers-Susse and J. Loners. J. Mater. Sci 28 (1993) 3547.

[34] M. Kagamida, H. Kanda, M. Akaishi, A. Nukui, T. Osawa and S. Yamaoka. J Cryst Growth 94 (1989) 261.

[35] T. Endo, O. Fukunaga and M. Iwata. J. Mater. Sci. 14 (1979) 1676.

[36] H. Hiraguchi, H. Hashizume, O. Fukunaga, A. Takenaka and M. Sakata. J. Appl Crystallogr. 24 (1991) 286.

[37] T. Sato, T Endo, S Kashima, O Fukunaga and M. Iwata. J. Mater. Sci. 18 (1983) 3054.

[38] T. Endo, O. Fukunaga and M. Iwata. J. Mater. Sci. 16 (1981) 2227.

[39] S. Nakano, H. Ikawa and O. Fukunaga, Diamond Relat. Mater. 3 (1993) 75.

[40] T. Taniguchi and K. Watanabe, J. Cryst. Growth 303 (2007) 525.

[41] H. Saito, M. Ushio and S. Nagao, Yogyo-Kyokai-Shi 78 (1970) 1

[42] R. H.Wentorf Jr., W. A. Rocco, US Patent 3,918,219 (Nov. 11, 1975).

[43] R. C. DeVries and J. F. Fleischer, US Patent 3,918,931 (Nov. 11, 1975).

[44] W. A. Rocco and R. H. Wentorf Jr., US Patent 3,743,489 (Jul. 3, 1973).

[45] D.W. He, M. Akaishi and T. Tanaka, Diamond Relat. Mater. 10 (2001) 1465.

[46] T. Sasaki, M. Akaishi, S. Yamaoka, Y. Fujiki and T. Oikawa. Chem Mater 5 (1993) 695.

[47] T. Taniguchi, New Diamond Front. Carbon Tech. 14 (2004) 289

[48] O. Fukunaga, S. Nakano and T. Taniguchi, Diamond Relat. Mater. 13 (2004) 1709.

[49] H. M. Strong, R. E. Hanneman, J. Chem. Phys. 46 (1967) 3668.

[50] R. H. Wentorf Jr., J. Phys. Chem. 75 (1971) 1833.

[51] H. M. Strong, R. M. Chrenko. J. Phys. Chem. 75 (1971) 1838.

[52] O. Mishima and K. Era in: Science and technology of boron nitride, Y. Kumashiro (ed.) Electric Refractory Materials, Marcel Dekker, New York (2000) 495.

[53] O. Mishima, S. Yamaoka and O. Fukunaga. J Appl Phys 61 (1987) 2822.

[54] Y. Kubota, K. Watanabe and T. Taniguchi, Jpn. J. Appl. Phys. 46 (2007) 311-314.

[55] Y. Kubota and T. Taniguchi, Jpn. J. Appl. Phys. 48 (2009) 071004 1-4.

[56] Y. Kubota, K. Kosuda and T. Taniguchi, Jpn. J. Appl. Phys. 46 (2007) 7388-7391.

[57] O. Fukunaga, S. Takeuchi and T. Taniguchi, Diamond Relat. Mater. 20 (2011) 752.

[58] A. Onodera, K. Inoue, H. Yoshihara, H. Nakae, T. Matsuda and T. Hirai, J. Mater. Sci. 25 (1990) 4279.

[59] T. Ohashi, K. Yamamoto, Y. Yamada and T. Tanase, Intl. J. Ref. Metals Hard Mater. 16 (1996) 403

[60] T. Taniguchi, M. Akaishi and S. Yamaoka, J Mater. Res. 14 (1999) 162.

[61] J. Angseryd, M. Elfwing and E. Olsson, H.-O. Andrén, Intl. J. Ref. Metals Hard Mater. 27 (2009) 249.

[62] X. Z. Rong and O. Fukunaga in: M. Homma (ed.) Advanced Materials '93, I/B, Elsevier Science B.V. 1994 pp.1455.

[63] R. Lv, J. Liu, Y. Li, S. Li, Z. Kou and D. He, Diamond Relat. Mater. 17 (2008) 2062.

[64] X. Rong, T. Tsurumi, O. Fukunaga and T. Yano, Diamond Relat. Mater. 11 (2002) 280.

[65] B. K. Agarwala, B. P. Singh and S. K. Singhal, J. Mater. Sci. 21 (1986) 1765.

[66] M. M. Bindal, R. K. Nayar, S. K. Singhal, A .J. Dhar and R. Chopra, J. Mater. Sci. 21 (1986) 4347.

[67] Y. Li, S. Li, R. Lv, J. Qin, J. Zhang, J. Wang, F. Wang, Z. Kou and D. He, J. Mater. Res. 23 (2008) 2366.

[68] H. S. Jia, Y. L. E, J. Li, X. P. Jia, H. A. Ma, F. Z. Liu, L. H. Liu and H. B. Li, Intl. J. Ref. Metals Hard Mater. 41 (2013) 138.

[69] N. Tan, C. J. Liu, Y. J. Li, Y. W. Dou, H. K. Wang, H. Ma, Z. L. Kou and D. W. He, Eur. Phys. J. Appl. Phys. 53, 11501 (2011)

[70] D. H. Jack, Materials & Design 7 (1986) 267.

[71] V. Richter and M. Fripan in: PCBN cutting tools in a competitive market, Proceedings of EURO PM2006 (2006) 115.

[72] P. J. Heath, in: Ultrahard Tool Materials, J. R. Davis (ed) A.S.M. Handbook, 9th ed., Vol. 16, 105

[73] E. M. Trent and P. K. Wright, Metal Cutting (2000) 227

[74] M. Fleming and A. Wickman, Industrial Diamond Rev. 2/06 (2006) 26.

[75] S. N. Monteiro, A. L. D. Skury, M. J. Azevedo and G. S. Bobrovnitchii, J. Mater. Res. Tech. 2 (2013) 68.

[76] Mitsubishi Carbide General Catalog - CBN PCD Inserts (2013) 12

[77] R.D.Pehlke and J.F.Elliot, Trans Met. Soc. AIME 218 (1960) 1088.

[78] H. Wada and R. D. Pehlke, Met. and Mat. Trans. B 12 (2) (1981) 333.

[79] R. G. Blossey and R. D. Pehlke, Trans Met. Soc. AIME 236 (1966) 28.

Chapter 2 Experimental methods

2.1. HPHT apparatus

High pressure and high temperature experiments were carried out by using a modified belt-type high pressure and high temperature (HPHT) apparatus. The schematic illustration and the image of the belt apparatus are shown in Fig. 2.1 and Fig. 2.2 respectively.

This apparatus was designed to utilize HPHT synthesis of diamond and related materials in the approximate pressure range 3–8 GPa [1–4].
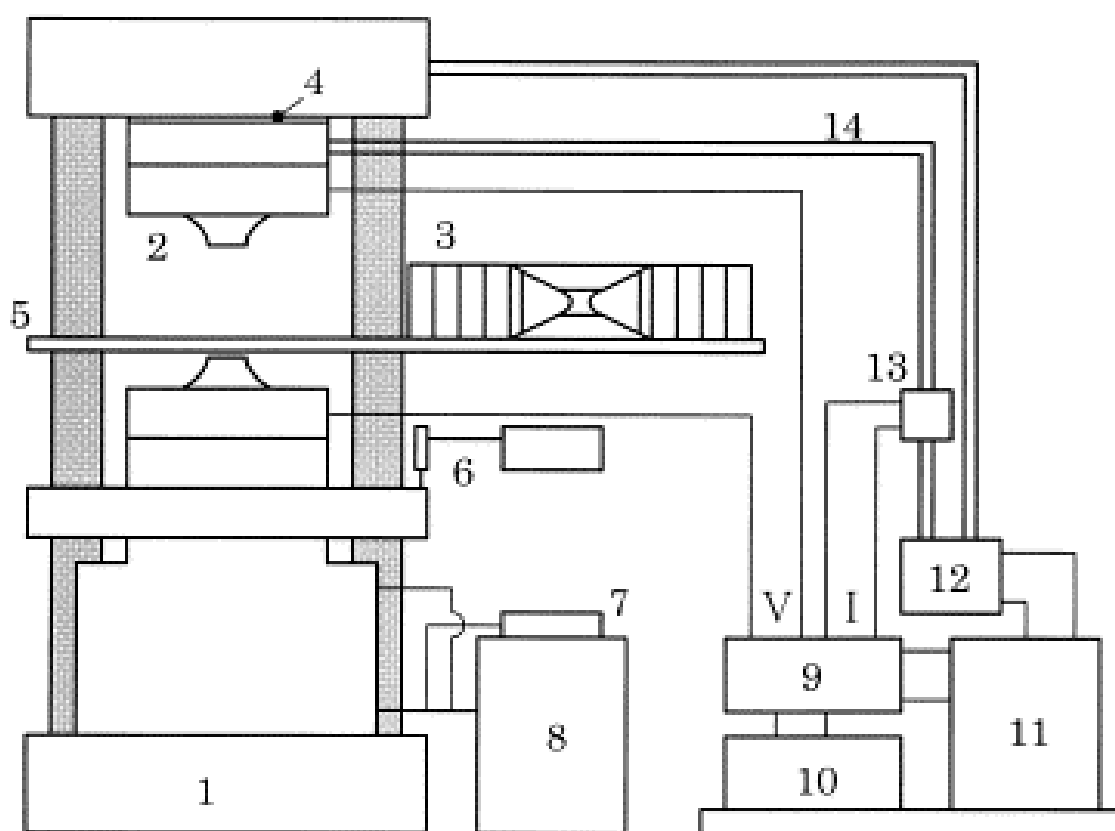

Fig. 2.1. Schematic illustration of FB apparatus:
1 Hydraulic press; 2 High pressure anvil; 3 High pressure cylinder; 4 Insulation sheet; 5 Carrier of cylinder; 6 Measuring scale of anvil displacement; 7 Auxiliary high pressure pump; 8 Pressure pump and control unit; 9 Input–output unit of the heating power; 10 Program unit; 11 Thyrister unit; 12 Step-down transformer; 13 Current transformer; 14 Heating power lead.
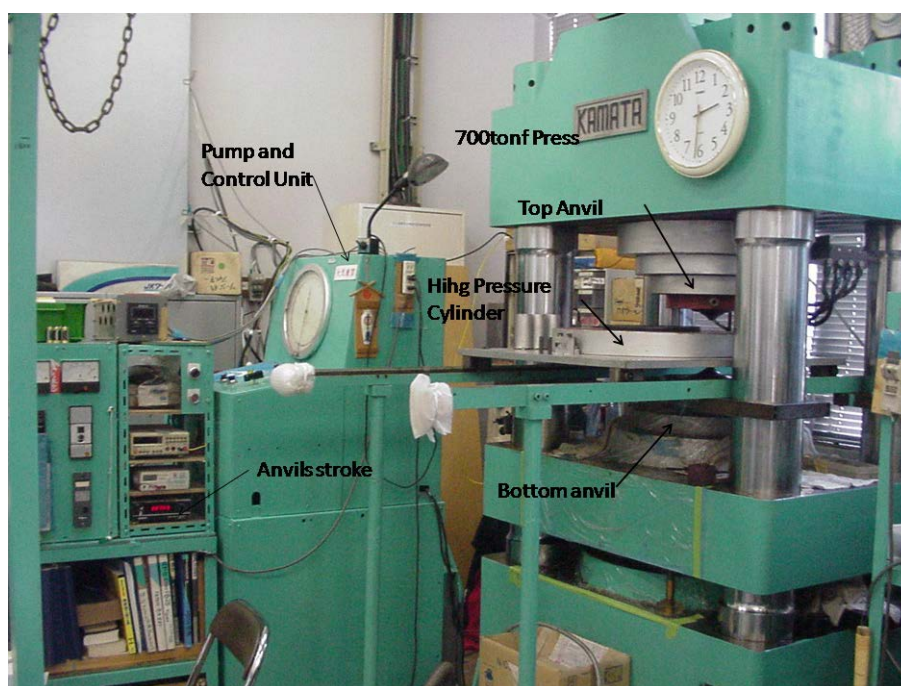
Fig. 2.2. Photo of the 700 tonf belt type press.

Figure 2.1 illustrates the Flat-Belt (FB) apparatus and pressure-temperature control system schematically. We used a 700 metric tonne load up-stroke type hydraulic press (Kamata Machine Co., Saitama, Japan) to install the anvils and high pressure cylinder of the FB apparatus. The upper anvil of the FB apparatus was tied to the upper press plate via an electrical insulation sheet. The sample and lower gasket assembly were set on the lower anvil, they were approached upwardly with the cylinder, and then the upper gasket assembly was inserted. So the assembled sample and gasket were compressed at a speed of about 0.6 mm/min to the designed press load value. The anvil displacement (0.01 mm of sensitivity) versus press load (1 tonne of the sensitivity) curve was checked every run to estimate sample volume change during compression.

The press load was controlled using an auxiliary small plunger pump. A cooling water supply was introduced to the gap between anvil and cylinder with a water seal rubber jacket. Heating power was supplied to the graphite heater while monitoring the voltage and current in the heater. Power from the thyrister unit was supplied to keep a balance between power from the heater and the signal of the program unit. In all experimental runs, power and the electrical resistance to the heater were monitored.

2.2. Sample assembly and gasket preparation

The sample and gasket assembly is shown schematically in Fig. 2.3. The image of the parts we used in the experiments was also shown in Fig. 2.4. We placed the current ring assembly for each end of the sample. The current ring assembly was composed of current plates (stainless steel, 21 mm diameter and 0.5 mm thick for the anvil side; and molybdenum plate, 21 mm diameter and 0.5 mm thick for the sample side), stabilized ZrO_2 ceramic and a hard steel ring 4 mm thick. The current ring assembly could supply a large heating current to the graphite heater keeping good thermal insulation to the tungsten carbide anvil.
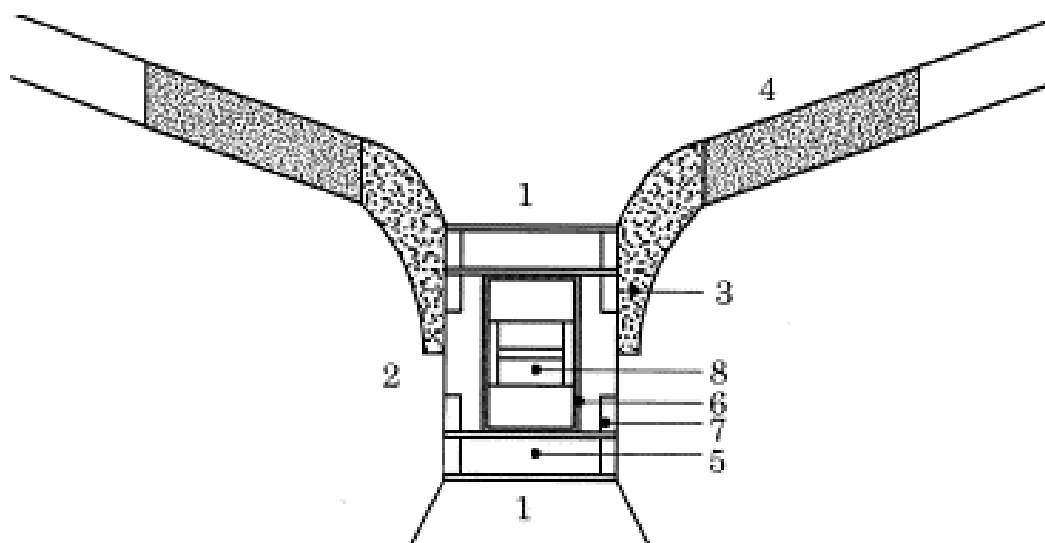

Fig. 2.3. High pressure cell assembly:
1 Anvil top; 2 High pressure cylinder core; 3 Pyrophyllite gasket; 4 Laminated paper gasket; 5 Current ring assembly; 6 Graphite heater; 7 Outer salt sleeve with steel ring; 8 Sample chamber surrounded by salt parts.

The central part of the sample cell was composed of outer NaCl plus 10 wt% stabilized zirconia (hereafter called salt) compact. The salt sleeve was 21 mm in diameter and 17.4 mm in length and was used as furnace insulator and pressure medium. At the end of the outer salt sleeve, a soft steel ring 5 mm thick, was bounded to prevent deformation of the sleeve. The graphite heater (ISO-63 isotropic graphite, Toyo Tanso Co., Osaka, Japan) of 12 mm outer diameter and 10 mm inner diameter was press fitted to the outer salt sleeve. Inside the graphite heater, a thin inner salt sleeve was used for electrical insulation between the sample and the heater.
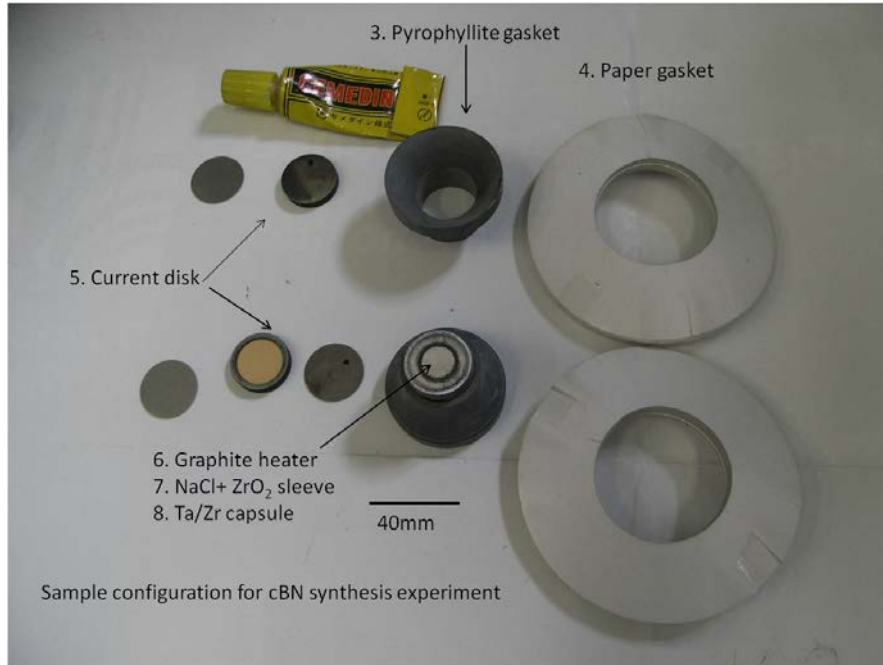
Fig. 2.4. Various parts used in HPHT experiments

The sample zone to be utilized for cBN/ diamond synthesis and sintering was about 7 mm in diameter and 6-8 mm in length. In case of cBN synthesis, two sets of hBN/solvent samples were placed with separated by a 1 mm thick salt plate. All the salt parts were formed with added water (about 3%) at 400 MPa, using a tungsten carbide die and punch. The pyrophyllite gaskets shown in Fig. 2.4 were lathe machined using similar shaped tungsten carbide tools. Outer laminated paper gaskets were press formed using laminated 0.44 mm thick papers. The deformation characteristic of the laminated paper was checked and selected so as to maintain good performance of the compressible gasket action [3].

Some images regarding the sample assembly on the belt press were shown in Fig. 2.5 with the upper image is the sample assembled set on the cylinder (top anvil side) and the lower image is the sample assembled at the bottom anvil.
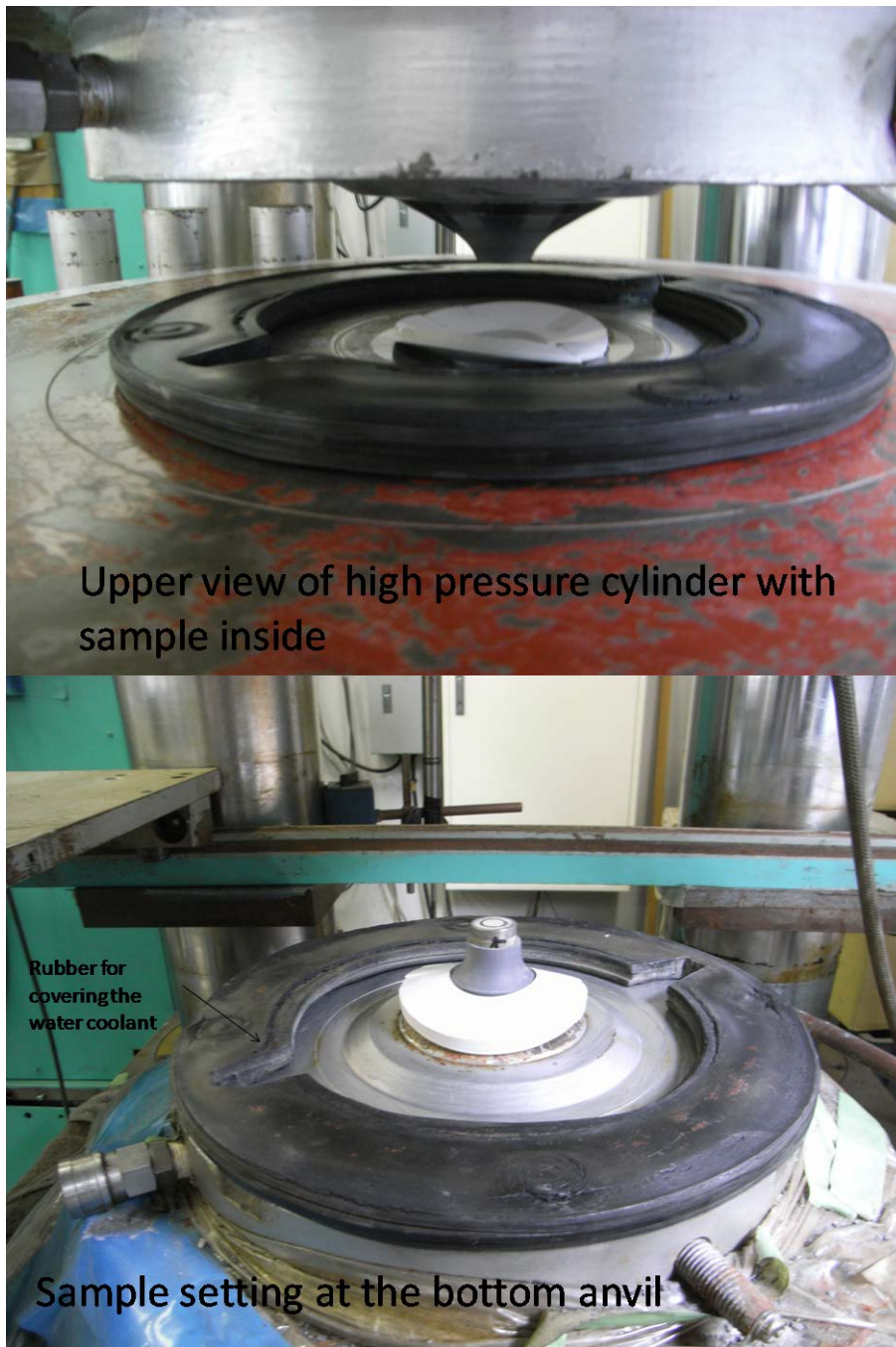
Fig. 2.5. Sample assembly on the belt press

An example of the sample assembly after the HPHT process could be seen in the Fig. 2.6. The upper image is the NaCl sleeve covered cBN synthesis sample sandwiched with the current disk on both side while the lower image is the as recovered cBN with its metal solvent source.
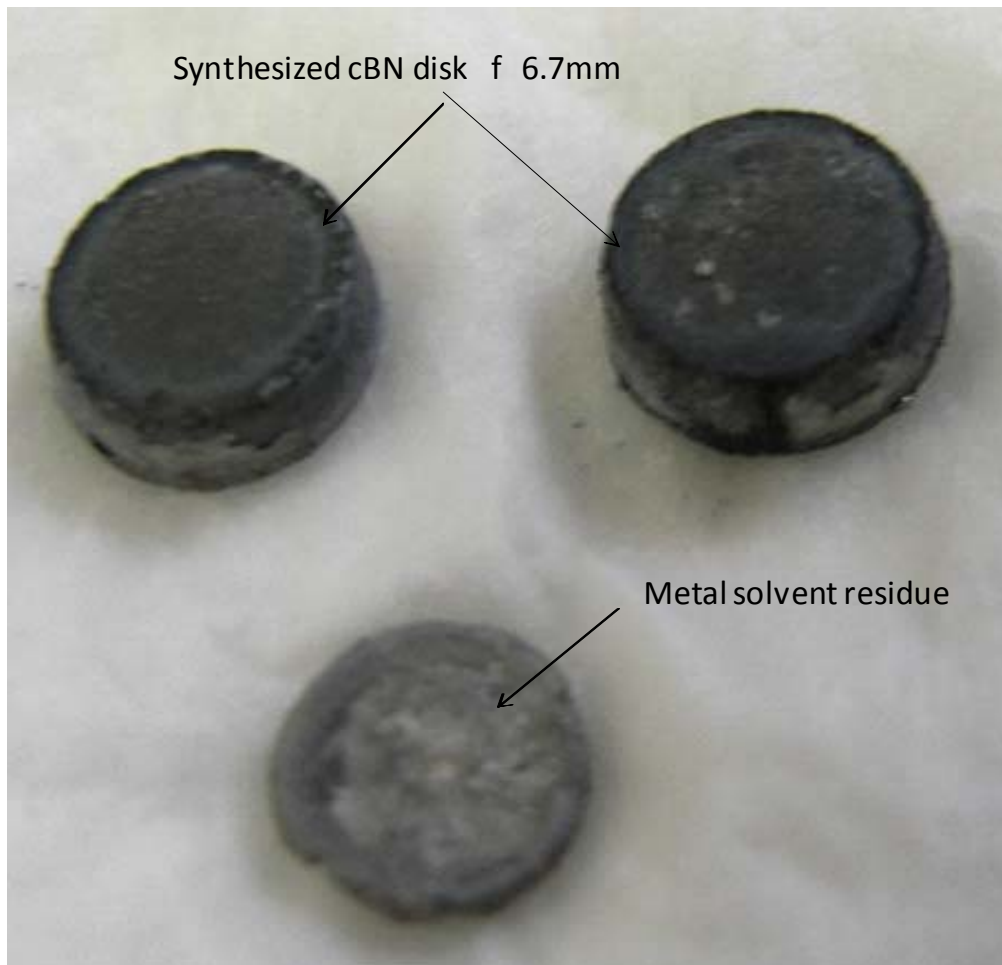
Fig. 2.6. An example of the recovered sample after HPHT experiment

2.3. Estimation of absolute pressure and temperature at HPHT

The pressure calibration at room temperature was measured based on the phase transitions in bismuth (I–II, 2.55 GPa), thallium (II–III, 3.68 GPa) and barium (I–II, 5.3 GPa). As the pressure at the high temperature increase as the result of the NaCl melts in the sample assembly, the pressure at high temperature was also need to be measured [5].

In the present study, the absolute pressure and temperature values in the cBN synthesis region were estimated based on the minimum Pressure-Temperature (P-T) points of diamond formation in Ni, Co and invar solvent systems. We considered minimum P-T conditions of diamond formation in the graphite–solvent systems as a candidate for both pressure and temperature standards. The P-T region of diamond formation was bounded by two distinct lines, namely a graphite–diamond equilibrium line and a carbon–solvent eutectic line. Thus the minimum P-T point of diamond formation was defined as the intersection of the two lines. We adopted the graphite–diamond equilibrium line

determined by Kennedy [6]. The equilibrium boundary expressed as P(GPa)=T(°C)/400+1.94 which is basically consistent with the calculated boundary by Berman and Simon [7] and [8]. After confirming the minimum P-T condition of the diamond formation in Ni, Co and invar solvent systems as a function of press load and heater power, the relation between heater power and temperature and the relation between the press load and the absolute pressure could be estimated using already published and recognized data of the minimum P-T of the diamond formation in each metal solvent system [7-10]. Additional experiments to evaluate the accuracy of pressure estimation based on the minimum P-T standards of diamond formation was also performed using a phase boundary between garnet and perovskite phase of CaGeO$_3$ which the phase boundary could be shown as a function of P(GPa)= 6.9−T(°C)/1250 [11].

The results of the measurement on the absolute pressure and temperature are shown in the fig. 7 and 8 respectively. As shown in Fig. 2.6, the variation of measured temperature values was about 60°C (about 4%) at 1500°C from three different runs. From fig. 2.7, the absolute pressure in the diamond formation temperature region must be accounted to about 20% pressure increase from room temperature when we use a salt pressure cell.
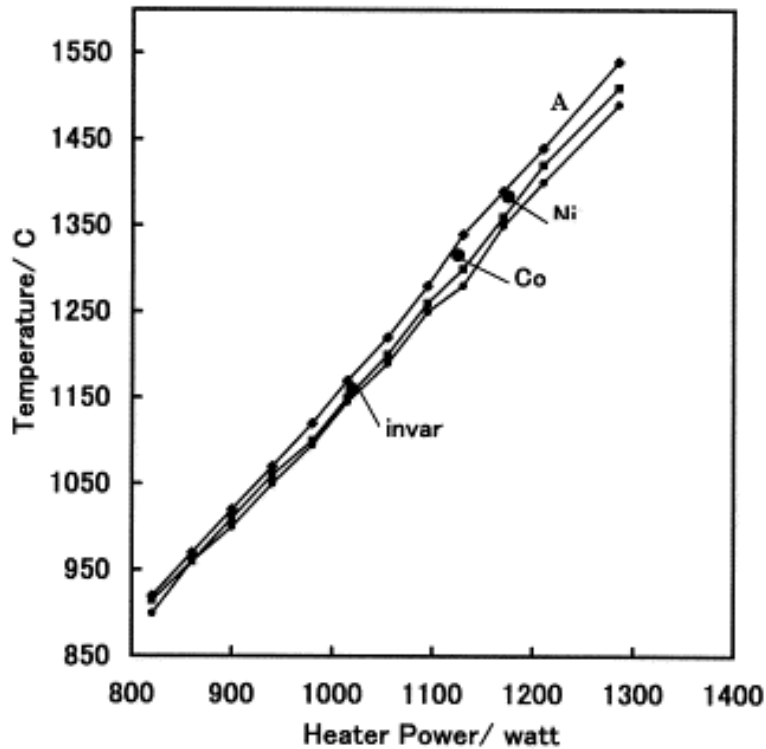

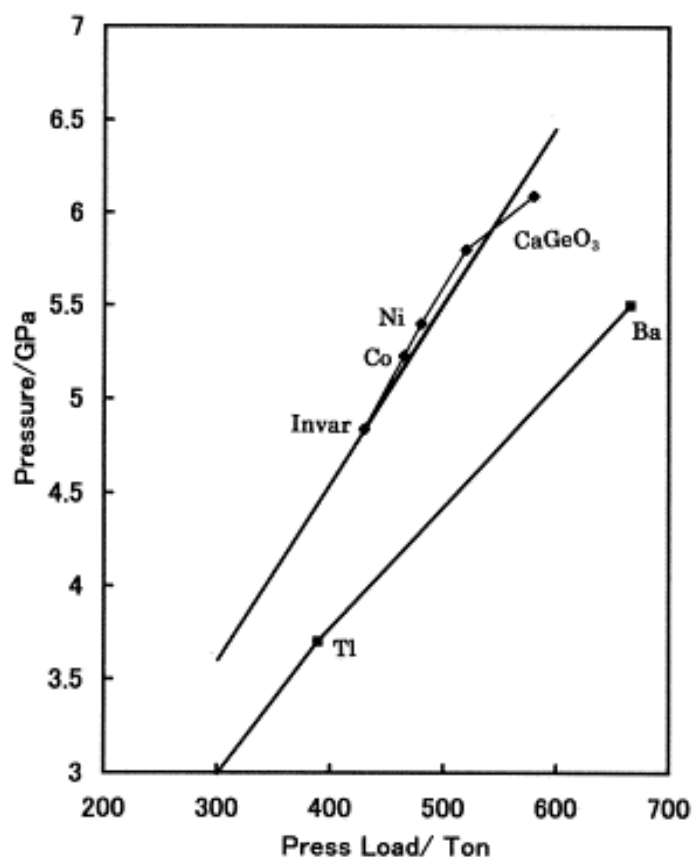Fig. 2.6. Temperature measurements using Pt-Pt13%Rh thermocouple.

Fig. 2.7. Pressure calibration curve at high temperature.

2.4. Sample analysis

  Phase identification of the product was made by the X-ray powder diffraction (XRD) method. The measurements were made using a Cu (1.54 Å) target. The measurement conditions were as follows: acceleration voltage was 40kV; beam current was 30mA; and the scanning rate was 4°/min. In the cubic BN synthesis experiments, the conversion rate from hexagonal BN to cubic BN was estimated from the X-ray diffraction intensity ratio of cubic BN to hexagonal BN.

  A high resolution electron microscope and an ordinary electron microscope were used. High resolution of Field Emission-Scanning Electron Microscope (FE-SEM) was used in the observation of the grain boundary of the cBN bonding in the cBN sintering related experiments and ordinary FE-SEM was used mainly in the hBN-cBN synthesis related experiment.

  When necessary, energy dispersive X-ray Spectroscopy was taken to identify the substance. The substance identification and its distribution on some samples were also analyzed the using electron probe micro analyzer or EPMA.

  The average grain size of the obtained sample was measured from the SEM image and

was confirmed using grain boundaries identification from the crystal orientation of the electron backscatter diffraction (EBSD) analysis.

5. Physical properties evaluation

The hardness of the sintering sample was measured using a micro Vickers hardness tester with the load fixed at 1.0 kg. The samples were mirror polished by diamond abrasives.

To evaluate the cutting performance of the obtained sample, cutting test on the NC lathe were carried out using FC300 gray cast iron and FCD700 ductile cast iron as a work material. The details of the cutting tests conditions will be described in the chapter 7. Flank wear was measured and a cutting edge was observed.

References

[1] O. Fukunaga, M. Akaishi, T. Endo and S. Yamaoka, J. High Press. Soc. Japan, 14 (2) (1976) 91.

[2] O. Fukunaga, S. Yamaoka, T. Endo, M. Akaishi and H. Kanda, High Pressure Science and Technology, Vol. 1Plenum (1979) 846.

[3] O. Fukunaga, S. Yamaoka, M. Akaishi, H. Kanda, T. Osawa, O. Shimomura and T. Nagashima, M.H. Manghnani, Y. Syono (Eds.), High Pressure Research in Mineral Physics, Sci. Terra, Tokyo (1987) 17.

[4] S. Yamaoka, M. Akaishi, H. Kanda, S. Osawa, T. Taniguchi, H. Sei and O. Fukunaga, J. High Press. Soc. Japan, 30 (1992) 249.

[5] O. Fukunaga, Y.S. Ko, M. Konoue, N. Ohashi and T. Tsurumi, Diamond Relat. Mater. 8 (1999) 2036.

[6] C. S. Kennedy and G. C. Kennedy, J. Geophys. Res., 81 (1976) 2467.

[7] R. Berman, F. Simon and Z. Elektrochem. 59 (1955) 333.

[8] R. Berman, Physical Properties of Diamond, Clarendon Press, Oxford (1965) 371.

[9] H. M. Strong, Act. Metall. 12 (1964) 1411.

[10] H. M. Strong and R. E. Tuft, Technical Rep. No. 74CRD118, G.E. Corp. R and D, Schenectady NY, July, 1974.

[11] J. Susaki, M. Akaogi, S. Akimoto and O. Shimomura, Geophys. Res. Lett. 12 (1985) 729

Chapter 3 Morphology of cubic BN crystals synthesized from hexagonal BN disk source using (Fe, Co, Ni)-(Cr, Mo)-Al alloy solvents

3.1. Introduction

The effective converting solvent from hBN to cBN must be contained elements to increase both boron and nitrogen solubility in the liquid alloys at high pressure [1]. As shown in Fig. 1.8, Pehlke and Elliot [2] reported nitrogen solubility in liquid binary Fe-M alloy where M=Mo, Mn, Ta, Cr, Nb and V. The nitrogen solubility at 6 wt% of M-elements in the Fe alloy were Mo=0.05 wt%, Mn= 0.06 wt %, Ta=0.07 wt%, Cr=0.085, wt% Nb=0.11 wt%, and V=0.17 wt% [2]. The increase of the nitrogen solubility was also confirmed in the Ni alloy [3] and Co alloy [4] as seen in Fig. 3.1 for the Ni alloy and Fig. 3.2 for the Co alloy.
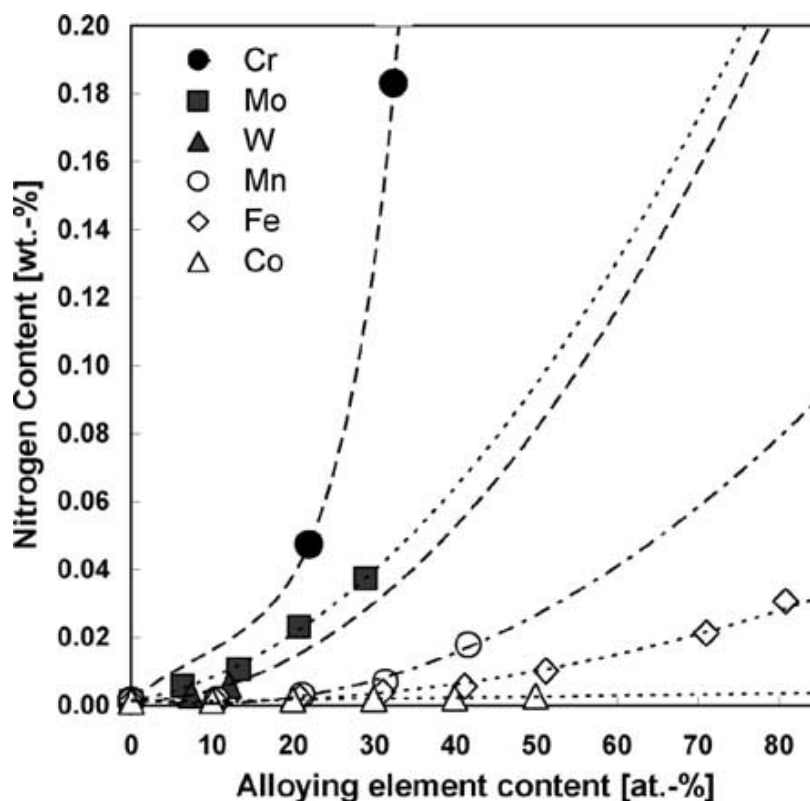

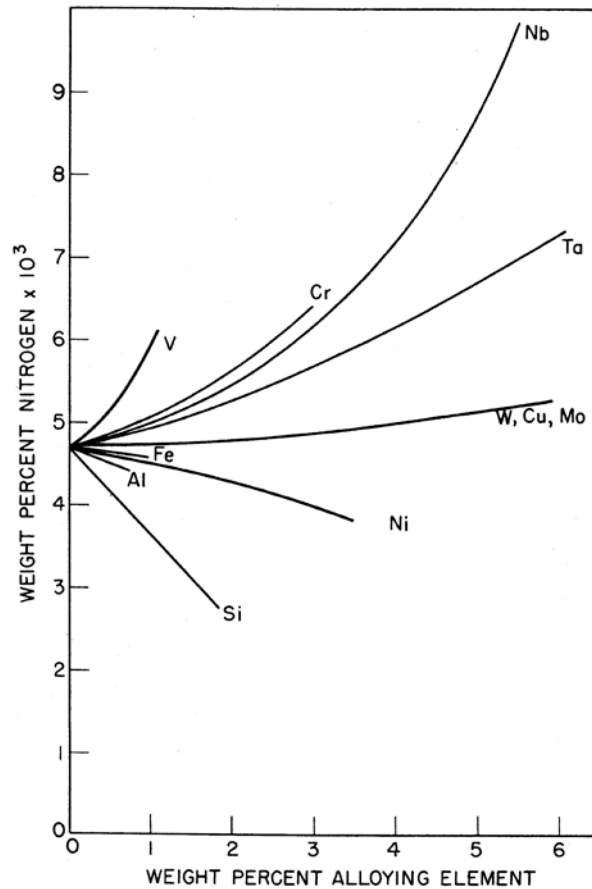Fig. 3.1. Nitrogen solubility in Ni alloy [3]

Fig. 3.2. Nitrogen solubility in Co alloy [4]

From the above data, then it is assumed that addition of M-elements into the Fe-Ni-Co liquid alloy is effective to increase nitrogen solubility in the solvent system. Based upon this scheme, we described alloy solvent system as a combination of boron soluble elements, (Fe, Ni and Co), elements of increase nitrogen solubility, (Mo, Mn, Ta, Cr, Nb and V) and Al, such as (Fe, Co)-Cr-Al.

In this chapter, we examined pressure temperature (P-T) condition of the growth cBN using (Fe, Ni)-Cr-Al and Co-(Cr, Mo)-Al solvents. As typical contents for these solvents, we selected (Fe52.5, Ni5.8)-Cr38.8-Al2.9 wt% solvent and Co47-(Cr30, Mo20)-Al3 wt% solvent for the determination of the P-T region of cBN growth.

The (Fe, Ni)-Cr-Al solvents of which we select were Fe rich or Ni rich composition but content of Cr were about 30-40 wt% as referred to the Cr content between 21-47 wt% reported by DeVries and Fleischer [5]. We present P-T regions of cBN growth

using (Fe52.5, Ni5.8)-Cr38.8-Al2.9 wt%. For the content of Co-(Cr, Mo)-Al solvent, Co content was kept at about 46-47 wt% and the content of Cr plus Mo were kept at about 50%. The P-T region of cBN growth was examined using Co47-(Cr 30, Mo20)-Al3 wt% solvent. Crystal size and morphology of cBN crystals were examined using optical microscope and SEM.

3.2. Experiments

3.2.1 Preparation of the sample

  Starting BN source was hot pressed hBN rod (Denka N-1 type, Purity: $\geqq$ 99%, Denki-kagaku, Tokyo), which contain about 0.1 wt% of oxygen as impurity. The hBN rod was machined to 7mm diameter and 2-3 mm of thickness. We used powder mixture of constitutional metals. The powders of Ni (99.9%), Co (99.9%), Fe (90%), Cr, Mo (99.9%) and Al (99.99%) were used. The metal powders were weighed and mixed in an ethanol using agate pestle and mortar.

3.2.2 High pressure experiments

   The belt type (FB25H) high pressure apparatus [6] as described in chapter 2 was used in the experiments. Detailed method of pressure and temperature calibration was described in the previous chapter 2. The sample container was lined by Mo or Zr foil of 0.02 mm thickness. The hBN source disks were laminated with pressed powder of the solvent alloy and packed into the container. Figure 3.1 showed the sample assembly for synthesis experiments.

hBN disk
Metal solvent powders
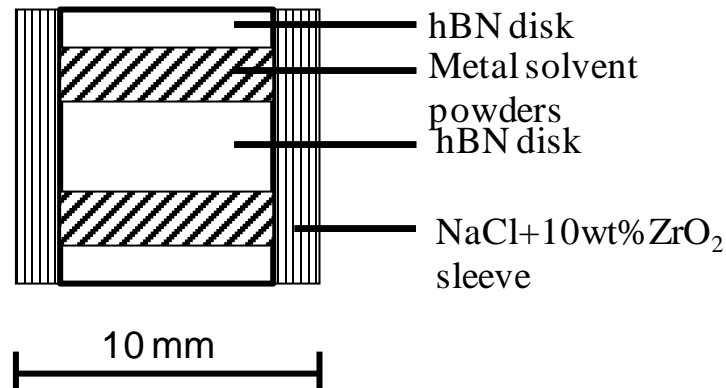hBN disk
NaCl+10wt%ZrO_2 sleeve

10 mm

Fig. 3.1. Sample assembly for high pressure-high temperature (HPHT) synthesis of cBN using metal catalyst.

The sample assembly was compressed at room temperature to the designed press load and at designed pressure at first before the sample heating program was started. After HPHT runs, heating current was cut within 10 min. and then press load was decreased slowly. Recovered sample was examined using optical microscopy, SEM and XRD method.

3.2.3 Solvent compositions

At the initial stage of the present experiments, we tried to check minimum pressure of cBN formation using (Fe9.4, Ni53)-Cr33.6-Al4 wt% solvent. The composition of this solvent was closed to the composition of Ni49-Cr49-Al2 wt% or (Fe8, Ni43)-Cr47-Al2 wt% solvents, which have been reported the synthesis of cBN at 5.25 GPa and 1450 °C by DeVries and Fleischer [5]. The P-T region of the cBN growth on the Fe-Ni-Cr-Al system was widely checked using the (Fe52.5, Ni5.8)-Cr38.8-Al2.9 wt% alloy system.
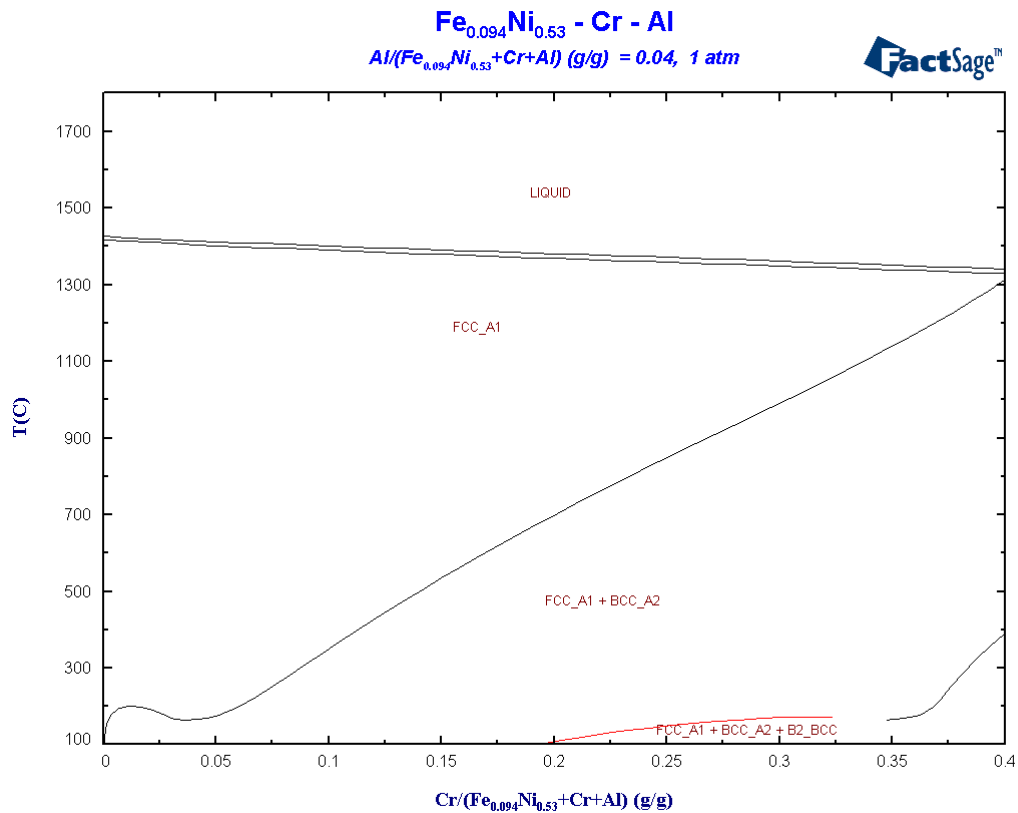

Fig. 3.2. Calculated equilibrium diagram of the (Fe9.4, Ni53)-Cr-Al4 wt% pseudobinary system at 1 atm.

As references, the liquidus temperature of the above alloys system at the ambient pressure was calculated using the FactSage thermochemical software and databases. The results were shown in Fig. 3.2 for the (Fe9.4, Ni53)-Cr33.6-Al4 wt% alloy system and Fig. 3.3 for the (Fe52.5, Ni5.8)-Cr38.8-Al2.9 wt% alloy system. The liquidus temperature of these alloys was confirmed at about 1300 to 1350 °C. As the alloy solvent will react with the B and N, it was suggested that the actual liquidus temperature will be lower.
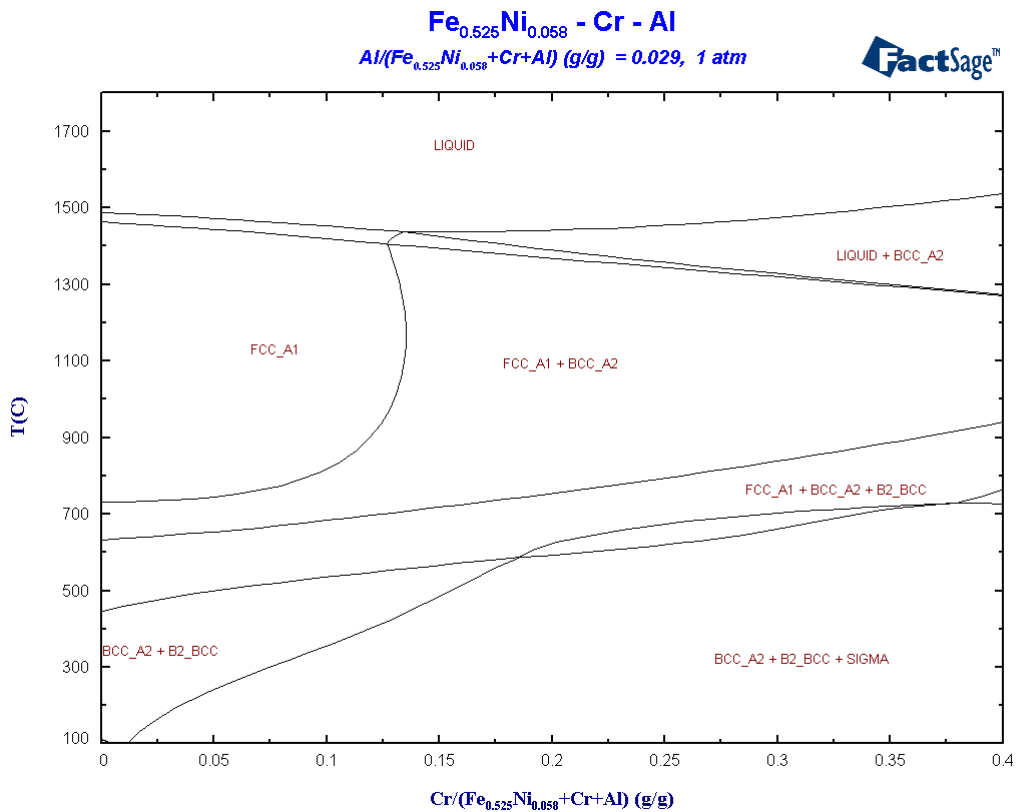

Fig. 3.3. Calculated equilibrium diagram of the (Fe52.5, Ni5.8)-Cr-Al2.9 wt% pseudobinary system at 1 atm.

The same calculation to determined the liquidus temperature for the Co-(Cr, Mo)-Al was also performed on the Co47-(Cr30, Mo20)-Al3 wt% and the result was shown in Fig. 3.4. From the Fig. 3.4, it could be confirmed that the liquidus temperature of the Co47-(Cr30, Mo20)-Al3 wt% system at 1 atm is about 1300 °C.
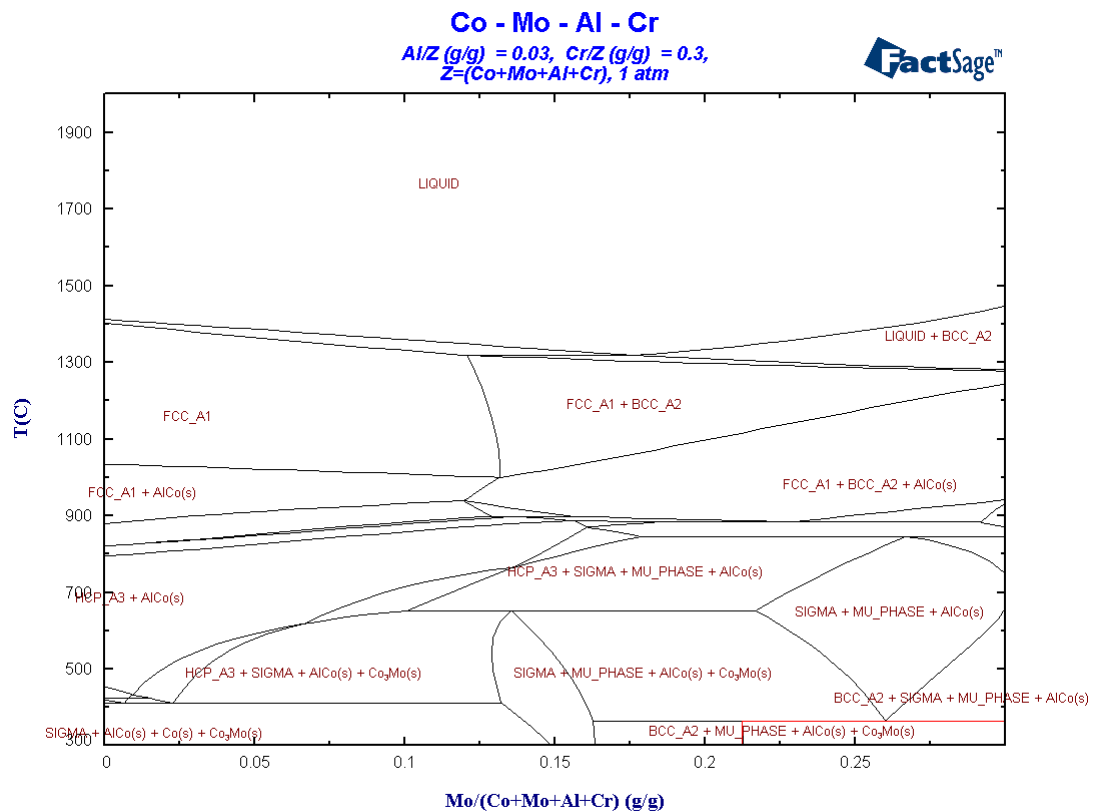
Fig. 3.4. Calculated equilibrium diagram of the Co47-Cr30-Mo-Al3 wt% pseudobinary system at 1 atm.

3.3. Results and Discussion

3.3.1 Pressure-temperature region and morphology of the growth of cBN crystals using (Fe, Ni)-Cr-Al solvent

We determined minimum cBN formation condition at about 4 GPa and 1320 °C using (Fe9.4, Ni53)-Cr33.6-Al4 wt% solvent. This result indicated that addition of Cr into the Al alloy of Fe and Ni decreased minimum formation pressure of cBN. The minimum pressure of cBN growth in a Fe-Ni-Al alloy was estimated at about 6 GPa [7].

The SEM images of the sample reacted hBN with (Fe9.4, Ni53)-Cr33.6-Al4 wt% solvent at 4.2 GPa and 1394 °C for 1 h. is shown in Fig. 3.5. All grains in the figure were cBN crystals and the yield of cBN in the sample was estimated to more than 90%. The morphology of cBN crystals shown in Fig. 3.5 was irregular in shape and the size of the grains was about 100-200 µm.

The crystallization of cBN was started at the interface between source hBN disk and molten solvent layer. The B and N species are dissolved into liquid alloy solvent from hBN to more than solubility limit of cBN. Density of cBN nucleation is depended on the degree of super-saturation of cBN in the liquid alloy. Crystallization of cBN in the liquid prompts the liquid layer to migrate into the hBN layer. Higher rate of cBN crystallization accelerate the migration of liquid alloy layer.
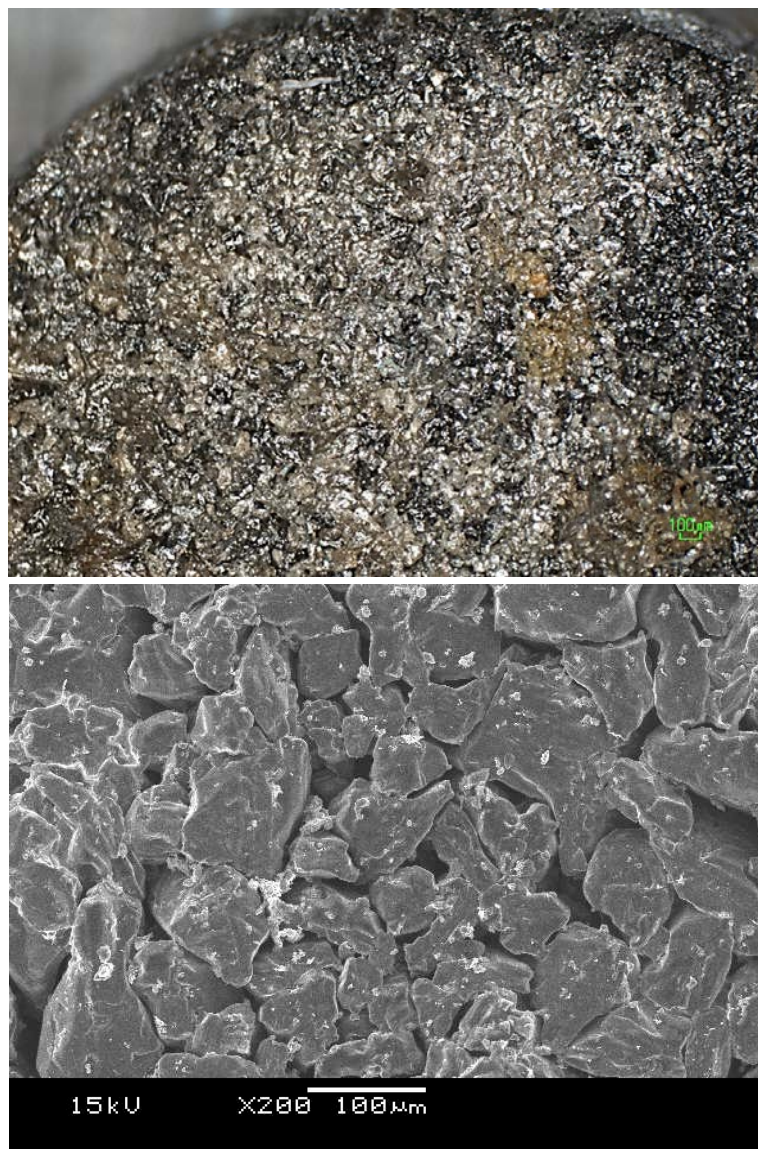

Fig 3.5. Optical and SEM images of the sample reacted hBN with (Fe9.4, Ni53)-Cr33.6-Al4 wt% solvent at 4.2 GPa and 1394 °C for 1 h.

The liquid alloy solvent layer was migrated to the source hBN disk with converting hBN to cBN. Thus the migration speed of molten alloy was corresponded to the rate of cBN growth. The texture of cBN crystals as shown in Fig. 3.5 suggested high growth rate of cBN crystal by rapid migration of liquid solvent.
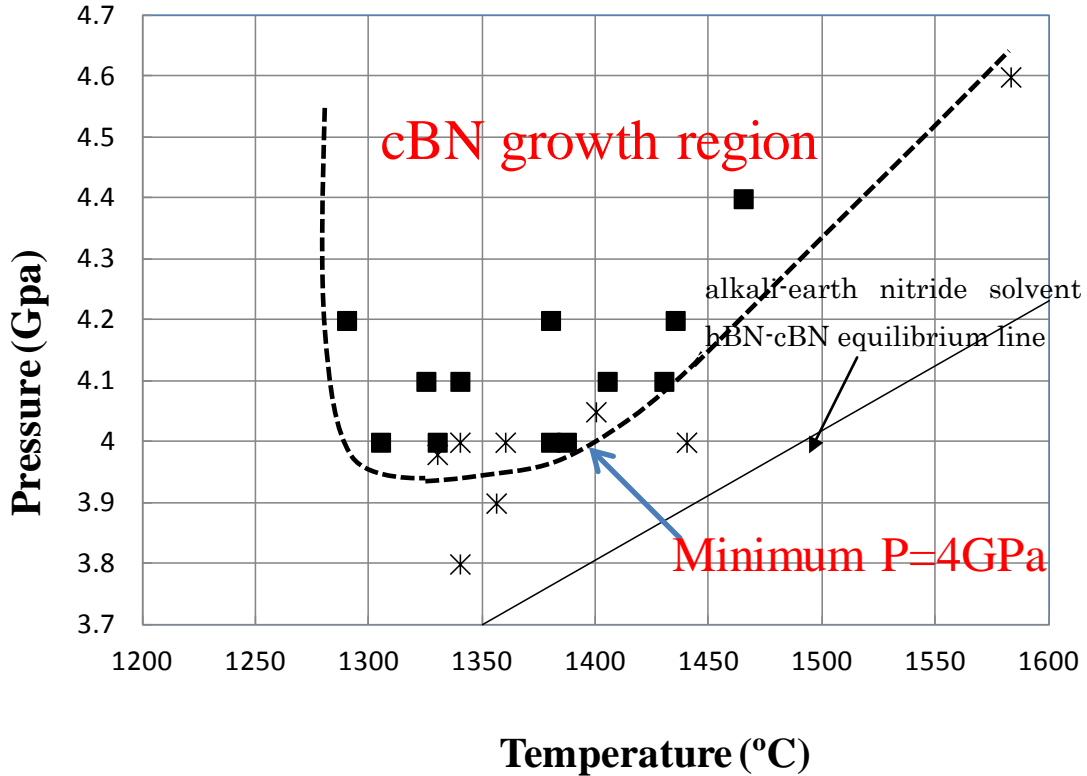

Fig. 3.6. P-T region of cBN growth using (Fe52.5, Ni5.8)-Cr38.8-Al2.9 wt% solvent.

We examined the P-T region of cBN growth using (Fe52.5, Ni5.8)-Cr38.8-Al2.9 wt% solvent and illustrated the result in Fig. 3.6. The minimum cBN forming pressure in Fig. 3.6 was about 4 GPa at 1300-1400 °C, which close to the results used (Fe9.4, Ni53)-Cr33.6-Al4 wt% solvent. But cBN crystals were detected in some runs at 4 GPa, but no cBN was found in the other runs at 4 GPa. At lower pressure range of at about 4 GPa, experimental results of cBN formation were scattered by small variation of P-T condition. At 4.2 GPa, cBN was precipitated in the all samples examined.

The cBN grains grown in the (Fe52.5, Ni5.8)-Cr38.8-Al2.9 wt% solvent are shown in Fig. 3.7 to Fig. 3.9 with increase of reaction pressure from 4 to 5 GPa. The image shown in Fig. 3.7 are collected the sample reacted at 4 GPa and 1350 °C for 0.5 h. The small numbers (about 25 grains on the disk of 7 mm in diameter) of cBN crystals were

deposited on one surface of solvent layer. The migration speed of liquid alloy layer was very slow in this case, cBN crystals were grown at the interface between the solvent and source hBN. The grain size of facetted cBN crystals was about 300-500 μm.

Fig. 3.7. Optical photograph of cBN synthesized using Fe52.5Ni5.8-Cr38.8-Al2.9 solvent at 4 GPa 1350 ℃ 0.5 h.

The images of optical microscopy of the sample reacted at 4.2 GPa and 1280℃ for 1h are shown in Fig. 3.8. Due to near lowest pressure condition, migration rate of liquid layer of the solvent was relatively slow. Semi-spherical pocket of liquid alloy was observed at the central portion of the sample. The grain size of cBN was about 300 μm reflected slow growth rate of cBN.

Fig. 3.8. Optical photograph of cBN synthesized using Fe52.5Ni5.8-Cr38.8-Al2.9 solvent at 4.2 GPa 1280 ℃ 0.5 h.

The cBN grains reacted at 4.4 GPa and 1465 °C for 1 h. and at 5 GPa and 1320 °C for 1 h. grown in (Fe52.5, Ni5.8)-Cr38.8-Al2.9 wt% solvent are shown in Fig. 3.9 and 3.10. These samples were reacted at higher pressure than the sample shown in Fig. 3.7 and 3.8. The migration speed of liquid solvent layer was estimated very high, thus the yield of cBN reached almost 100 %. The shape of the cBN crystals was very rough and non-faceted morphology and the crystal size was about 150 μm for both Fig. 3.9 and 3.10. The morphology of cBN crystals precipitated in the (Fe52.5, Ni5.8)-Cr38.8-Al2.9 wt% solvent was normally irregular in shape and 100-500 µm of grain size depending on the reacted pressure. With increasing reacted pressure, grain size of cBN was decreased due to rapid nucleation and growth of cBN crystals in the liquid solvent.
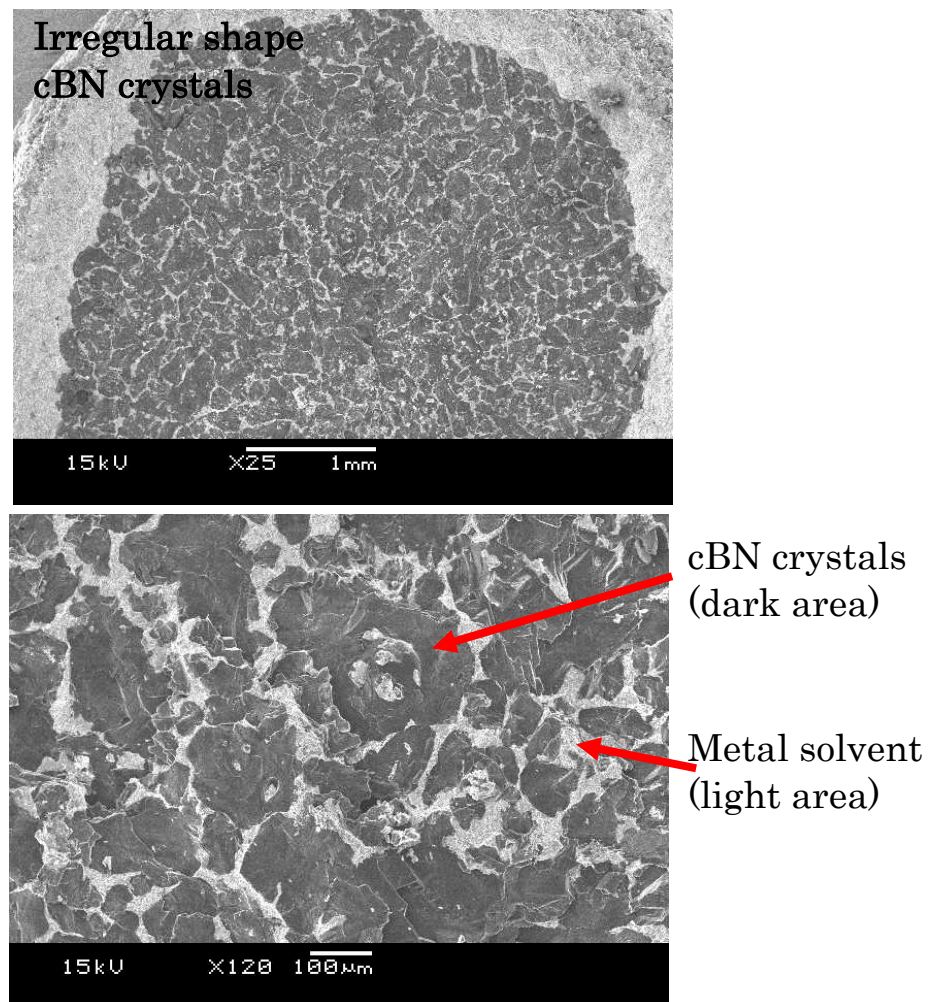

Fig. 3.9. SEM image of cBN synthesized using Fe52.5Ni5.8-Cr38.8-Al2.9 solvent at 4.4 GPa 1465 °C 1 h.
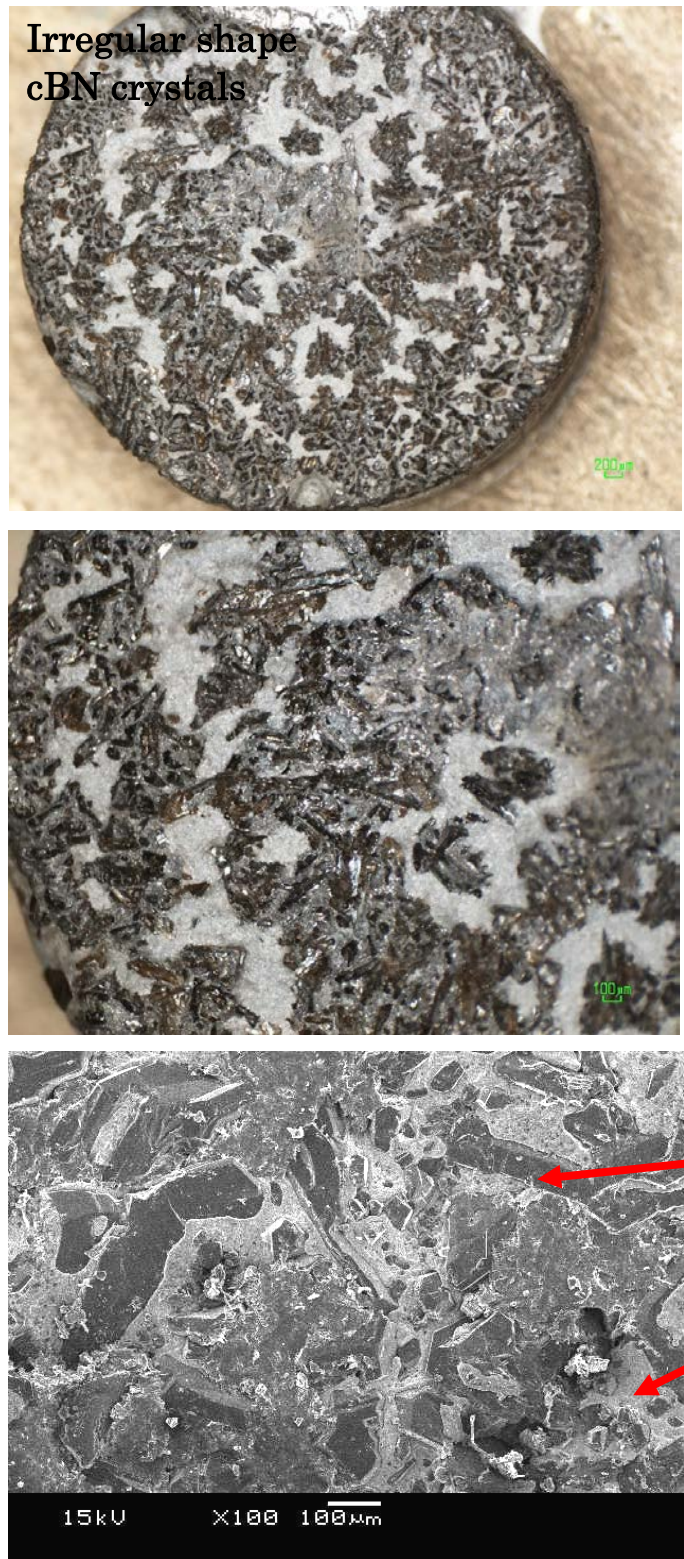
Fig.3.10. Optical photograph and SEM image of cBN synthesized using Fe52.5Ni5.8-Cr38.8-Al2.9 solvent at 5 GPa 1320 ℃ 1 h.

3.3.2 Pressure-temperature region and morphology of the grown cBN crystals using Co-(Cr, Mo)-Al solvents
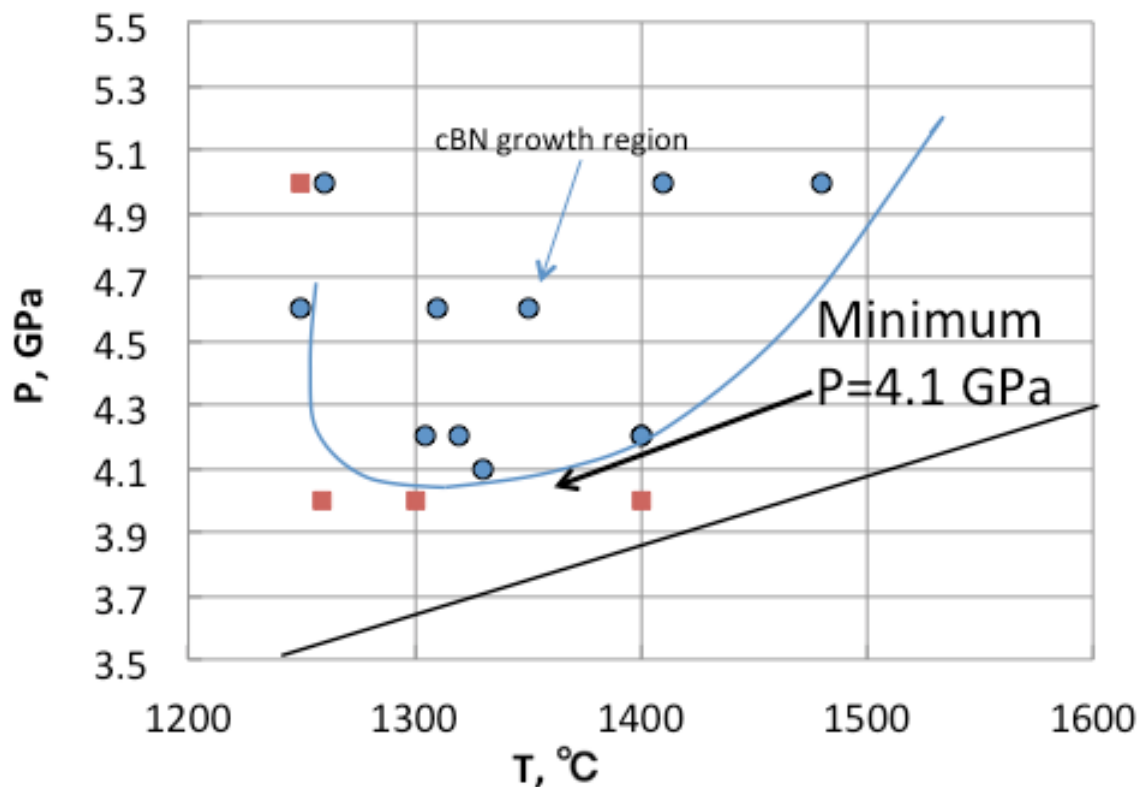

Fig. 3.11. P-T diagram of cBN formation in the solvent Co47-Cr30-Mo20-Al3 wt%

In this section we intend to examine the effect of Mo content to the morphology of cBN crystals using solvents Co-(Cr, Mo)-Al. As a first step, P-T diagram of cBN formation in the solvent Co47-(Cr30, Mo20)-Al3 wt% was determined and illustrated in Fig. 3.11. As shown in the figure, minimum pressure of cBN formation in the Co47-(Cr30, Mo20)-Al3 wt% solvent was about 4.1 GPa at 1300 °C. This result of the pressure limit of cBN formation was lower than that of Co67.6-Mo38.4-Al4 solvent reported previously [1]. The minimum pressure of cBN formation was about 4.6 GPa at 1300°C for Co-Mo-Al solvent. Addition of Cr into the Co-Mo-Al solvent system increased nitrogen solubility in the liquid alloy solvent and decreased minimum pressure of cBN formation. The P-T region of cBN growth shown in Fig. 3.11 was very similar to the results of (Fe52.5, Ni5.8)-Cr38.8-Al2.9 wt% solvent shown in Fig. 3.6.

Fig. 3.12. The morphology of cBN crystals reacted at 4.2-4.5 GPa and 1300-1400 °C 1 h. with various Mo content.

The morphology of cBN crystals reacted at 4.2-4.5 GPa and 1300-1400 °C are observed with the change of Mo content in the Co-(Cr, Mo)-Al solvent and showed in Fig. 3.12. When Mo content was increased to higher than about 65 wt%, cBN crystals showed two-dimensional plate-like morphology as shown Fig 3.12. (a), (b) and (c). The planar (111) face of cBN crystal was formed at the initial stage of the growth, but smooth layer growth was prevented by many random nucleation and growth of cBN crystals having about 100 µm size as shown in Fig. 3.12 (b). The SEM images taken from Fig. 3.12 (b) are shown in Fig. 3.13.
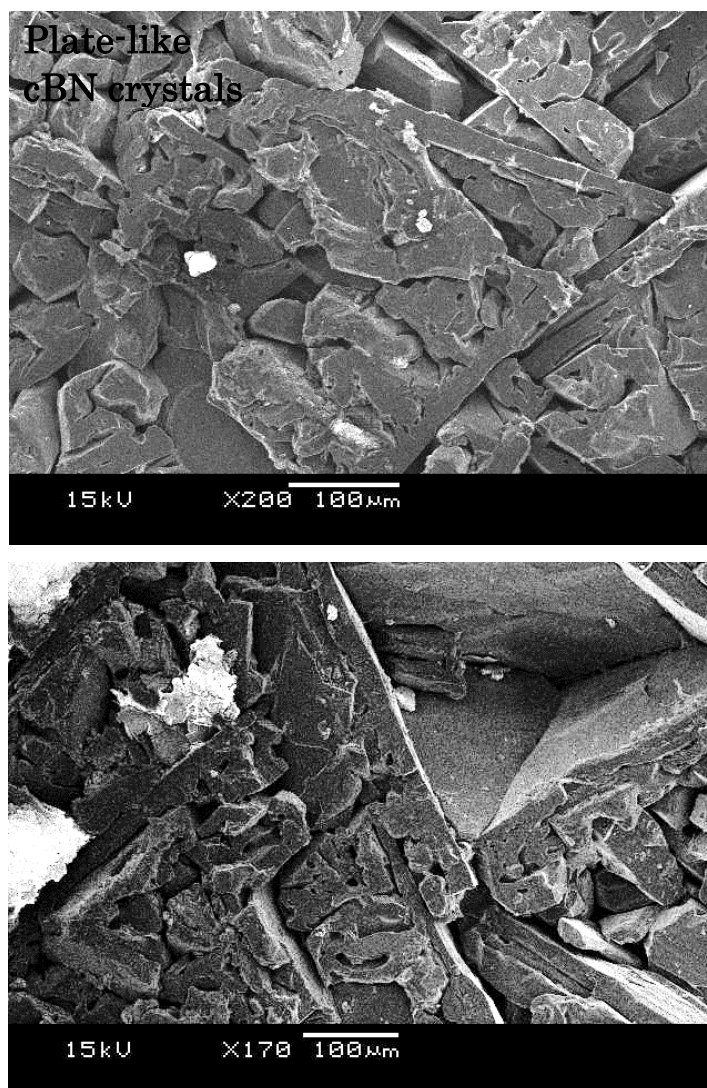

Fig. 3.13. SEM images of the cBN synthesized with Co48.65Cr16.2Mo32.43 Al2.7 at 4.5 GPa 1400 °C 1 h. Mo/(Mo+Cr)=66.7wt%

46

When the Mo content C, (C=Mo/(Mo+Cr) wt%) was decreased to about 30-40 wt%, morphology of cBN crystal was changed to more three-dimensional growth pattern. As shown in Fig. 3.14, the Mo content C=40 wt%, population of facetted cBN crystals were increased. These facetted crystals were precipitated at moderate migration speed of liquid solvent. cBN crystals of about 150 µm in size was confirmed from this synthesis condition. The selection of appropriate amount of Mo addition controlled migration speed of liquid solvent and hence the amount of facetted cBN crystals was increased.
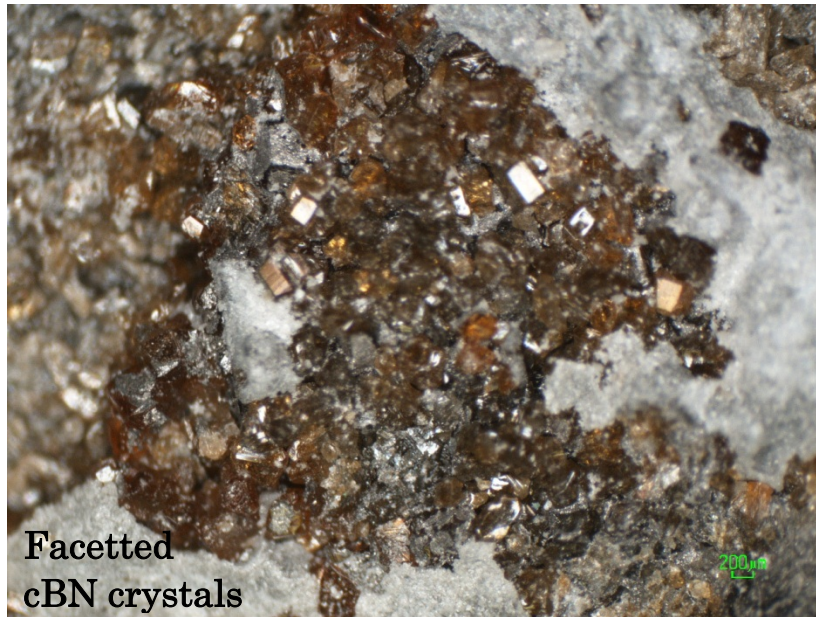
Fig. 3.14. cBN crystals synthesized with Co47Cr30Mo20Al3 at 4.6 GPa 1300 ° C 0.5 h. Mo content, Mo/(Mo+Cr)=40 wt%.

3.3.3 The effect of solvent composition to the cBN morphology in the Co-(Cr, V)-Al solvent.

In this section we present brief example of another compositional effect of solvent to the morphology of cBN crystals. In Fig. 3.15, we showed SEM image of cBN sample reacted at 4.2 GPa and 1330 ℃ for 1 h. using Co64-(Cr20, V13)-Al3 wt % solvent. As seen here, the change of Mo addition with V in the molten solvent drastically decreased grain size of cBN. The shape of the cBN crystals was very rough and non-faceted morphology and the crystal size was about 20-30 μm.
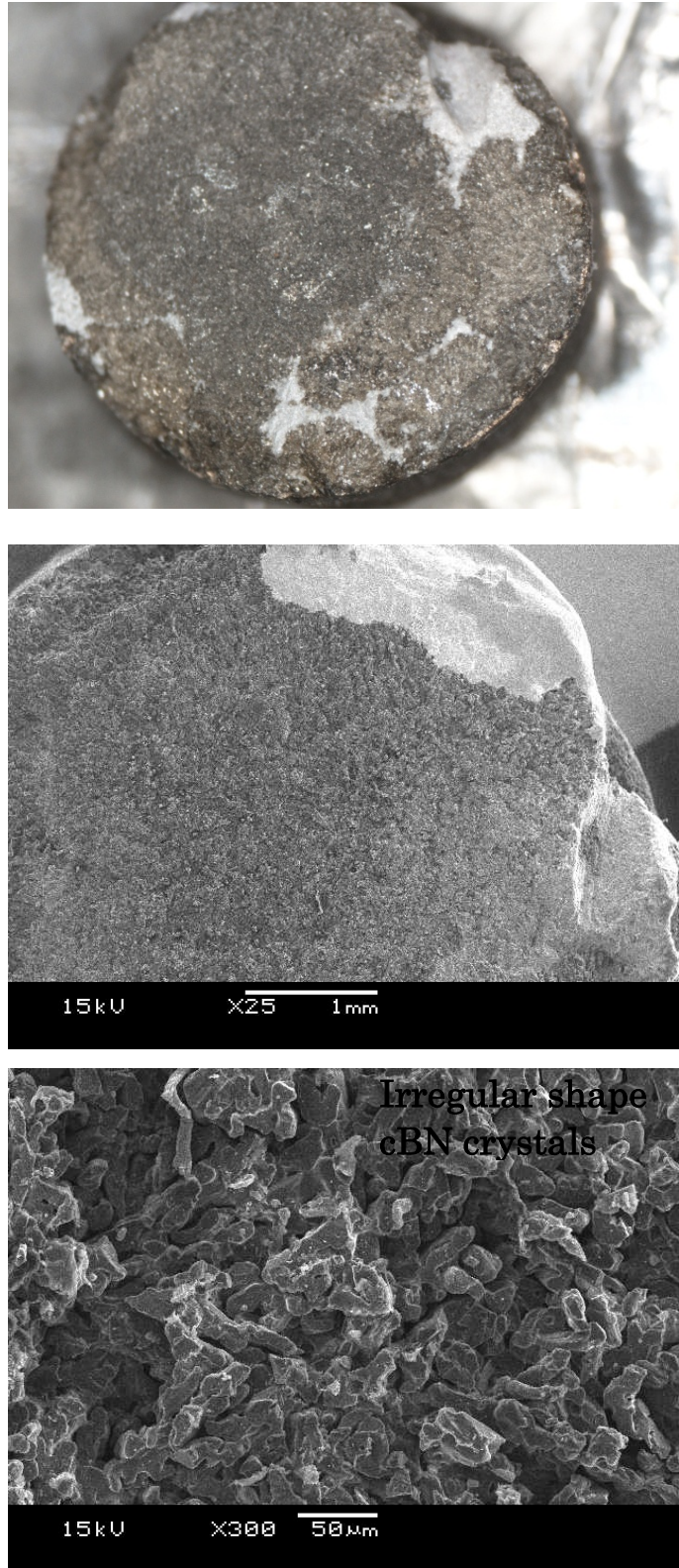
Fig. 3.15. Optical photograph and SEM images of cBN synthesized using Co64-Cr20-V13-Al3 at 4.2GPa 1330 ℃ 1 h. Cr/(Cr+V)=60.6wt%

To reconfirm such V effect on the cBN morphology and grain size, we took off V from the alloy solvent and check the morphology of cBN crystal under Co-Cr-Al solvent system when it was synthesized under similar synthesis condition. Fig. 13.16 showed the SEM images of the cBN crystal synthesized with Co58.2-CR38.8-Al3 wt% solvent at 4.2 GPa and 1370 ℃ for 1 hour. As seen here, relatively large cBN yield was obtained. The crystal shapes showed regular (111) morphology.

Fig. 3.16. SEM images of the cBN crystal synthesized with Co58.2-Cr38.8-Al3 wt% solvent at 4.2 GPa and 1370 ℃ for 1 hour.

Comparing the morphology and the grain size of the cBN crystal synthesized with Co-Cr-V-Al system in Fig. 3.15 and the one synthesized with Co-Cr-Al system in Fig. 3.16, it was suggested high density of cBN nucleation by rapid migration of liquid solvent occurred under the alloy solvent containing vanadium.

3.3.4 Nucleation behavior of cBN in the (Fe, Co, Ni)-(Cr, Mo)-Al alloy solvents
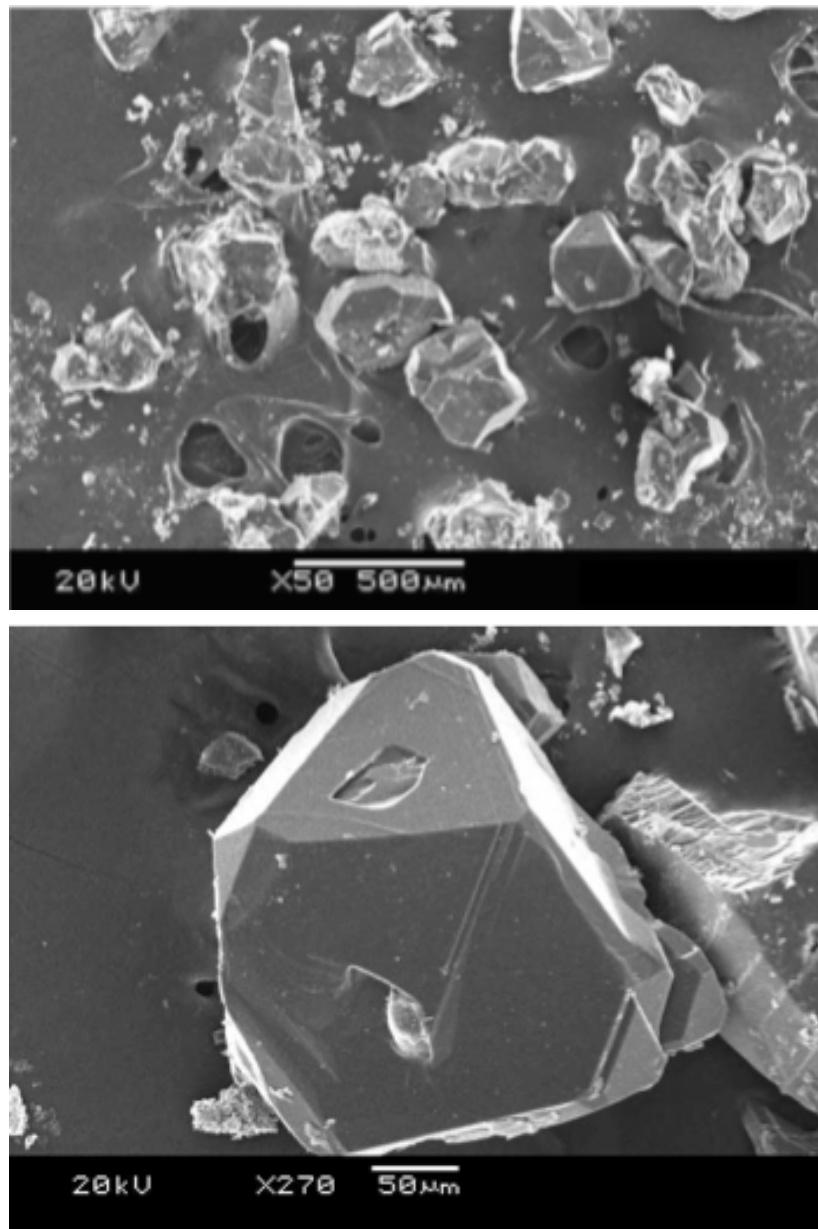
DeVries and Fleischer [8] reported phase relation in the system Li_3BN_2 solvent and BN. They showed that the growth region of cBN at constant pressure was between eutectic temperature and the maximum at boundary temperature of hBN/cBN. Present P-T diagrams of cBN growth shown in Fig. 3.6 and 3.11 were bounded by minimum formation temperature at about 1250 ˚C and the maximum temperature determined by the reaction pressure. These behaviors were coincided with the scheme of cBN formation by DeVries and Fleischer [8].

Diamond formation from carbon and solvent metal system showed similar behavior under certain temperature region at constant pressure [9]. Strong and Hanneman examined unseeded diamond growth in Ni-graphite at the temperature of 1455 ˚C by changing the pressure from 5.4 to 5.67 GPa and showed that the number of spontaneously nucleated diamond crystals increased rapidly with the increasing pressure. The nucleation of diamond crystals was very sensitive against the excess pressure above equilibrium line between graphite and diamond.

As we showed in (Fe52.5, Ni5.8)-Cr38.8-Al2.9 wt% solvent system, the spontaneously nucleated 100-150 µm size agglomerate cBN crystals were grown between 4.4-5 GPa at 1320-1465 ˚C. The feature of cBN agglomerate crystals were very similar to the diamond crystals obtained at 5.67 GPa and 1455˚C [8].

The nucleation of diamond was also changed with change of the temperature at any constant pressure. At lower temperature near to the Ni-C eutectic, the solubility difference between graphite and diamond was high and it decreased to zero at equilibrium of graphite/diamond. The spontaneous nucleation of diamond was maximum at the lowest temperature and number of euhedral crystals was increased with increasing temperature.

The series of solvent system from Co-Mo-Al to Co-(Cr, Mo)-Al and Co-(Cr, V)-Al

were reflected continuously increasing of nitrogen solubility in the alloys. The solubility of nitrogen into the Co-Mo-Al alloy was the smallest and it increase with increase of Cr content in Co-(Cr, Mo)-Al system and further increase of nitrogen solubility in the Co-(Cr, V)-Al was realized with increase the content of vanadium. The grain size of cBN was decreased with increasing nitrogen solubility of the alloy system and small agglomerate crystals were appeared in the Co-(Cr, V)-Al system.

While the composition change of Fe, Ni, Co element in the (Fe, Ni, Co)-(Mo, Cr, V)-Al solvent system also affected the nitrogen solubility change in the system, it was thought that the increase of nitrogen solubility in the (Fe, Ni, Co)-(Mo, Cr, V)-Al solvent system was mainly came from the composition change of Mo, Cr, V element. As shown in Fig. 3.17, Abdulrahman et al. [10] studied the change of the nitrogen solubility in the Ni-Co, Ni-Cr and Ni-18.09%Cr-Co system and found that nitrogen solubility in the liquid Ni was drastically increase by the addition of Cr element and almost unchanged by the addition of Co. They also showed that the addition of Co element into the Ni-18.09%Cr slightly changed the nitrogen solubility in the system.
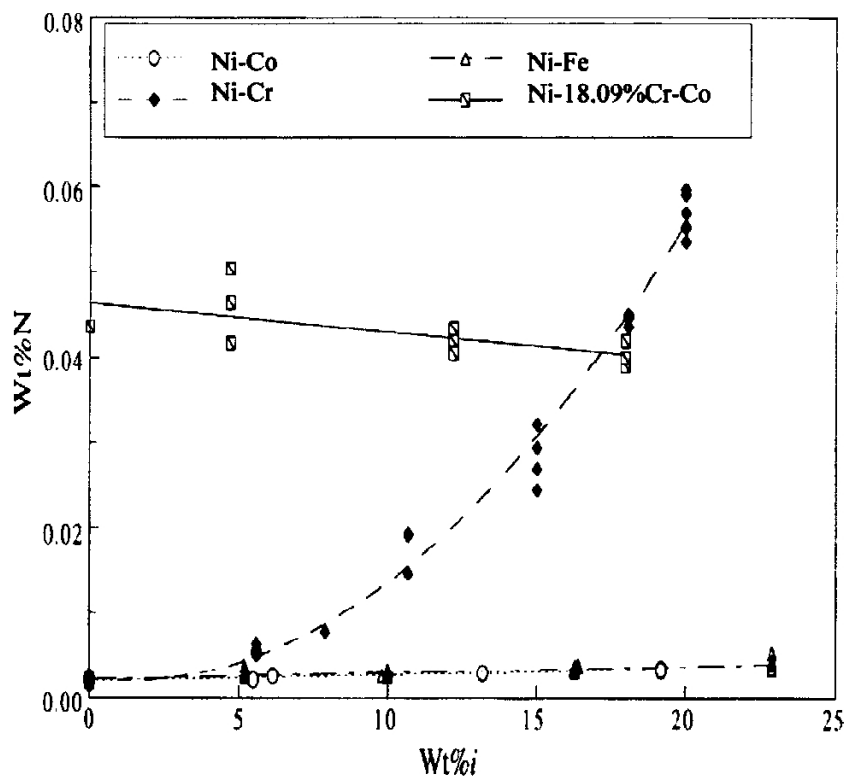

Fig. 3.17. Effect of alloying elements on the equilibrium solubility of nitrogen in nickel.

3.4. Conclusions

  In the present study, we confirmed that minimum pressures of cBN formation in both (Fe, Ni)-Cr-Al and Co-(Cr, Mo)-Al solvents were about 4.1 GPa. The minimum pressure of cBN formation was almost similar to that in the traditional alkali or alkali-earth B-N solvents [6]. The application of the alloy solvents with various combination of alloy composition could open the new field in cBN synthesis technology. The variation of alloy composition provides various morphology and grain size of cBN crystals. Boron and nitrogen solubility can be changed continuously by the variation of (Fe, Co, Ni)-(Cr, Mo)-Al system. Accordingly, we can control crystal growth parameters such as solubility, diffusion constant of B and N in the alloy. We present the results of the variety of cBN morphology employed the (Fe, Ni, Co)-(Cr, Mo)-Al solvent. The results indicated possible application of metallic solvent in the production of cBN abrasive grains. The morphology of cBN crystals is important information to the practice of cBN abrasives. The crystal size and morphology of the cBN were different due to P-T condition and content of the solvents employed in the experiment.

References

[1] O. Fukunaga, S. Takeuchi, T. Taniguchi, Diamond Relat. Mater., 20 (2011)752.

[2] R. D. Pehlke and J. F. Elliot, Trans Met. Soc. AIME 218(1960) 1088.

[3] C. Kowanda and M. O. Speidel, Scripta Materialia 48(2003) 1073.

[4] R. G. Blossey and R. D. Pehlke, Trans Met. Soc. AIME 236 (1966) 28.

[5] R. C. DeVries and J. F. Fleischer, US Patent 3,918,931 (Nov. 11, 1975)

[6] O. Fukunaga, S. Nakano and T. Taniguchi, Diamond Relat. Mater., 13 (2004)1709.

[7] O. Fukunaga, Y. S. Ko, M. Konoue, N. Ohashi, and T. Tsurumi, Diamond Relat. Mater., 8 (1999) 2036.

[8] R. C. DeVries and J. F. Fleischer, J. Cryst. Growth., 13/14(1972) 88.

[9] H. M. Strong and R. E. Hanneman, J. Chem. Phys., 46 (1967) 3668.

[10] R. F. Abdulrahman and A. Hendry, Met. Mat. Trans. B 32B (2001) 1103.

Chapter 4 Synthesis and grain size control of cubic BN using Co-V-Al and Co-Cr-V-Al base alloy solvents

4.1. Introduction

As described in the previous chapter, the addition of Mo in the Ni and Co solvent improves the extremely low solubility of nitrogen in molten Ni or Co. Moreover, the addition of Cr to Ni solvent, which can better enhance the nitrogen solubility in molten Ni than Mo, resulted in further increasing the crystal size [1]. The same as Mo, vanadium was also reported by Wada et al. to be effective in increasing the solubility of the nitrogen in the Fe-V and Fe-Cr-Ni-V system [2].

In this study, Co-Cr-Al base solvent and we exchanged Cr with Mo or V in the solvent to control the grain size of cBN crystals was employed. The effect of V addition into the Co-Al and Co-Cr-Al in comparison with Co-Cr-Mo-Al metal solvent during cBN synthetic process was studied. The P-T region of the cBN growth was determined by both Co-(Cr, Mo)-Al and Co-(Cr, V)-Al alloys as the synthetic solvent. It showed that Mo addition into the Co-Cr-Al alloys promote the grain growth of cBN crystals and obtained more than 400 μm size cBN crystals. On the other hand V addition into the Co-Cr-Al system grain size of cBN was decreased to about 20 μm. The ratio of Cr and V under Co-Cr-V-Al solvent system was also changed to compare the cBN growth rate and its morphology between Co-V-Al and Co-Cr-Al solvents system.

4.2. Experimental methods

Co, Cr, V, Mo, Al metal powders (Rare Metallic, 99.9%) as the solvents was used. The solvents were pre-mixed before pressed to form the green compact. The hexagonal BN source was hot-pressed hBN disk from Denka Co. (type N1, Purity: $\geqq$99%).

High pressure and high temperature (HPHT) experiments were carried out by using a modified belt-type HP apparatus at pressures between 4 to 6 GPa and temperatures between 1200 to 1700 °C for 60 min with a conventional quenching method. [3].

Figure 4.1 shows the sample assembly used in this study. The pre-mix metal solvent green compact was placed between the hBN disks (7 mm of diameter and 3 mm of the thickness) in the inner NaCl sleeve. Laminated hBN/alloy solvent/hBN samples were covered with 0.05 mm Ta foil. The HPHT runs were conducted with pressure increases at room temperature and then temperature increases. At about 750 °C, temperature was kept for 10 min. to homogenized Al melt and Co, Cr, Mo, V powders. After keeping for 1 hour at designed temperature, current supply to the heater was quickly decreased and then press load was decreased slowly.

hBN disk
Metal solvent powders
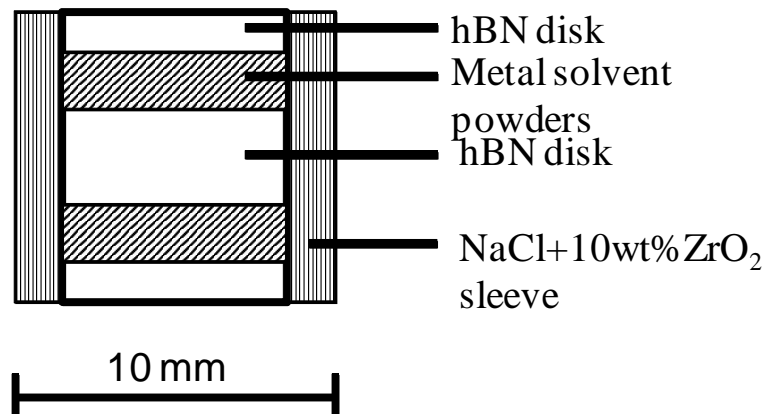hBN disk
NaCl+10wt%ZrO$_2$ sleeve

10 mm

Fig.4. 1. Sample assembly for high HPHT synthesis of cBN using metal catalyst.

The treated samples were recovered by removing the Ta capsule with a grinding wheel. To get the cross section, the recovered samples were then encapsulated in a hot mounting press before lapped with a diamond disc on the horizontal lapping machine. The samples were examined using the X-ray powder diffraction method (XRD) to confirm the cBN transformation, a scanning electron microscope (SEM) for cBN grain size/morphology observation and an EBSD to reconfirm the cBN grain size measurement.

Co - V - Al
Al/(Co+V+Al) (g/g) = 0.1, 1 atm

FactSage™

LIQUID

LIQUID + AlCo(s)

LIQUID + BCC_A2

BCC_A2

FCC_A1 + AlCo(s)

BCC_A2 + AlCo(s)

ALTA_SIGMA + AlCo(s)

BCC_A2 + AlCo(s) + CoV$_3$(s)

HCP_A3 + AlCo(s)
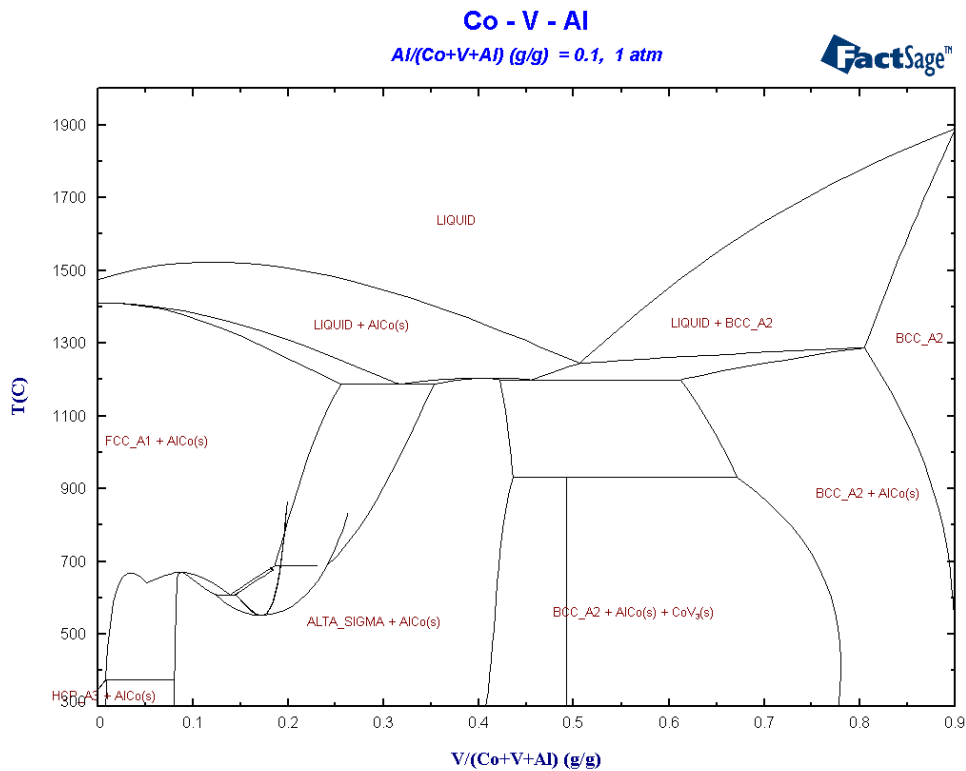
T(C)

V/(Co+V+Al) (g/g)

Fig. 4.2. Calculated equilibrium diagram of the Co-V-Al10 wt% pseudobinary system at 1 atm.

54

In these experiments, the cBN growth P-T region was checked using Co65-V25-Al10 wt% solvent and Co47-(Cr30, Mo20)-Al3 wt% solvent mainly. As a reference, the liquidus temperature of the Co65-V25-Al10 alloy system at the ambient pressure was calculated using the FactSage thermochemical software and databases. The results were shown in Fig. 4.2. The liquidus temperature of the of the Co65-V25-Al10 alloy system is about 1250 °C at ambient pressure.

The cBN yield was determined from the the hBN (002) and cBN (111) peak ratio of the XRD. The relation between the hBN/cBN peak ratio and the cBN yield was obtained by performed a calibration measurement using the mixed powder of hBN and cBN in some different ratios.

4.3. Result and Discussions

4.3.1 Pressure and temperature region of cBN growth using Co-Cr-Al base alloy systems
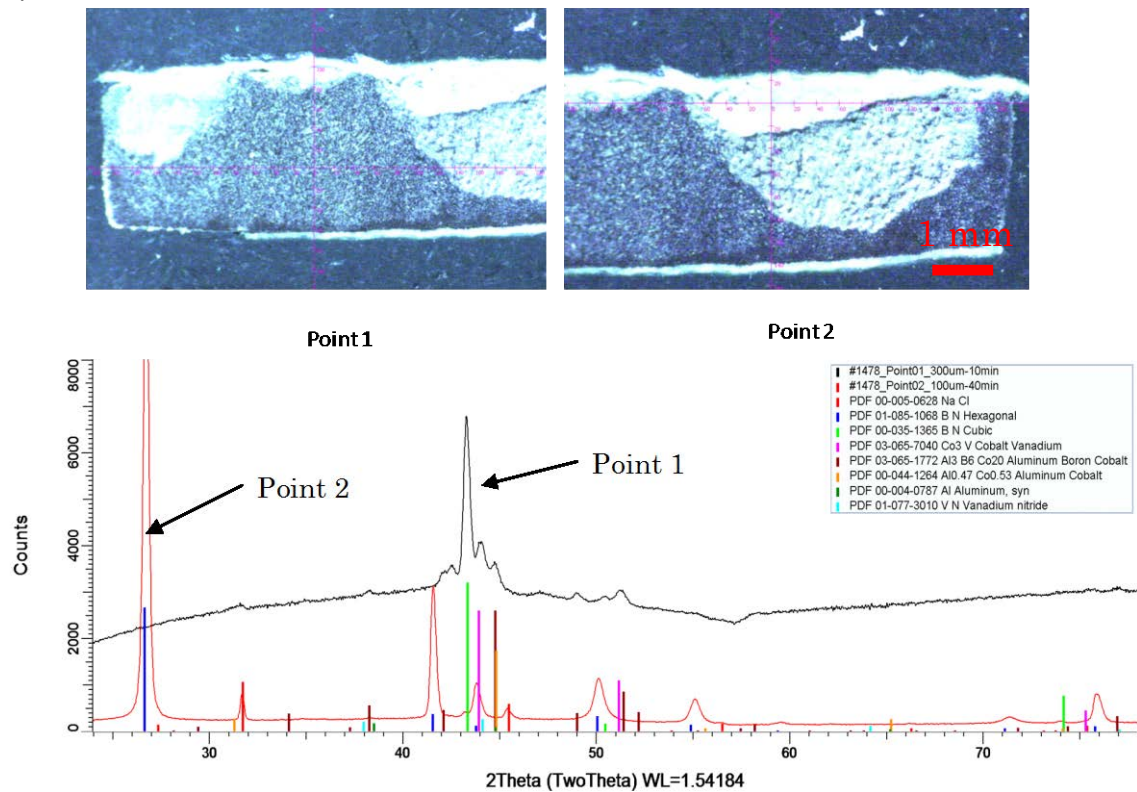

Fig. 4.3. XRD measurement result from the sample synthesized at 4.6 GPa, 1330 °C

To clear up the cBN grain growth process in the molten alloy solvents, it is important to check the P-T region of cBN growth using various Mo or V content in the

Co-Cr-Al base alloy. As described later in Fig. 4.5, which showed an example of cBN grain growth, the grain size of cBN crystals were different by any different P-T conditions. Normal trend of the cBN grain size was decrease with the increase of the reacted pressure because higher pressure tended to promote nucleation density of cBN. Thus effect of cBN grain size by introducing additional elements to the base alloy must be evaluated under similar P-T conditions.

An example of the raw result of the XRD measurement of the sample obtained at 4.6 GPa and 1330 °C is shown in figure 2. The XRD measurement was performed on 2 different points thought to be an area where cBN is completely synthesized (point 1 in Fig. 4.3) and an area where the cBN source is still remains (point 2 in Fig. 4.3). From this figure it was clearly confirmed the cBN peak in the measurement at point 1 and an hBN peak from the measurement result at point 2 in Fig. 4.3.
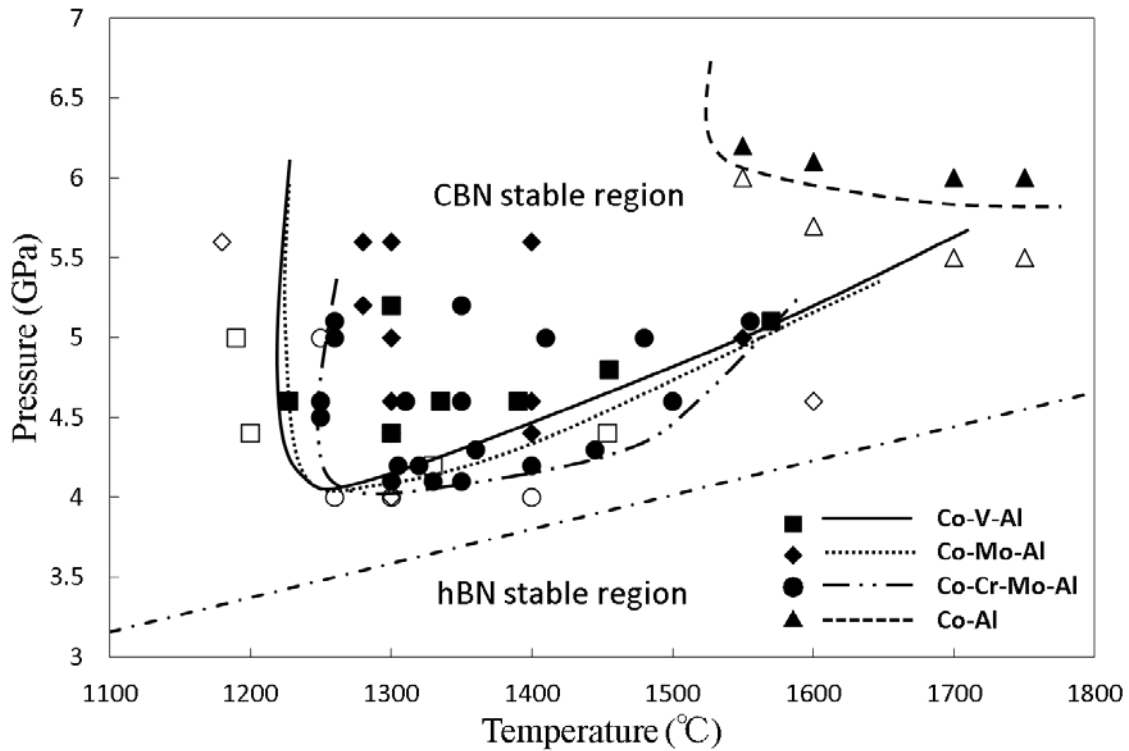
Fig. 4.4. P–T region of cBN formation with Co65V25Al10 and Co47Cr30Mo20Al3 wt% alloy solvent. The square marks are the results of Co-V-Al solvent system and circle marks are from Co-Cr-Mo-Al solvent system. The closed marks denote cBN results and the open ones denote no cBN results. The diamond marks represent the region of cBN formation in the Co-Mo-Al system [4] while the triangles are the cBN formation region under Co-Al solvent [4]. The dot-dashed line denotes the equilibrium line determined by alkali and alkali-earth nitride solvents [5].

The P–T region of cBN formation in the Co-V-Al (C065-V25-Al10 wt%) solvent is shown in Fig. 4.4 with the solid line as an estimated minimum pressure and temperature conditions and the squares in the figure indicate the various experimental conditions as listed in the Table 1.

Table 1. Various P-T conditions performed for determining the cBN growth region under Co65V25Al10 metal solvent.

Sample No:	Solvent (wt%)	Pressure (GPa)	Temp. (°C)	Holding Time (min)	Result (Vol%)
1	Co65V25Al10	4.6	1400	60	60%cBN
2	Co65V25Al10	4.8	1450	60	80%cBN
3	Co65V25Al10	4.6	1330	60	60%cBN
4	Co65V25Al10	4.4	1290	60	60%cBN
5	Co65V25Al10	4.6	1230	60	50%cBN
6	Co65V25Al10	5.1	1560	60	80%cBN
7	Co65V25Al10	4.4	1450	60	100%hBN
8	Co65V25Al10	5.2	1300	60	100%cBN
9	Co65V25Al10	4.2	1330	60	100%hBN
10	Co65V25Al10	4.4	1200	60	100%hBN
11	Co65V25Al10	5.0	1200	60	100%hBN

The reaction time of each experiment was 1 hour. In these figures, we denoted P–T points of cBN obtained by solid marks while the open marks denoted no cBN results. To be noted here, that the solid squares marks denoted cBN formation in the figure contained some amount of the residual hBN starting material. The yield of the cBN at each condition will be discussed later. Along with the P-T region of the cBN formation under Co-V-Al, we also plotted the P-T region of cBN formation under Co-Mo-Al (Co58-Mo38-Al4 wt%) and Co-(Cr, Mo)-Al (Co47-Cr30-Mo20-Al3 wt%) as comparison.

The double-dot-dashed line in Fig. 4.4 is an estimated minimum pressure and temperature conditions of cBN formation in the Co-(Cr, Mo)-Al (Co47-Cr30-Mo20-Al3 wt%) solvent system while the circle marks indicate its various experimental conditions.

The dotted line along with the diamond marks indicate the cBN-formation region in the Co-Mo-Al system obtained from a previous experiment while the dashed line along with the triangles indicate the cBN-formation region in the Co-Al system obtained from a previous report [4]. A line representing phase equilibrium between cBN and hBN [5] is also shown in Fig. 4.4 with dot-dashed lines.

Comparing the P–T region of cBN formation using Co-V-Al solvent system with the minimum pressure and temperature for cBN synthesis under Co-Al solvent system which is about 6 GPa and 1550 °C [4], the results from Fig. 3 suggested that adding vanadium to the Co-Al solvent system could decrease the pressure and temperature region of cBN synthesis for about 1.8 GPa, the same as molybdenum did in the Co-Al solvent system [4].

We checked the P-T region of cBN formation using wide range of the composition of Co-(Cr, Mo)-Al and Co-(Cr, V)-Al alloy solvent and concluded that P-T region of cBN growth were almost similar within Co-(Cr, V, Mo)-Al systems.

The addition of V into Co-Al solvent system increased the solubility of the nitrogen in the molten solvent [2], hence enhancing the hBN-cBN phase transformation.

4.3.2 Texture of the composite containing cBN crystal and alloy solvent matrix

Fig. 4.5 (a) showed the optical photographs of the cross-section from the recovered sample synthesized with Co65V25Al10 alloy solvent at 4.6 GPa and 1400 °C. Fig. 4.5 (b) showed a close up SEM-BSE image of the cBN forming zone from the same sample. The XRD pattern of the cBN forming zone in Fig. 4.5 (b) mainly showed strong cBN (111) and (220) peaks and extra diffraction peaks due to alloy components. Weak hBN peak (002) was identified from this sample indicating that hBN was not completely transformed at this reacted pressure and temperature as confirmed from the optical photographs of the cross-section.

The residual of the hBN source was also confirmed at the opposite side of the metal source indicating that the cBN transformation was not complete at this P-T condition. The cBN growth was relatively homogenous with an average grain size about 18 µm as it was measured from SEM observation.
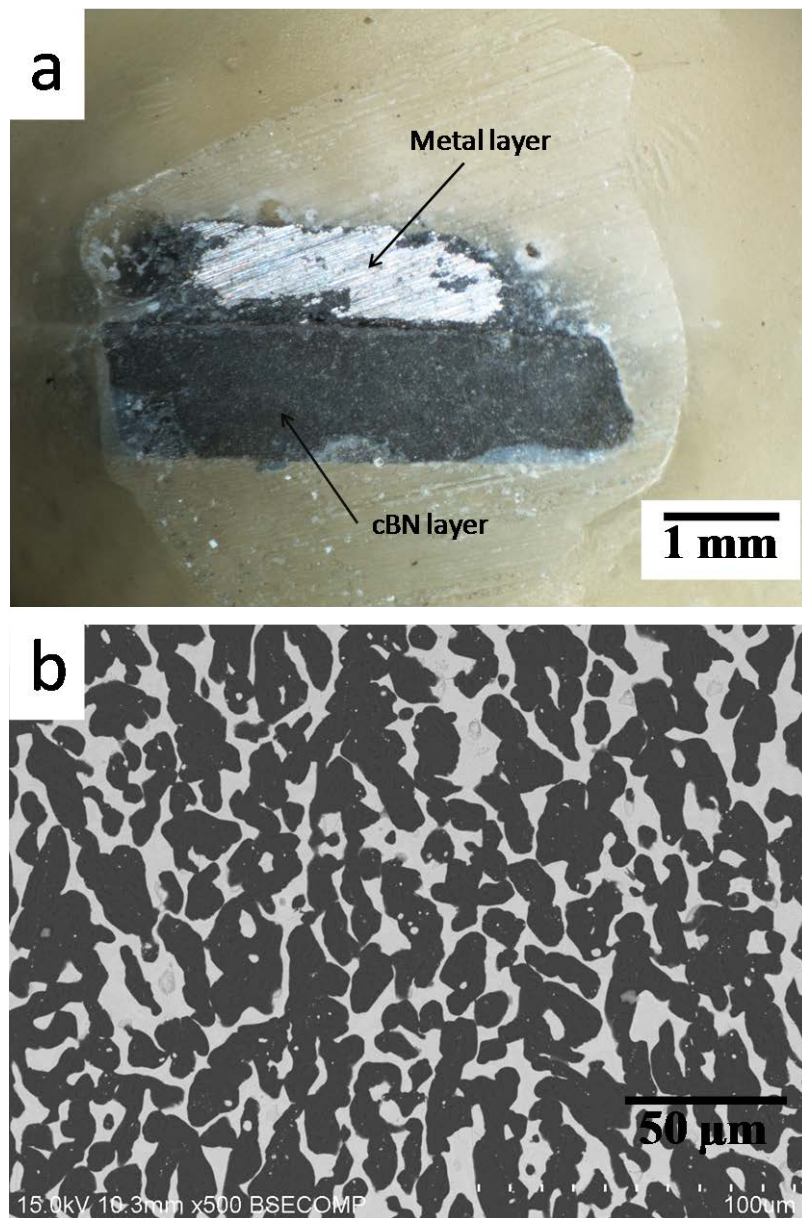
Fig. 4.5. (a) Optical photographs of the cross-section of the recovered sample synthesized with Co65-V25-Al10 solvent, and (b) a close up image of the cBN forming zone. Experimental conditions were 4.6 GPa and 1400 °C for 1 h.

The grain size measurement was also performed base on the IPF image of the EBSD as a comparison. Figure 4.6 showed the SEM-BSE image along with the cBN only IPF map (ND) of the same sample shown in Fig. 4.5. From this image, it can be seen that the cBN crystal formed a domain during the growth. When we colored one cBN crystal with one unique color (the color does not have any meaning) we can easily measure the average grain size the cBN crystal in the overall area.
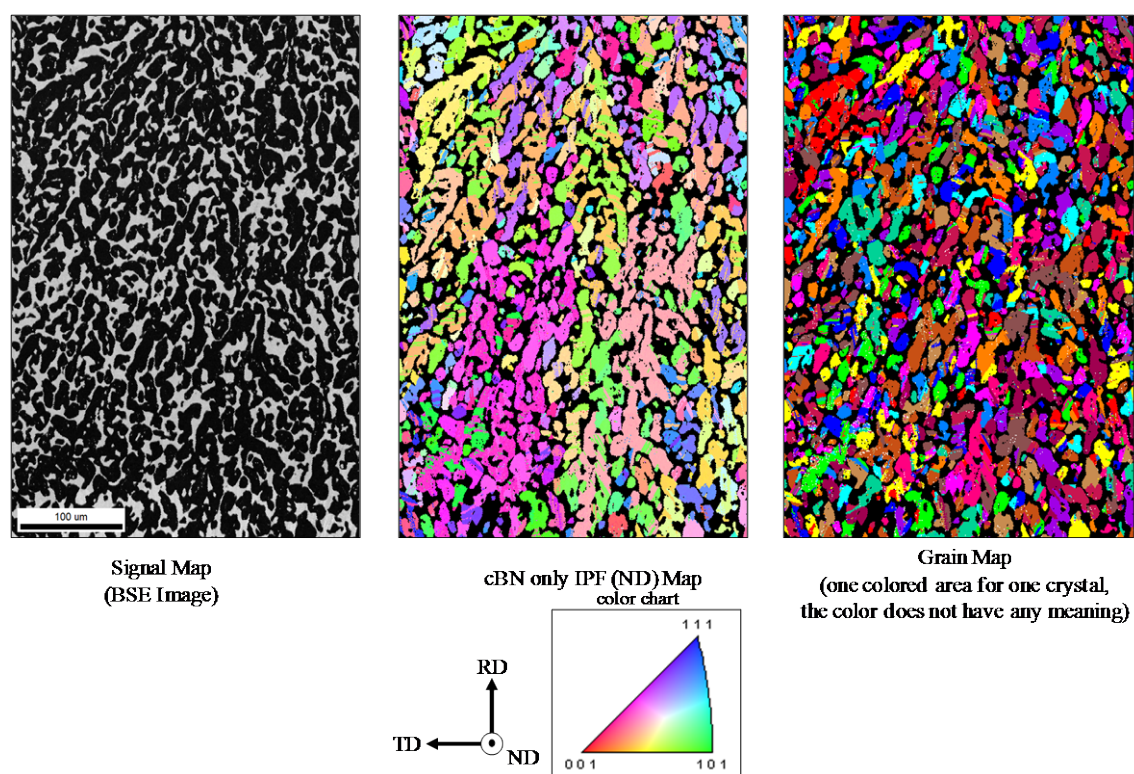
Fig. 4.6. EBSD analysis result of the cBN forming zone. Experimental conditions were 4.6 GPa and 1400 °C for 1 h.

From the image of Fig. 4.5 (b), we can postulate that the hBN-cBN transformation was occurred at the interface between the metal solvent and source hBN layer and with increasing reaction time, the characteristic texture of the cBN crystal (dark elongated area) and metal matrix (gray continuous zone) was formed as shown in Fig. 4.5 (b)

Figure 4.7 showed the SEM observation result from the polished cross-section of the recovered samples synthesized with two different P-T conditions. Fig. 4.7 (a) and (c) were observed just above the metal-hBN source interface while Fig. 4.7 (b) and (d) were observed at the opposite side. From the SEM-EDS and as it was confirmed by XRD, the dark irregularly shaped area in the figure is the cBN grains. The gray regions were solidified alloy solvent. As shown in the figures, the cBN crystals obtained are irregular in shape with the grain size less than 40 µm. The small irregular shape of the crystals may have been due to relatively slow grain growth as an effect of vanadium addition after a spontaneous nucleation of cBN in the molten solvent.
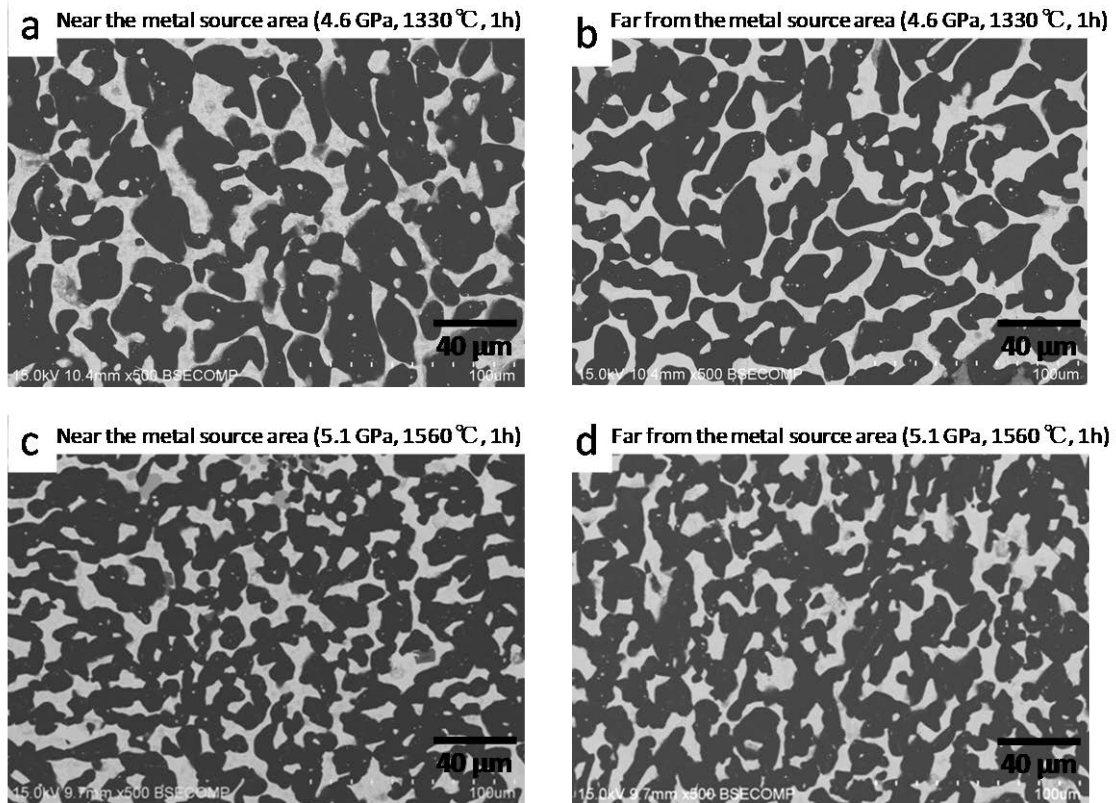
Fig. 4.7. SEM-BSE images of the cBN forming zone synthesized with Co65-V25-Al10 at 2 different P-T conditions observed near the metal-hBN source interface, and the far side of the metal source.

The grain size of cBN tended to increase at lower pressure and temperature because the rate of metal infiltration into the hBN source is depending on the P-T condition. Rate of migration of the molten alloy into the source hBN was decreased at lower temperature [4]. The comparison of the cBN grain size obtained at two different conditions could be observed from above Fig. 4.7. Figure 4.7 (a) and (b) which is synthesized at 4.6 GPa and 1330 °C have relatively coarser grain size comparing with the one from Fig. 4.7 (c) and (d) which is synthesized at 5.1 GPa and 1560 °C.

Using the same measurement method as mentioned above, the cBN grain size of the other samples synthesized with Co65V25Al10 alloy solvent was confirmed to be fine with 40 µm is the biggest average size depending on their P-T condition. The growth of cBN with such fine grain sizes under Co-V-Al system will be discussed later in the next chapter.

As the conversion from hBN to cBN was started at the interface between molten

solvent and hBN layer, the thickness of the precipitated cBN zone could be measured and the yield of cBN can be estimated as a relative thickness of cBN zone. The cBN yield was also estimated using the XRD intensity ratio of the reflection of cBN (111) to the reflection of hBN (002).

The yield of the cBN increased as the reacted pressure is getting higher. It is thought that lower cBN yield in relatively low reacted pressure is due to the smaller excess pressure (the reacted pressure minus equilibrium). This kind of phenomenon is similar with the result of the cBN synthesis using the other metal solvents such as Co-Mo-Al and Ni-Cr-Al that has been already reported [4, 6].

4.3.3 Effect of grain sizes of cBN crystal with addition of Mo or V

We showed optical micrographs of the surface aggregated by cBN crystals attached with solvent alloys in Fig. 4.8 (a) and (b). Photograph of Fig. 4.8 (a) shows the surface covered with fine cBN grains reacted at 4.2 GPa and 1300 °C for 1 hour using Co64-(Cr20, V13)-Al3 wt% solvent.

Fig. 4.8 (b) shows coarse cBN grains precipitated at 4.2 GPa and 1300 °C using Co49-(Cr19, Mo32)-Al 3 wt% solvent. These results clearly suggested that Mo addition into the Co-Cr-Al base alloy solvent was effective to increase the grain size of cBN crystals. When we change the content of Mo into the Co-Cr-Al alloy, largest grain size of cBN (~500 μm) can obtain around Mo =40-50 wt % in Cr + Mo weight.

The result of such high rate cBN grain growth under the Co-Cr-Mo-Al alloy system was similar with the one obtained by Co-Mo-Al solvent where the cBN grain size was observed around 0.3 mm [4]

These coarse cBN grain sizes obtained from Co-Cr-Mo-Al solvent confirmed that the absence of vanadium in metal solvent affected the cBN growth in the molten solvent.
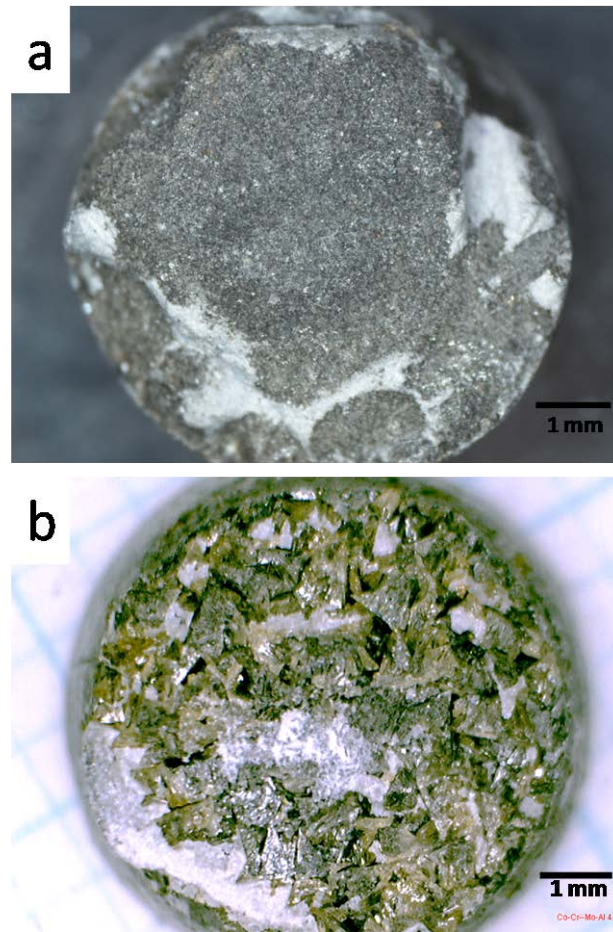
Fig. 4.8. Optical photographs of the recovered cBN crystals at the hBN source-metal solvent interface of the sample obtained after HP-HT treatment. (a) Sample with Co64-Cr20-V13-Al3 solvent, And (b) sample with Co49-Cr16-Mo32-Al3 solvent. Synthesis conditions were 4.2 GPa and 1300 °C for 1 h.

4.3.4 Grain size control in Co-(Cr, V)-Al alloy solvent system

We also studied the change of the cBN grain size synthesized under such metal solvent system where both chrome and vanadium exist. We examined precipitation of cBN at one fixed P-T conditions by the change of Cr and V content in the Co-(Cr, V)-Al solvent. We compared the growth rate of the cBN in Co-V-Al, Co-Cr-Al and Co-Cr-V-Al with various content ratio of Cr against (Cr + V). The compositions of the metal alloys were summarized in Table 2.

Table 2. Various Cr and V contents in the Co-(Cr-V)-Al solvent used to study the relation between Cr (V) content and the synthesized cBN grain size. (4.6 GPa and 1300 °C for 1 h.)

Co (wt%)	Cr (wt%)	V (wt%)	Al (wt%)
70	22	0	18
70	19	3	18
63	20	13	14
40	20	20	20
64	8	18	10
65	0	25	10

Figure 4.9 showed the trend of the cBN grain size versus content ratio of Cr against (Cr + V) in the metal solvent at the pressure and temperature conditions of 4.6 GPa and 1300 °C for 1 hour reaction time. Some examples of the cBN microstructures synthesized using some different chemical compositions of Cr and V were also shown in the graph. These SEM-BSE images were observed at the area near the metal-hBN source interface of each recovered sample.

The results in Fig. 4.9 showed that cBN grain size increased gradually until the content ratio of Cr against (Cr + V) in the Co-Cr-V-Al solvent reached for about 50 wt%. At these P-T conditions, the cBN grain size was about 12 µm under Co-V-Al system and increased to about 20 µm when the Cr content ratio reached about 50 wt%. The cBN grain size drastically became coarser when the metal solvent contains more Cr than V. The cBN grain size was about 60 µm when Cr content ratio reached 86 wt% and was about 100 µm when we completely substituted V with Cr.

These experiments results suggest that controlling the synthesized cBN grain size could be done by changing the chemical composition of the metal solvent. By changing the pressure and temperature region of the cBN synthesis, the ranges of the grain size

could be moved to the finer or coarser side as the cBN grain size was also depended on the P-T conditions itself.
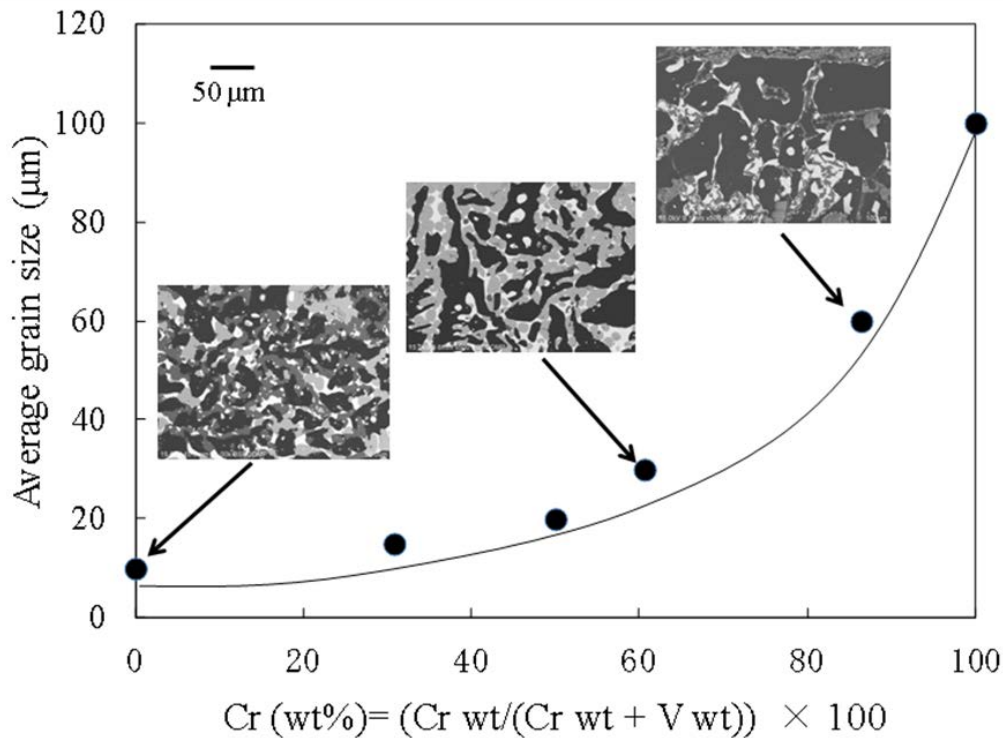

Fig. 4.9. Relation between cBN grain size and the Cr content ratio against (Cr + V) in Co-Cr-V-Al metal solvent system at 4.6 GPa and 1300 °C for 1-h reaction.

The introduction of vanadium is not only increasing the solubility of the nitrogen in the system but also work as a grain growth inhibitor. Although the detailed mechanism of the role of vanadium during the cBN growth is not known yet, adding some amount of Vanadium could be the way in controlling the cBN growth during cBN synthesis process.

Pehlke and Elliot [7] studied the effect of additional element to the nitrogen solubility in molten iron, and they showed that about 6% of addition of Mo, Cr and V increased nitrogen solubility to 0.06% for Mo, 0.08% for Cr and 0.17% for V. The increase of the nitrogen solubility by the vanadium addition was also confirmed in the Co alloy [8]. If V addition into Co-Cr-Al can increase nitrogen solubility remarkably, higher V content in the Co-Cr-Al alloy precipitated high density cBN nuclei in the system. If nitrogen solubility was decreased by the replacement of Cr with Mo, extraordinary large grain size of cBN grown in the Co-(Cr, Mo)-Al can be explained by same view point of nitrogen solubility.

4.4. Conclusions

In this chapter, we examined grain growth control in the Co-Cr-Al base alloy by exchanging Cr with Mo or V. First, we examined pressure temperature region of cBN growth in the wide range of Co-(Cr, Mo)-Al and Co-(Cr, V)-Al alloy solvent systems, and confirmed that the P-T region of cBN formation was not change remarkably by the change of Mo or V content in the metal solvent. Secondly, based on the data, we compared grain size of cBN crystal reacted at about 4.6 GPa and 1300 °C for 1h. We showed that exchange Mo to the Cr was very effective to obtain up to about 400-500 μm size cBN crystals. Thirdly, replace Cr with V resulting fine grain size cBN crystals to about 10 μm. Systematic change of grain size of cBN in Co-(Cr, V)-Al system was confirmed.

References

[1] Y. Kubota, K. Watanabe, O. Tsuda and T. Taniguchi, Chem. Mater. 20 (2008) 1661.

[2] H. Wada and R. D. Pehlke, Met. and Mat. Trans. B Vol. 12 (2) (1981) 333.

[3] O. Fukunaga, Y. S. Ko, M. Konoue, N. Ohashi and T. Tsurumi, Diamond Relat. Mater. 8 (1999) 2036.

[4] O. Fukunaga, S. Takeuchi and T. Taniguchi, Diamond Relat. Mater. 20 (2011) 752.

[5] F. P. Bundy, R. H. Wentorf Jr., J. Chem. Phys. 38 (1963) 1144.

[6] Y. Kubota and T. Taniguchi, Jpn. J. Appl. Phys. 48 (2009) 071004 1.

[7] R. D. Pehlke and J. F. Elliot, Trans. Met. Soc. AIME 218 (1960) 1088.

[8] R. G. Blossey and R. D. Pehlke, Trans Met. Soc. AIME 236 (1966) 28.

Chapter 5 The microstructure of cubic BN-metal composites synthesized from hexagonal BN with Co-V-Al and Co-Cr-Al metallic solvents

5.1. Introduction

The production of sintered compacts of high cBN content materials are normally performed using pre-mixed cBN and binder powder. Another process reported in the patents was infiltration process of molten metallic solvent into the BN layer to synthesized composites of cBN and metallic binders.

The previous reports on the sintering solvent of metal alloys including transition metals (Fe, Ni, Co, Mn) , nitrogen solvents (Mo, Cr, V) and Al suggested as a candidate to realize homogeneous cBN-metal composite for cutting tool applications [1-3]. However, few experimental studies on cBN-metal composite were available in the literatures. In the previous chapter, it was showed that the minimum pressure and temperature for the cBN growth in the molten metal solvents were greatly decreased by the addition of vanadium. The

In this study, cBN-metallic alloy composites was synthesized using hBN to cBN transformation and molten metal infiltration processes. At the P-T region where cubic is a stable phase of the BN and where the alloy is completely melted, molten alloy solvents penetrate into the hBN layer, starting the phase transition of the BN from hexagonal to cubic phase. The precipitated cBN grains are grown and coagulated to form cBN-metal composite.

As the metal solvent for cBN synthesis and the metal catalyst for cBN sintering are in general the same, it was suggested that metal alloy solvent or catalysts which are able to suppress the cBN grain growth during cBN synthesis, should also be useful in order to produce the cBN compact with a homogenous microstructure during the infiltration sintering method. Therefore it was deduced that adding an element that would act as a grain growth inhibitor into the already well studied metal solvent during the cBN synthesis process and observing the morphology of its cBN crystal, could be a starting point in investigating the metal catalyst for sintering cBN with infiltration method.

In the present report, the effect of vanadium addition into the Co-Al and Co-Cr-Al metal solvent during cBN synthetic process was studied. It was presumed that vanadium would act not only as a solvent of nitrogen atoms but would also act as a cBN grain growth inhibitor. Metal alloy solvents containing vanadium for cBN growth, could provide basic knowledge of cBN-metal polycrystalline systems to develop new polycrystalline cBN cutting tools.

5.2. Experimental methods

Co, Cr, V, Al metal powders (Rare Metallic, 99.9%) were used as the solvents. The solvent was prepared by mixing each metal powder, which were then pressed to form a green compact. The BN source used in this study was hot-pressed hBN disk (Denka, type N1).

The modified belt type high pressure apparatus [4] as described in chapter 2 was used for HPHT experiments.
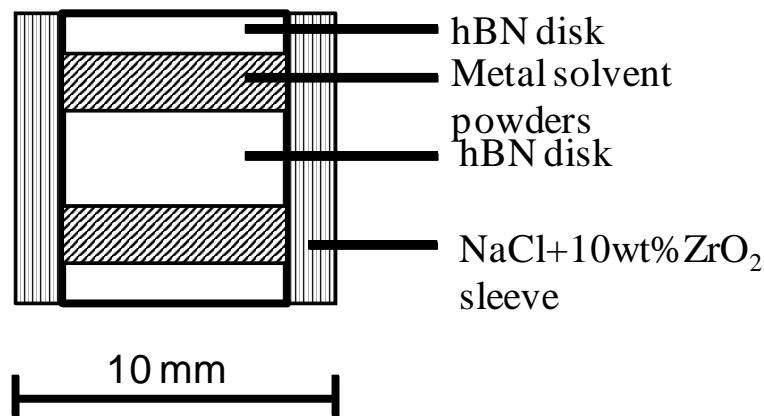

Fig. 5.1. Sample assembly for high pressure-high temperature (HPHT) synthesis of cBN using metal catalyst.

Figure 5.1 shows a sample assembly used in this study. The pre-mix metal solvent green compact was placed between the hBN disks (7 mm of diameter and 3 mm of the thickness) in the inner NaCl sleeve. Laminated hBN/alloy solvent/hBN samples were covered with 0.05 mm Ta foil. The HPHT runs were conducted with pressure increases at room temperature and then temperature increases. At about 750 °C, temperature was kept for 10 min. to homogenized Al melt and Co-Cr or Co-V powders. After keeping for 30 min. at designed temperature, current supply to the heater was quickly decreased and then press load was decreased slowly.

As already described in previous chapter, the minimum pressure and temperature (P-T) for cBN transformation in the system using Co-Cr-Al, Co-Cr-V-Al and Co-V-Al solvents were about 4.2-4.5 GPa and 1300-1400 °C [5]. P-T conditions with enough pressure and temperature to grow cBN was selected in the present study. The samples composition to study the effect of synthesis conditions and the effect of the amount of V in the metal solvent on the microstructure of the obtained cBN-metal composites was summarized in Table 1.

Table 1 cBN synthesis condition of each metal catalyst

Sample No.	Metal catalyst composition (Weight %)	Pressure (GPa)	Temperature (℃)	Holding time (min.)
1	Co80V10Al10	5.6	1700	30
2	Co80V10Al10	4.8	1720	30
3	Co84V6Al10	5.6	1700	30
4	Co70Cr22Al8	5.6	1720	30
5	Co70Cr22Al8	5.0	1700	30
6	Co70Cr19V3Al8	5.6	1720	30

The same with already described alloys solvent in previous chapters, the liquidus temperature of the Co70-V-Cr-Al8 alloy system at the ambient pressure was calculated using the FactSage thermochemical software and databases. The results were shown in Fig. 5.2. The liquidus temperature of the Co70-Cr22-Al8 alloy and Co70-Cr22-Al8 alloy system are about 1370 °C at ambient pressure.
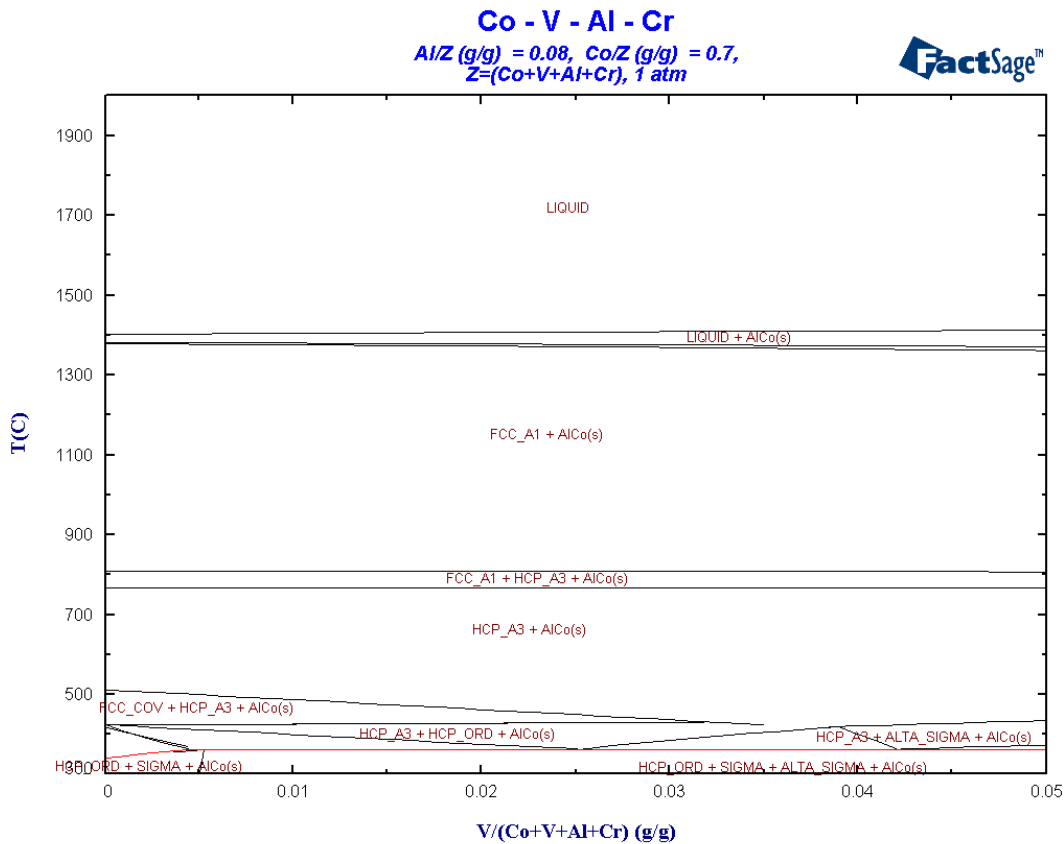

Fig. 5.2. Calculated equilibrium diagram of the Co70-Cr-V-Al8 wt% pseudobinary system at 1 atm.

The treated samples were recovered by removing the Ta capsule with a grinding wheel. To get the cross section, the recovered samples were then encapsulated in a hot mounting press before lapped with a diamond disc on the horizontal lapping machine. The samples were examined using the X-ray powder diffraction method (XRD) to confirm the cBN transformation, a scanning electron microscope (SEM) for cBN grain size/morphology observation and an Electron Probe Micro Analyzer (EPMA) for analyzing the infiltration and the distribution of the metal solvent in the BN layer.

5.3. Result and Discussions

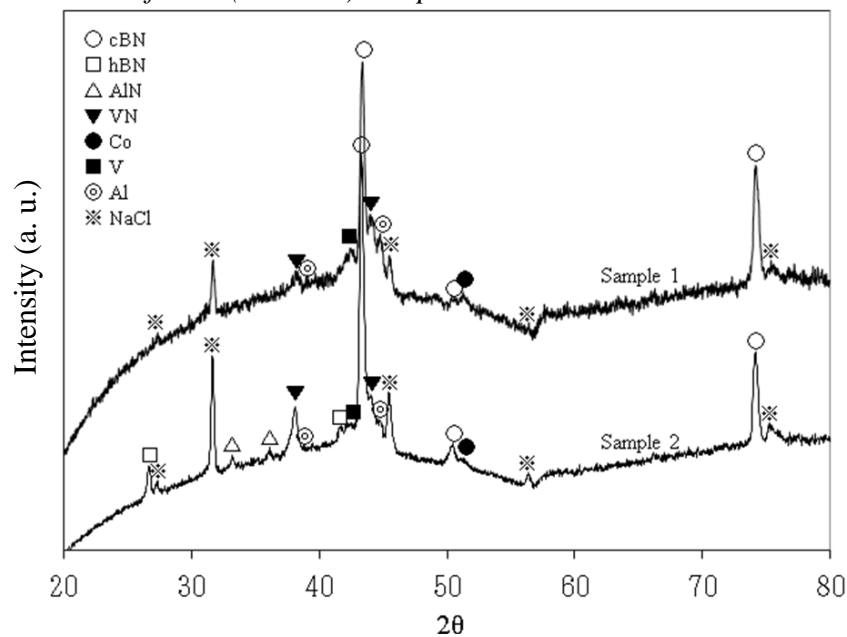### 5.3.1 Microstructure of cBN-(Co-V-Al) composites

Fig. 5.3. XRD pattern of sample 1 (upper line) and sample 2 (lower line) cross section after lapping.

The XRD pattern of sample 1 and 2 are shown in Fig. 5.3. The pattern mainly showed strong cBN (111) and (220) peaks, NaCl (200) peak and extra diffraction peaks due to alloy components. No residual hBN peaks were identified from sample 1. The peak of NaCl from the above result indicates that the metal capsule which covered the cBN and metal solvent collapsed during HPHT process causing the NaCl infiltration into the sample. The presence of NaCl was also observed by SEM image. An example of the SEM image and the SEM-EDS result that confirmed the presence of NaCl inside the composites was shown in Fig. 5.4. From the above result it is confirmed that complete hBN-cBN transformation occurred under the Co-V-Al solvent system at 5.6 GPa and 1700 °C.
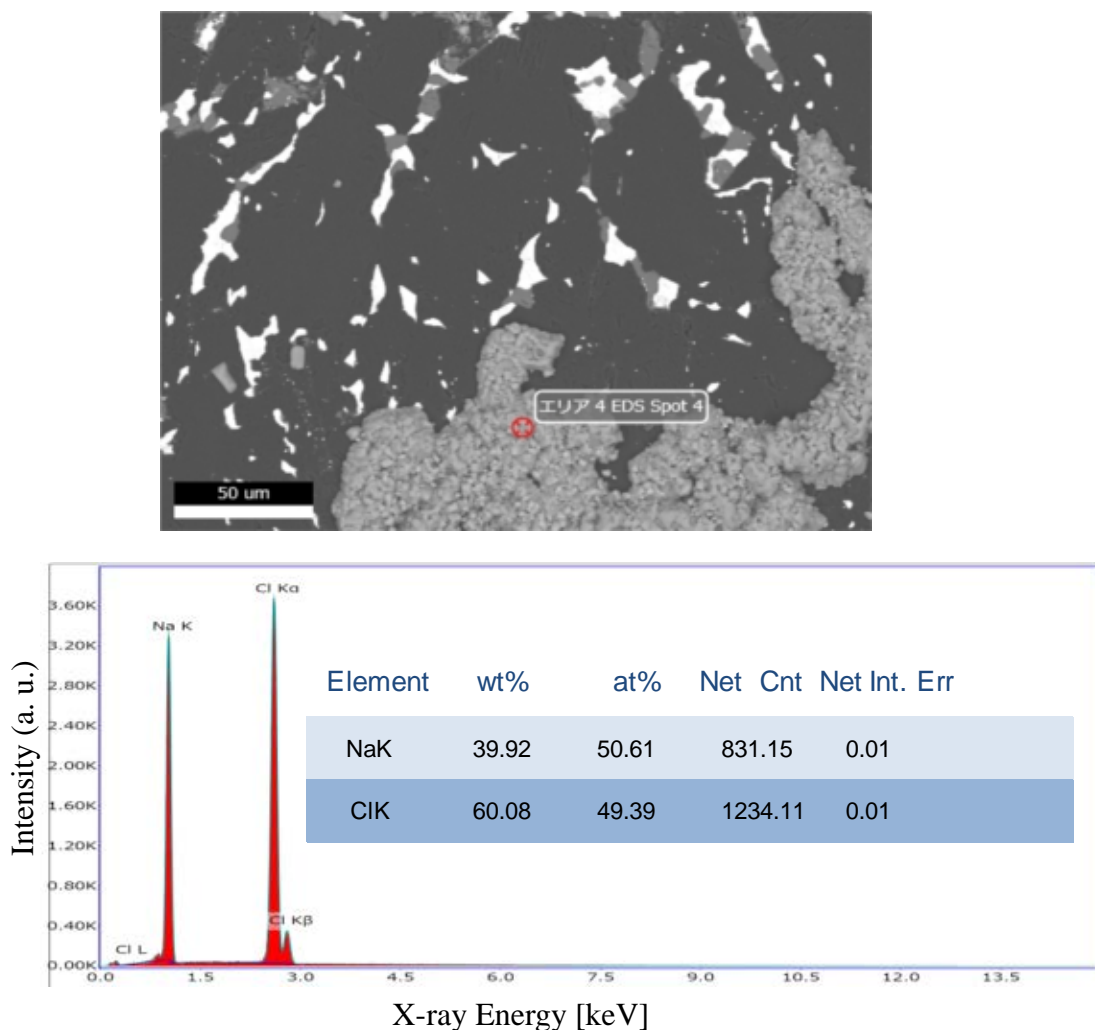
Fig. 5.4. SEM-BSE and SEM-EDS result showed the NaCl inside the cBN-metal composite of sample 4.

By using the same analysis method, cBN transformation was also confirmed from the sample 2 and 3. The hBN (002) peak was detected from sample 2 indicating lower cBN yield at lower reacted pressure. The lower cBN yield was also checked by SEM observation of the sample cross-section. As the conversion from hBN to cBN was started at the interface between molten solvent and hBN layer, the thickness of the precipitated cBN zone could be measured and the yield of cBN can be estimated as a relative thickness of cBN zone.

It is thought that this lower cBN yield in sample 2 is due to the smaller excess pressure (the reacted pressure minus equilibrium) at 1700 °C. Based on the equilibrium curve between hBN and cBN of P (GPa) = T (°C) / 465 + 0.79 [6], the equilibrium

pressure at this temperature was estimated to be 4.4 GPa and the excess pressures would be 1.2 and 0.4 GPa each for 5.6 and 4.8 GPa reacted pressures. The yield of cBN clearly increased with an increase in excess pressure. The change in the cBN yield under various HPHT condition was already described in previous chapter.

Comparing the reacted pressure of cBN synthesis using Co-V-Al solvent system as in sample 2 with the minimum pressure and temperature for cBN synthesis under Co-Al solvent system which is about 6 GPa and 1550 °C [3], the above results also suggested that the adding of vanadium to the Co-Al solvent system could decrease the pressure region of cBN synthesis for about 0.8 GPa, the same as molybdenum did in the Co-Al solvent system [5]. It is thought that the adding of vanadium into Co-Al solvent system increased the solubility of the nitrogen in the molten solvent [7], hence enhancing the hBN-cBN phase transformation.

The result of low cBN yield in the sample 3 where the quantity of vanadium in the metal solvent is 6 wt% less than the one in sample 1, confirmed the role of vanadium in enhancing the cBN transformation. Under equal reacted pressure and temperature, lower vanadium quantity in the molten solvent decreased the solubility of nitrogen and consequently lowered the yield of cBN.

Figure 5.5 showed the SEM observation result from the polished cross-section of the recovered sample 1. Figure 5.5 (a) was observed just above the metal-hBN source interface and Fig. 5.5 (b) was observed at the opposite side. From the SEM-EDS and EPMA results and as was confirmed by XRD, the dark irregularly shaped area in the figure is the cBN grains. The dark grayish regions correspond to the AlN, the light gray regions were identified as VN and the white area is the solidified Co alloy solvent. As shown in both figures, the cBN crystals obtained are irregular in shape with the grain size less than 20 µm. The small irregular shape of the crystals may have been due to relatively slow grain growth as an effect of vanadium addition after a spontaneous nucleation of cBN in the molten solvent. The result of such fine grain cBN under Co-V-Al metal solvent system was also confirmed in the previous chapter on the cBN-(Co65V25Al10) solvent system. Comparing Fig. 5.5 (a) and (b), it is clear that AlN was mainly developed near the metal-hBN source interface, suggesting that the distance of Al movement in the molten metal is limited to this area. Such result was also confirmed from the other samples.
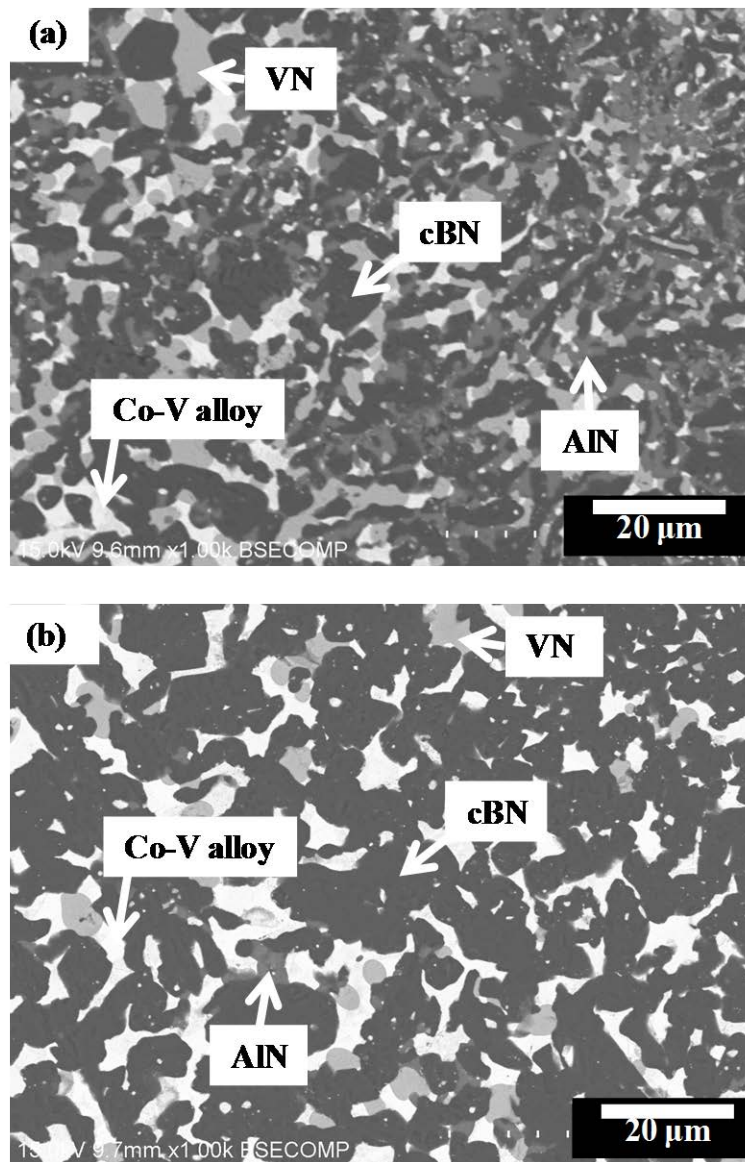
Fig. 5.5. SEM-BSE image of the cross-section of sample 1 (reacted at 5.6 GPa and 1700 °C 0.5 h. using Co80V10Al10 wt% solvent) after lapping. (a) near the metal-hBN source interface, and (b) far from the metal-hBN source interface.

While similar grain size of the cBN crystal was also recovered from sample 2, the cBN grain size in sample 3 consisted of 2 different types. The first type is the cBN crystal with the grain size less than 20 µm as seen in Fig. 5.6 (a) and the other type is the one with the grain size up to 50 µm as shown in Fig. 5.6 (b).

The result from SEM-EDS and EPMA showed that in areas where cBN grain grew rapidly as in Fig. 5 (b), vanadium contain or distribution was low. In contrast, in an area where the content of vanadium is relatively rich, the cBN grain growth was slow and

73

the cBN grain was finer. Such a large difference of microstructure of the cBN-metal composite was caused by the distance from the interface between molten solvent and BN layer. As shown in Fig. 5.6 (a), vanadium and Al content are higher at the interface than the inner part of the composites (Fig. 5.6 (b))
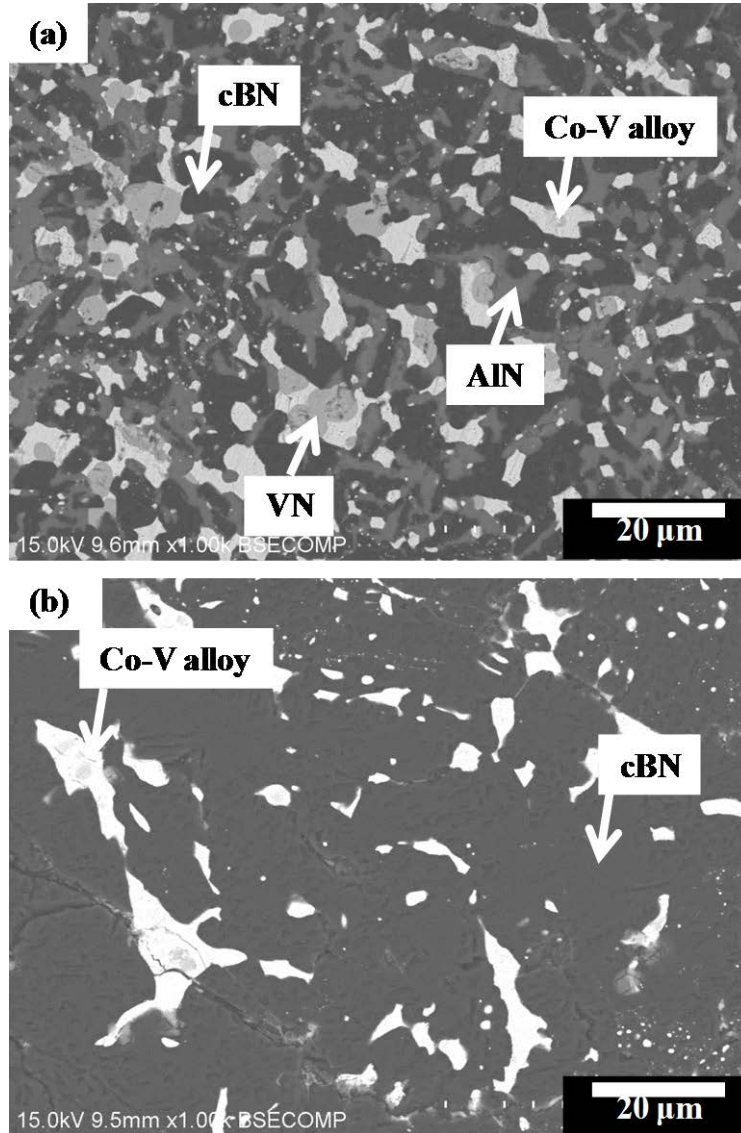

Fig. 5.6. SEM-BSE image of the cross-section of sample 3 (reacted at 5.6 GPa and 1700 °C 0.5 h. using Co84V6Al10 wt% solvent) after lapping. (a) Fine grains area, and (b) coarse grains area.

It is suggested that lower content of vanadium in the metal solvent decreased the speed of grain growth. Less vanadium in the molten solvent not only reduced the yield of cBN as already mentioned above but also advanced the grain growth of cBN. In other words, vanadium might act as cBN grain growth inhibitor.

5.3.2 Microstructure of cBN-(Co-Cr-Al) composites

To further confirm the effect of vanadium to inhibit the grain growth of cBN, vanadium was substituted from the metal solvent with chrome and carried out the cBN synthesis using Co-Cr-Al solvent system at the same reacted pressure and temperature of Co-V-Al solvent system as shown in sample 4 and 5 of Table 1.

The XRD results of both sample 4 and 5 showed that cBN was synthesized using Co70Cr22Al8 metal alloy solvent. The result from sample 5 where the experiment was conducted at 5 GPa and 1700 °C also confirmed that adding chrome into the Co-Al was effective to decrease synthesizing pressure of cBN in the same way that vanadium works in the Co-V-Al solvent system. The capability of chrome in increasing the solubility of nitrogen in the molten solvent, and as a result, decreasing the synthesizing pressure of cBN, has already been reported by Kubota et al. [8] in which the experiments were conducted using Ni-Cr-Al solvent system.
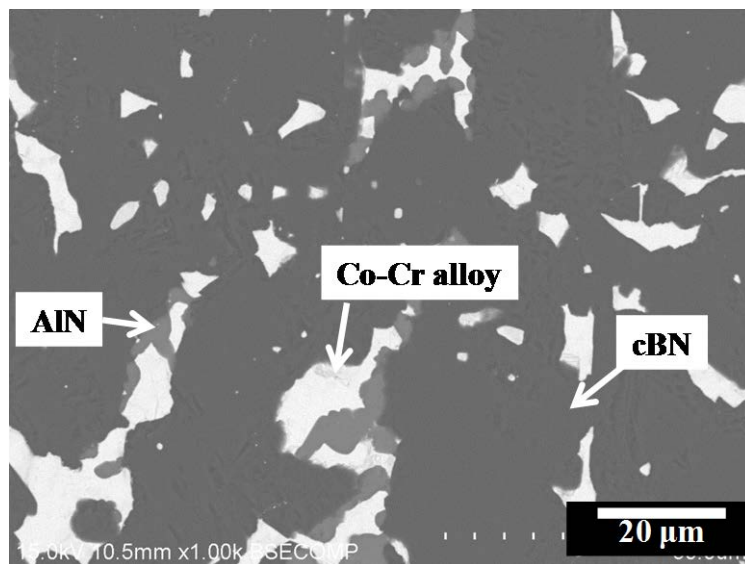

Fig. 5.7. SEM-BSE image of the cross-section of sample 4 after lapping.

Figure 5.7 showed the SEM-BSE image of sample 4 cross section. From the image, it could be seen that the cBN crystal from Co-Cr-Al solvent system has the grain size up to 50 μm. The same result of this up to 50 μm coarse cBN grain size was also observed from sample 5 in which the experiment condition was changed from 5.6 to 5.0 GPa to check the effect of the cBN synthesis reacted pressure on the cBN grain growth speed. The SEM-BSE image of sample 5 was shown in Fig. 5.8.

From the results of sample 4 and 5, it could be said that while the yield of the cBN is depends on the excess pressure as it was confirmed in Co-V-Al solvent system above,

there was no difference in terms of the cBN grain growth speed. The coarse cBN grain obtained under this Co-Cr-Al solvent system has no relation with the reacted pressure.
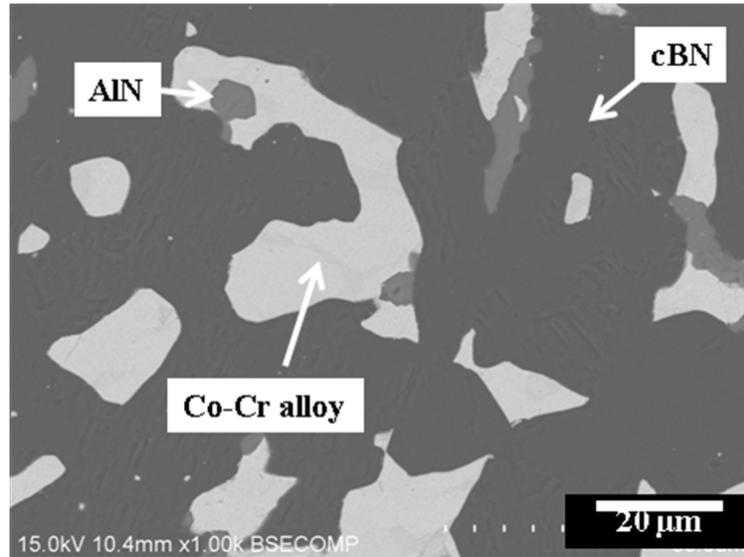

Fig. 5.8. SEM-BSE image of the cross-section of sample 5 (Co70Cr22Al8wt% solvent reacted at 5 GPa and 1700 °C 0.5 h.) after lapping.

Comparing the cBN grain size obtained from the sample 1 and 2 with the one from the sample 6 and 7, it was clear that under similar pressure and temperature condition, the cBN grain synthesized under Co-V-Al solvent system has finer size compared with the one synthesized under Co-Cr-Al solvent system. These coarse cBN grain sizes obtained from Co-Cr-Al solvent confirmed that the absence of vanadium in metal solvent affected the cBN growth in the molten solvent. Adding some amount of Vanadium could be the way in controlling the cBN growth during cBN synthesis process.

The microstructure of the cBN-(Co-Cr-Al) composites was also analyzed using EBSD to confirm the cBN grain size, the same as what was performed on the cBN-(Co-V-Al) sample as shown in previous chapter. Figure 5.9 showed the result from the EBSD analysis taken from sample 5. As seen here, the cBN was grown by forming a domain which is the same as on the Co-V-Al system but the grain size is much coarser comparing with the one from the Co-V-Al system as shown in Fig. 4.6 of chapter 4.
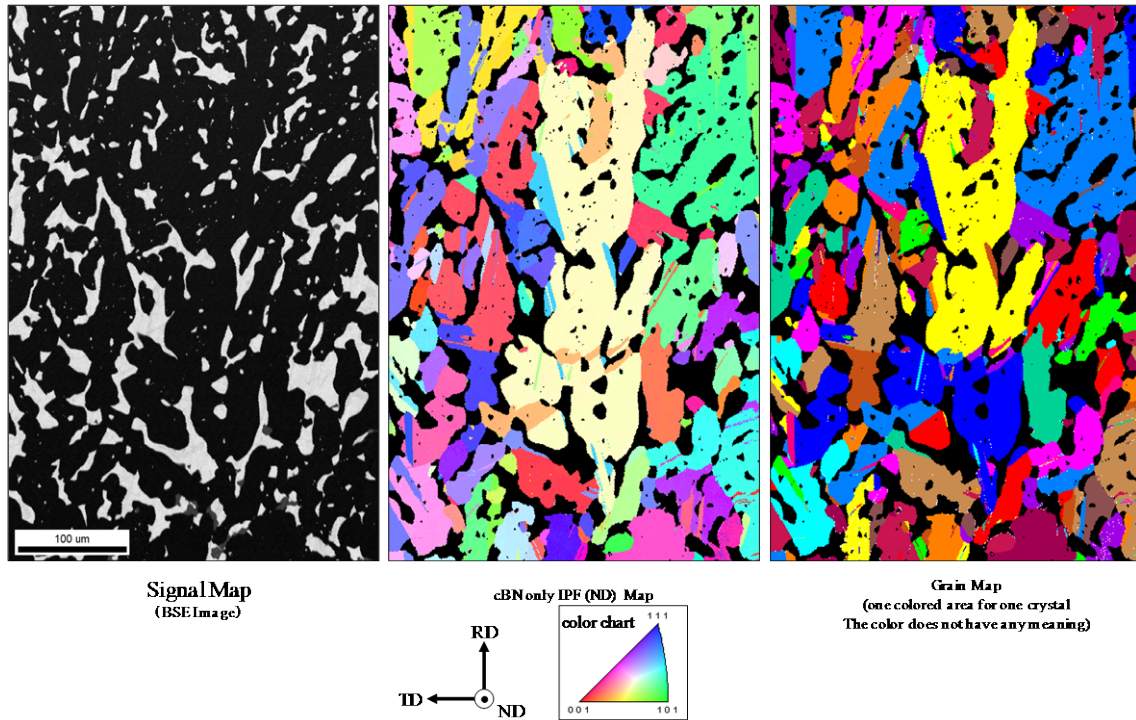

Fig. 5.9. EBSD analysis result of the cBN forming zone. Same sample of Fig. 7 (reacted at 5 GPa and 1700 °C 0.5 h. using Co70Cr22Al8 wt% solvent) was used for the analysis.
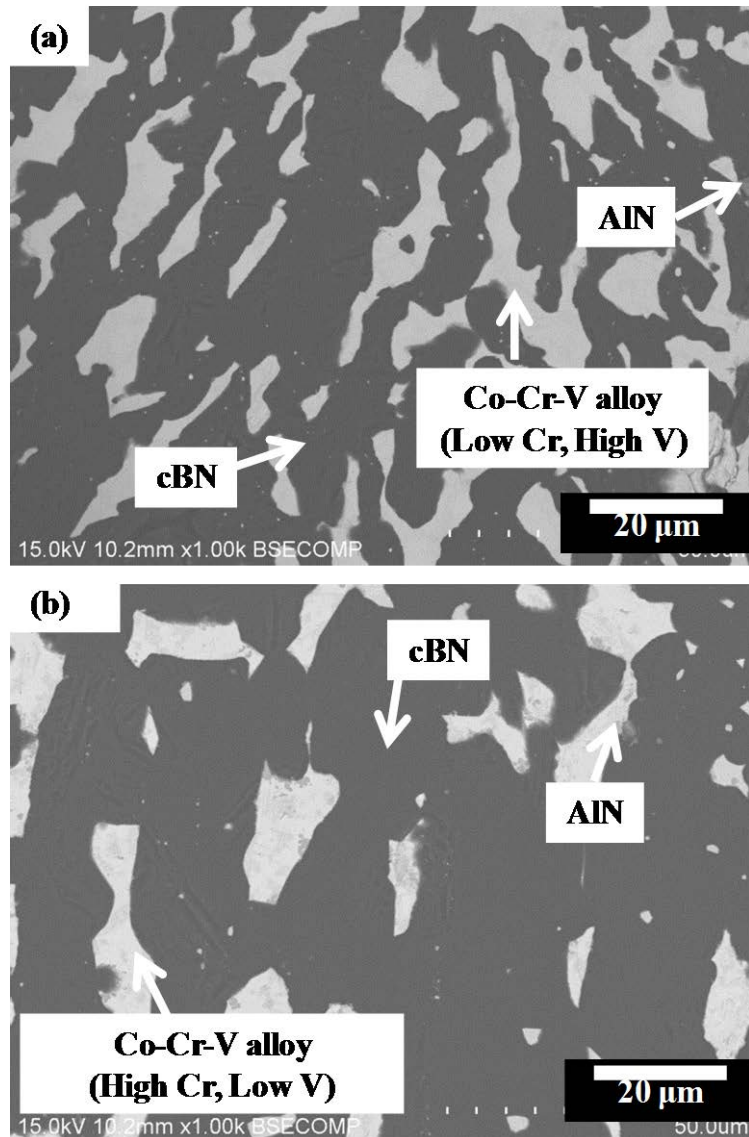
Fig. 5.10. SEM-BSE image of the cross-section of sample 6 (reacted at 5.6 GPa and 1720 °C for 0.5 h. using Co70Cr19V3Al8 wt% solvent) after lapping. (a) fine grains area, (b) coarse grains area.

Furthermore, cBN synthesis using Co70Cr19V3Al8 metal solvent was performed to see how the cBN grain will grow under such system where both chrome and vanadium exist. Figure 6 showed the SEM-BSE image of the polished sample 6 cross section. From the SEM-EDS result, it was found that there is a difference in term of chrome and vanadium content between Fig. 5.10 (a) and (b). The Co rich molten solvent in Fig. 5.10 (a) contains about 8.5 wt% of chrome along with 4.7 wt% of vanadium, while the

molten solvent in Fig. 5.10 (b) contains chrome and vanadium of about 14.3 wt% and 1.3 wt% each. As shown in the Fig. 5.10 (a), the high content of vanadium in the molten solvent could reduce the speed of the cBN grain growth in the Co-Cr-Al metal solvent. In contrast, as shown in Fig. 5.10 (b) where the presence of vanadium is relatively low, the cBN grain size is bigger compared with the one from the Fig. 5.10 (a).

An example of Cr rich area with coarse grain cBN and Cr poor area with fine grain cBN as analyzed with EPMA is shown in Fig.5.11. Figure 5.11 (a) is the area mapping from the area with coarse grain cBN and Fig. 5.11 (b) is the result from the area with fine grain cBN. Comparing the Fig. 5.11 (a) and (b), it could be confirmed that the Cr content level in Fig. 5.11 (a) is higher than in the Fig. 5.11 (b). As mentioned above, such difference in the composition of the metal solvent results in the difference in the microstructure of the cBN grain.

From the SEM-EDS and EPMA results of samples 1, 2, 3 and 5 that showed the segregation of vanadium nitride and the results of samples 4 and 5 that showed no segregation of chromium nitride, it was suggested that the formation of vanadium nitride in the molten solvent played important role in this phenomenon. The formation of VN and the absence of the CrN or Cr_2N could be explained by the difference on the free energy of formation of these nitrides in which the free energy of VN is much lower than CrN or Cr_2N [9]

From the above results, it was proved that adding Vanadium into the metal solvent could affect the grain growth of the cBN. Further study is still needed to find an adequate amount of vanadium in order to completely control the speed of the cBN growth.
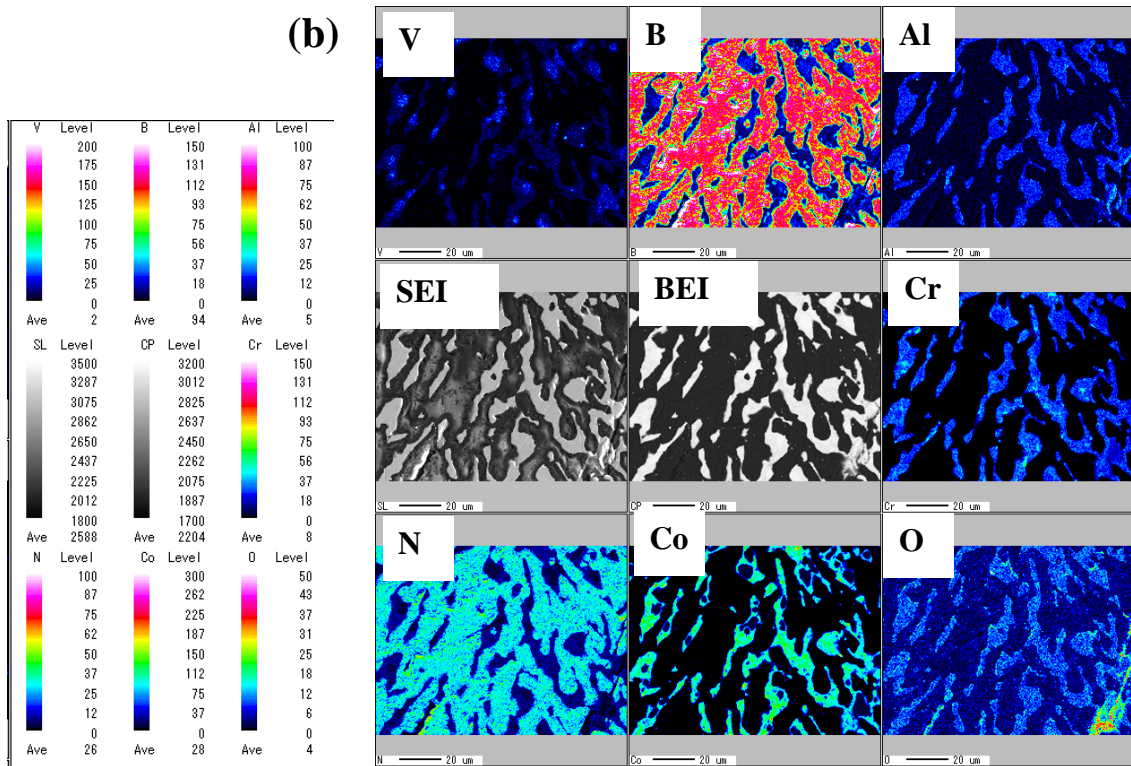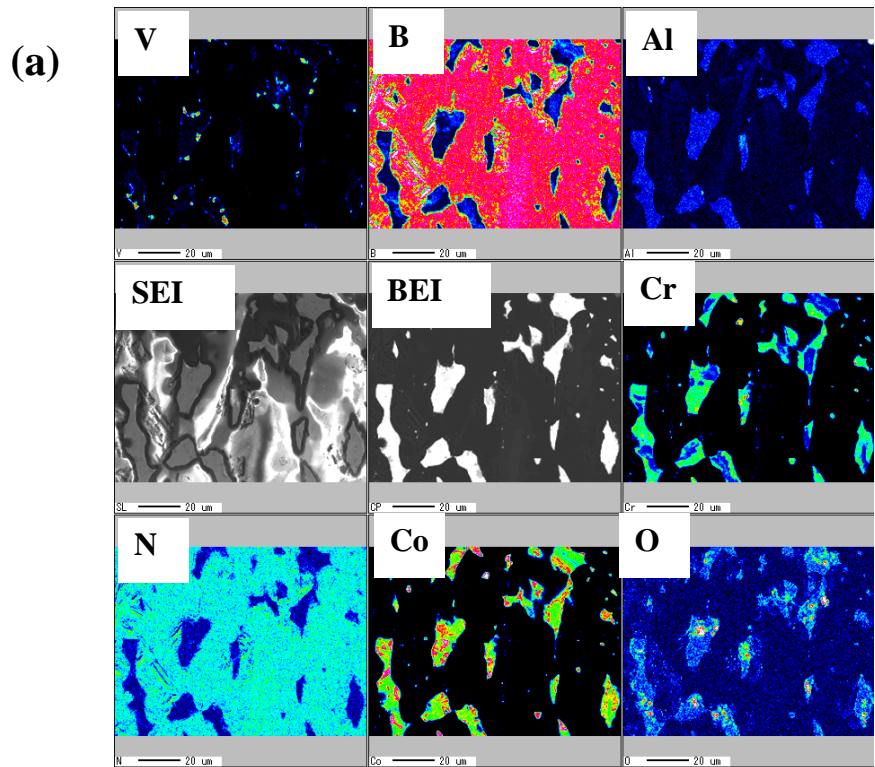
Fig. 5.11. EPMA area mapping on sample 6 (Co70Cr19V3Al8 wt% solvent reacted at 5 GPa and 1700 °C for 0.5 h.). (a) Coarse grain cBN area, (b) fine grain cBN area.

5.4. Conclusions

It was found that the size of cBN grains synthesized using Co-V-Al solvent was relatively finer compared with the ones synthesized using Co-Cr-Al. It was also confirmed that adding a small amount of V to the Co-Cr-Al solvent could suppress the cBN growth. It was suggested that V might be use as an additive in the metal catalyst during sintering of fine grains cBN compact where the microstructure homogeneity and the cBN abnormal grain growth are the important issues.

References

[1] R. H. Wentorf,Jr and W.A.Rocco, US Patent 3,918,219 (Nov.11,1975)

[2] R. C. DeVries and J. F. Fleischer US Patent 3,918, 931 (Nov.11,1975)

[3] O. Fukunaga, S. Takeuchi and T. Taniguchi, Diamond Relat. Mater. 20 (2011) 752.

[4] O. Fukunaga, Y. S. Ko, M. Konoue, N. Ohashi and T. Tsurumi, Diamond Relat. Mater. 8 (1999) 2036.

[5] A. Eko, O. Fukunaga and N. Ohtake, Diamond Relat. Mater. 40 (2013) 1

[6] O.Fukunaga, Diamond Relat. Mater., 9 (2000) 7.

[7] H. Wada and R. D. Pehlke, Met. Mat. Trans. B 12 (2) (1981) 333.

[8] Y. Kubota and T. Taniguchi, Jpn. J. Appl. Phys. 48 (2009) 071004-1.

[9] N. Ichinose and H. Kuwahara, Nitride ceramics, Nikkankōgyōshinbunsha (1998) 18.

Chapter 6 High pressure sintering of cubic BN using Co-V-Al alloy as bonding media

6.1. Introduction

The major applications of cBN are grinding wheel composed of cBN grains and bonding materials and sintered polycrystalline cBN (PCBN) cutting tools for machining ferrous materials. The cBN content varies depending on application; "low content cBN material" with ~50 vol% cBN plus ceramic type binder such as TiN, TiC (ceramic binder PCBN) can be used for turning case hardened steels and ball bearing steels, while "high content cBN material" with ~80-90 vol% cBN can be used in high speed machining of cast iron [1].

In the present study, metallic binder PCBN having high hardness and fracture toughness will be explored. The metallic binder PCBN reported previously contained simple binary system of Co-Al, Mn-Al, V-Al [2], or Co-W-Al [3]. Although, metallic binder composed of Al alloy of boron soluble transitional elements (Fe, Co, Ni) and nitrogen soluble elements selecting from V, Cr, Nb, Mn and Mo was designed and described in the previous chapters. The minimum pressure and temperature for the cBN growth in the molten metal solvents were greatly decreased with the adding of V or Cr to the Co-Al alloy solvent was reported [4]. The homogenous fine-grained cBN-metal composites was formed at 5.6 GPa and 1700 °C synthesis condition using hBN starting materials and Co-V-Al metal catalyst was also confirmed [5]. The previous reports on the synthesis solvent of metal alloys including transition metals (Fe, Ni, Co, Mn), nitrogen dissolver (Mo, Cr, V) and Al suggested as a candidate to realize homogeneous cBN-metal sintered composite for cutting tool applications. However, few experimental studies on metallic binder PCBN were available in the literatures particularly on the fine-grained cBN sintered compact with the grain sizes less than 2 μm. As the needs for the precision machining using PCBN cutting tools are steadily increase, the fine grained PCBN cutting tool along with the suitable cutting conditions is needed to achieve the best surface roughness during the machining [2].

While as synthesized cBN powder obtained in chapter 3 and 4 could be used as the starting materials for the sintering process, in the industrial practice, crushed cBN powder with irregular shape and homogenously classified by the grain size (range) was used as the starting materials.

In the present report, high content polycrystalline cBN compact with cBN powder as a starting material was sintered using Co-V-Al as metal solvent or catalyst. As the nitrogen solubility in the metal catalyst increased by the addition of vanadium or

chrome, it was predicted that the dissolution–precipitation process of the cBN grains in the molten metal catalyst during sintering process would be more active. Hence, enhancing the cBN-cBN direct bonding and resulting the increasement of the hardness in PCBN compacts sintered compacts. The change behavior in the hardness of the PCBN compacts sintered with Co-V-Al metal catalyst was compared with the already reported cBN-Al sintered compacts in the function of Al/(Al + BN) and the microstructure of the compact will be discussed.

6.2. Experimental methods

The starting materials were commercially available 0.5-2 and 2-4 μm cBN powders from Showa Denko type BN-F. Co, V, Al metal powders (Rare Metallic, 99.9%) were used as the metal catalysts. The metal catalyst was prepared by mixing each metal powder before finally re-mix it with cBN powders, which were then pressed to form a green compact. The SEM images of the starting materials were shown in Fig. 6.1.
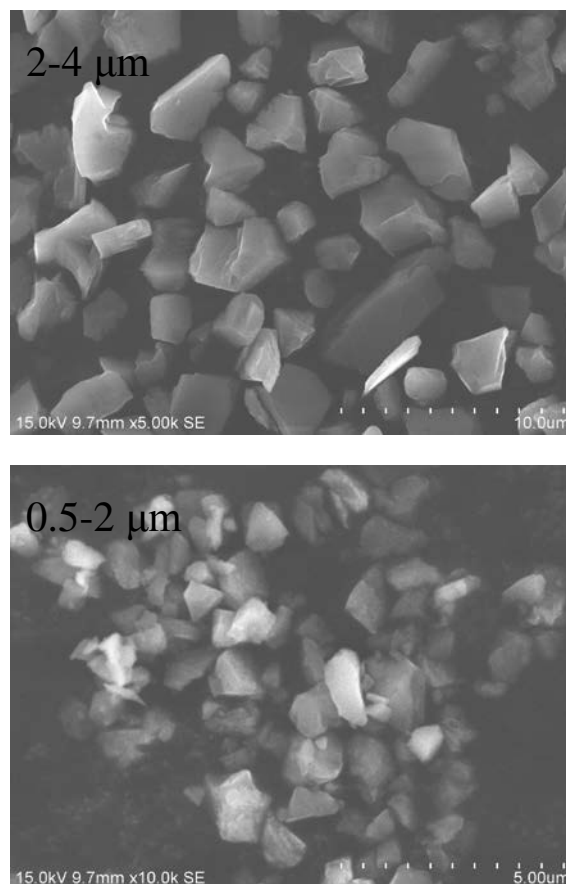

Fig. 6.1. SEM images of crushed irregular cBN powders used in the sintering process

The cBN content in the compacts was fixed to 80 and 90 wt%. In the Co-V-Al system, Co and V ratio was kept to about 7:3 in weight. The details of the metal solvent composition were summarized in Table 6.1.

Table 6.1. Various samples composition use in these experiments

cBN (2-4 μm) wt %	solvent	Al/(Al+BN) wt%
90	Co58V32Al10	1.1
90 (0.5-2 μm)	Co50V19Al31	3.3
90	Co50V19Al40	4.25
90	Co43V17Al50	5.26
90	Co28V7Al65	6.74
90	Co19V11Al70	7.22
80	Co63Cr33Al4	1
80	Co65V25Al10	2.44
80	Co60V25Al15	3.61
80	Co60V23Al17	4.08
80 (0.5-2 μm)	Co60V23Al17	4.08
80	Co55V20Al25	5.88
80	Co50V19Al31	7.2
80	Co43V14Al40	9.09
80	Co36V7Al65	11.1

The modified belt type high pressure apparatus [6] as described in chapter 2 was used for HPHT experiments. Figure 6.2 shows a sample assembly used in this study. The pre-mix cBN-metal green compact was covered by Zr capsule and placed between the NaCl + 10 wt% ZrO_2 disks in the inner NaCl sleeve. The HPHT runs were conducted with pressure increases at room temperature and then temperature increases. The samples were kept at 770 °C for 10 min before raised again to final designated temperature. After keeping for 30 min. at designed temperature, current supply to the heater was slowly decreased for about 1 hour back to room temperature to avoid cracking in the sintered samples before the press load was decreased slowly.
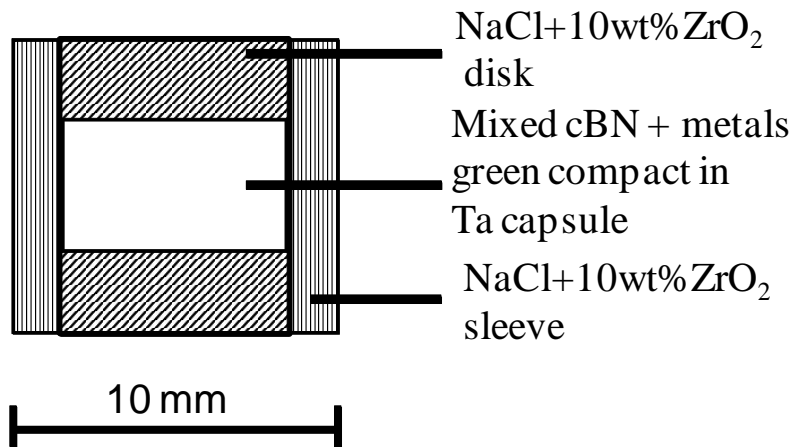
Fig. 6.2. Sample assembly for high pressure-high temperature (HPHT) sintering of cBN using metal catalyst.

The minimum pressure and temperature (P-T) for cBN transformation in the system using Co-Cr-V-Al or Co-V-Al solvents were confirmed at 4.2 GPa and 1400 °C in the previous report [5]. The pressure of 5.6 GPa and the temperature 1600 °C was selected and was fixed as the conditions to prepare the cBN-metals composites of the present study.

While the cBN content was fixed to 80 and 90 wt%, the content of Al in the cBN-Co-V-Al system were changed from about 1 to 11 wt% in the function of Al/(BN + Al). Mainly, cBN powders with the grain size of 2-4 μm were used for this kind of experiments. The suitable Al content to produce the cBN compact with high hardness using the Co-V-Al was determined.

After the HPHT sintering process, the recovered samples were then encapsulated in a hot mounting press before lapped with a diamond disc on the horizontal lapping machine. The samples were examined using the X-ray powder diffraction (XRD) to confirm the reactions during sintering process and a scanning electron microscope (SEM) for microstructure observation. The hardness of the obtained samples was measured on Vickers hardness test machine with the applied load of 9.807 N and 20 sec. dwelling time.

6.3. Result and Discussions

6.3.1. Hardness measurement

Figure 6.3 showed the Vickers hardness of each polycrystalline cBN-(Co-V-Al) composite against its value of Al/(BN + Al). The solid squares marks represent the hardness results measured from 2-4 μm cBN 80 wt% + (Co-V-Al) 20 wt% composites

and the solid line is our prediction of the hardness change behavior of this composites system. The solid diamond marks represent the results measured from 2-4 μm cBN 90 wt% + (Co-V-Al) 10 wt% composites and the dot line is the trend on its hardness change. As comparison, 2 sets of the data which compiled from previously published reports were also drawn in the figure. The solid triangle marks and its dashed line are the data of 10 μm cBN-Al mixtures on the WC-16 wt% Co substrates sintered at 5.0 GPa and 1400 °C as published by Li et al. [7]. The cross marks are the data from of the cBN-Al compact sintered at 5.75 GPa and 1400 °C for 20 min [8].
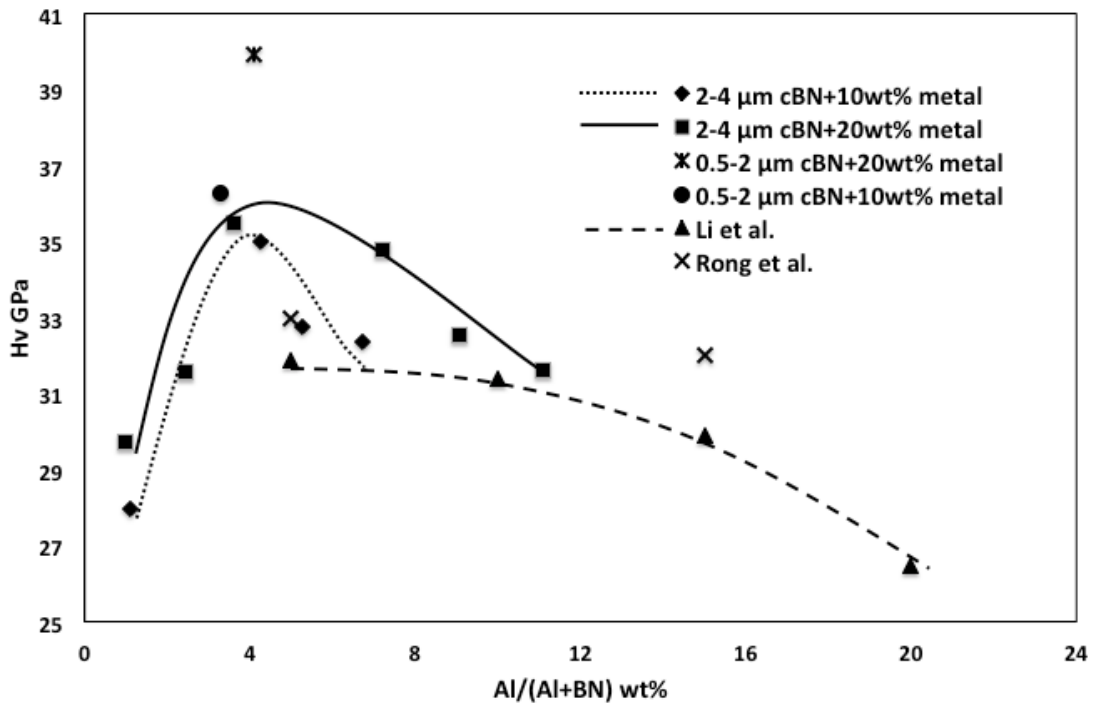
Fig. 6.3. Vickers hardness (Hv) of various cBN-(Co-V-Al) composites sintered at 5.6 GPa and the temperature 1600 °C for 30 min. as the function of Al/(BN + Al) wt% value.

In Fig. 6.3, at lower Al content (lower Al/(Al + BN)) region, Vickers hardness values were extraordinary low may due to poor bonding between cBN grains and precipitated AlN. The content of Co + V to the BN (Co + V/(Co + V + BN) was decreased with increase Al content in the Fig. 6.3. The results suggested that even enough amount of liquid Co-V alloy was present in the cBN system, initial cBN and AlN bonding was essential to form metallic binder PCBN.

When Al content was increased to about the level of Al/(Al + BN)=3-4 wt%, the dissolution–precipitation process of B-N species through the liquid Co-V alloy become active. Highest hardness values are obtained at Al/(Al + BN)= 3.61 wt% and Co +

V/(Co + V + BN)= 17.5 wt% for 2-4 µm cBN 80 wt% mixture and at A/(Al + BN)= 4.25 wt% and Co + V/(Co + V + BN)=6.25 wt% for 2-4 µm cBN 90 wt% mixture.

At high Al content, Co + V contents were decreased and the system was closed to pure cBN-Al system. At 7.2 wt% Al (Al/(Al + BN)=7.2 wt%), (Co + V)/(Co + V + BN) content was about 3.2 wt% for 2-4µm cBN 90 wt% mixture and the hardness value was closed to the value of cBN-Al system.

6.3.1.1. Effect of V addition into cBN-metals sintering system

From Fig. 6.3, it was confirmed that under the same Al content, the cBN compacts sintered with Co-V-Al catalyst have higher hardness comparing with the one sintered using Al on tungsten carbide substrate. The highest hardness of the 2-4 µm cBN 80 wt% + (Co-V-Al) 20 wt% composites obtained from our experiments was 35.5 GPa with Al/(BN + Al) value of 3.61 wt% while in the 2-4 µm cBN 90 wt% + (Co-V-Al) 10 wt% composites the highest hardness was 35.5 GPa with Al/(BN + Al) value of 4.25 wt%. Such higher value of the hardness in the present study is thought to be the result of the increasement in the cBN-cBN direct bonding ratio in the compact. The addition of the V in the metal catalyst enhanced the process of dissolution and precipitation of the nitrogen species in the molten catalyst. As reported previously, the cBN precipitation from the hBN source under Co-Al system begin at about 6 GPa and 1600 °C [9]. It is very much higher comparing with the lowest limit of the cBN precipitation under Co-V-Al system which is around 4.2 GPa and 1400 °C [22]. It was also reported that the excess pressure and temperature affecting the cBN yield during precipitation from the molten solvent [9].

Therefore, under the same sintering condition of pressure and temperature, the difference in enhancing the process of dissolution and precipitation of the cBN in the molten catalyst between cBN-Co-Al and cBN-Co-V-Al system is the main driving force behind the high hardness cBN compact forming in this present report. The ratio of cBN-cBN direct bonding in the obtained cBN compacts will also be observed later in this paper.

6.3.1.2. Effect of the Al content change in the cBN-Co-V-Al

The hardness of the composites was affected with the changing in the value of Al/(cBN + Al). The hardness decreased sharply when the value of Al/(BN + Al) reached below 1 wt% because cBN and AlN bonding was not formed homogeneously. Although the metallic Co and V content are relatively high at such low Al content region, dissolution and precipitation of the B-N species by liquid alloy phase to form the cBN-cBN direct

bonding was insufficient. This result is consistent with the report by Fukunaga et al. that under the same P-T condition, the amount of Al in the metal solvent affected the cBN formation limit [8]. For example, under Co-Mo-Al solvent at 6 GPa and 1750 °C for 30 min, cBN crystals were detected with the minimum Al content of 1.5 wt%.

When the value of Al/(BN + Al) was moved larger than 4 wt%, the hardness was also decrease gradually. Such decrease in the hardness value occured along with the increase of AlN as the chemical reaction product. As described in the previous papers the increase of the AlN will reduce the hardness of the cBN compact [8, 10]. The increase of the AlN in the compact along with the increment of Al content was also confirmed by XRD analysis. Higher Al addition will result higher AlN content in the cBN compact. It was also confirmed that when the Al content reached about 11wt% in the 2-4 μm cBN 80wt % + (Co-V-Al) 20 wt% composites, the hardness will be on the same region with the one from the cBN-Al compact published by Li et al. [7].

The sharply decrease in the hardness value on the 2-4 μm cBN 90 wt% + (Co-V-Al) 10 wt% composites when the value of Al/(BN + Al) is larger than 4 wt% was also confirmed. The hardness in 2-4 μm cBN 90wt% system decreased from Al 4.25 wt% to 7.22 wt% rapidly and the Co + V content also decreased rapidly from 6.3 wt% to 3.2 wt%. It is thought that small amounts of the Co and V alloy prevent homogeneous distribution of liquid in the cBN-AlN system during the sintering process. The confirmation of such inhomogeneity of the microstructure from the 2-4 μm cBN 90 wt% + (Co-V-Al) 10 wt% composite will be discussed later in this paper.

6.3.1.3. Effect of the cBN grain size

The sintering experiments using finer cBN powders of 0.5-2 μm was employed with Al content around 3.5-4 wt% which is best value of Al addition in sintering high hardness cBN compact with the 2-4 μm cBN powder as the starting materials. The same with above experiments, the cBN content were also fixed to 80 wt% and 90 wt%. The results were shown in Fig. 6.2 with the solid circle represent the result of 0.5-2 μm cBN 90 wt% + (Co-V-Al) 10 wt% composite and the asterisk represent the one from 0.5-2 μm cBN 80 wt% + (Co-V-Al) 20 wt% composite.

The hardness of 0.5-2 μm cBN 90 wt% with Al/(BN + Al) content of 3.3 wt% is 36.2 GPa while the hardness of 0.5-2 μm cBN 80 wt% with Al/(BN + Al) content of 4.08 wt% reached 39.9 GPa. Such considerable increase in the hardness of this fine-grained compact came from the higher specific surface area of the starting materials. Especially, 0.5-2 μm cBN 80 wt% with Al/(BN + Al) content of 4.08 wt% sample contained enough amount of Co+V alloy content ((Co + V)/(Co +V + BN)=17.2 wt%) to promote direct

bonding of cBN grains. As the process of dissolution and precipitation of the cBN to form the cBN-cBN direct bonding occurred on the cBN crystal surface, higher specific surface area means higher ratio of the cBN-cBN direct bonding. The systematic changes of the compact`s hardness in the cBN-Al compact has been studied by McKie et al. [11]. Their study showed that under the same amount of sintering catalyst, the cBN compact with finer grain size has higher hardness value.

6.3.2. Microstructure of the cBN-Co-V-Al composites
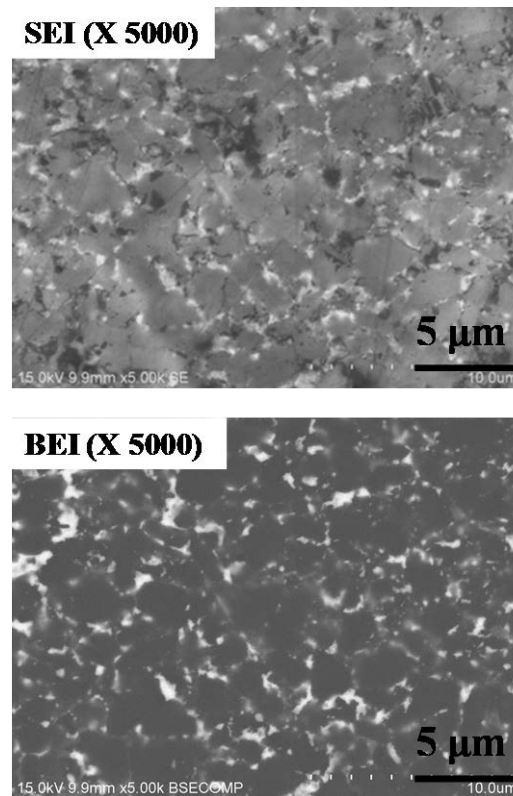
Fig. 6.4. SEM images of the 2-4 μm cBN 80 wt% + (Co60-V25-Al15) 20 wt% with the Al/(BN + Al) 3.61 wt%

The microstructure of the sintered cBN compact was observed by SEM to confirm the homogeneity and the cBN-cBN direct bonding. Fig. 6.4 showed the SEM image of the polished surface of 2-4 μm cBN 80 wt% + (Co60-V25-Al15) 20 wt% with the Al content of 3.61 wt%. As seen here, the cBN compact is well sintered with homogeneous microstructure. The dark side in the BSE image is the cBN grains and the light regions correspond to the solidified metal catalyst and its reaction product.

To confirm the cBN-cBN direct bonding in the compact, some of the sintered samples were treated in the strong acid of mixed HNO_3 + HF to remove the metallic binder. Fig.

6.5 showed the SEM image of the 0.5-2 μm cBN 80 wt% + (Co60-V23-Al17) 20 wt% composite after leaching in the strong acid for 24 hours. From the SEM-SEI image, it can be seen that cBN grains are directly bonded each other and the "necking" between the cBN crystals is quite advanced that it is difficult to identify the grain boundary. The addition of the V in the metal catalyst enhanced the process of dissolution and reprecipitation of the cBN in the molten catalyst during sintering process. As the result high ratio of the cBN-cBN direct bonding was homogenously formed.
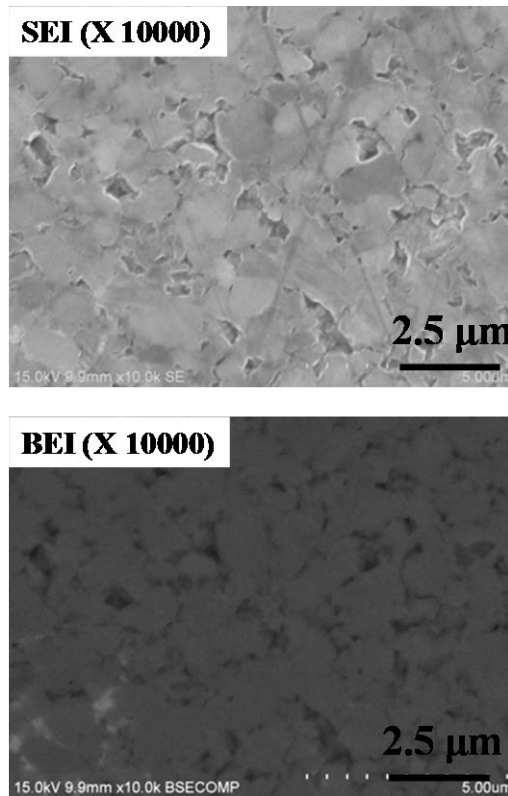
Fig. 6.5. SEM images of the polished surface of the 0.5-2 μm cBN 80 wt% + (Co60-V23-Al17) 20 wt% composite after treated in strong acid for 24 hours.

To check the fracturing mode of the cBN compact when it was broke, the same 0.5-2 μm cBN 80 wt% + (Co60-V23-Al17) 20 wt% sample was manually hit and broke with the hammer to observe the cross section of the fracture surface. Figure 6.6 showed the SEM-SEI image of the fracture surface. The image of Fig. 6.6 showed that the fracture of cBN compact proceeded through inter-granular fracture indicating that the cBN-cBN bonding is quite strong. The high hardness of the 0.5-2 μm cBN 80 wt% + (Co60-V23-Al17) 20 wt% sample could be explained by this high ratio of cBN-cBN direct bonding.
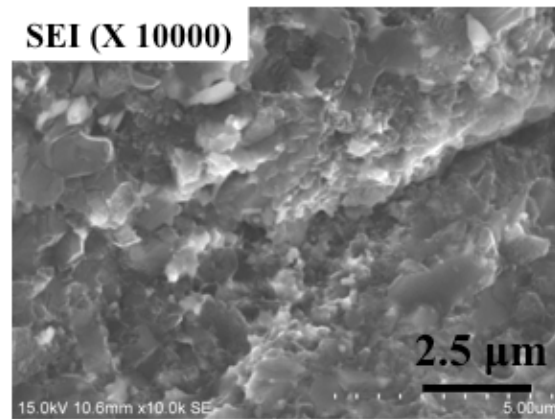
Fig. 6.6. SEM-SEI image of the fracture surface taken from 0.5-2 μm cBN compact

Figure 6.7 showed the microstructure of the 2-4 μm cBN 90 wt% + (Co43-V17-Al40) 10 wt% sample after treated at strong acid for 24 hours on their polished surface and as-sintered surface. As was confirmed from Fig. 6.7 (A) and (B), the polished surface of this sample is not as smooth as the surface of the 0.5-2 μm cBN 80 wt% + (Co60-V23-Al17) 20 wt% composite (Fig.4). The population of the cBN-cBN bonding in the 2-4 μm cBN 90 wt% + (Co43-V17-Al40) 10 wt% sample may be smaller compared to the sample of the 0.5-2 μm cBN 80wt% compact. Some cBN grains from the polished surface were left out during the acid treatment and creating some holes in the images. Such appearance was also observed from the shape of the cBN grains existed in the acid leached as-sintered surface. From the image, it was suggested that the direct bonding between cBN grains are occurred on some parts in the compact, however due to small amount of Co + V alloy components ((Co + V)/(Co +V + BN)=6.25 wt%), the dissolution and precipitation of cBN grains by the liquid alloy were not occurred homogenously.
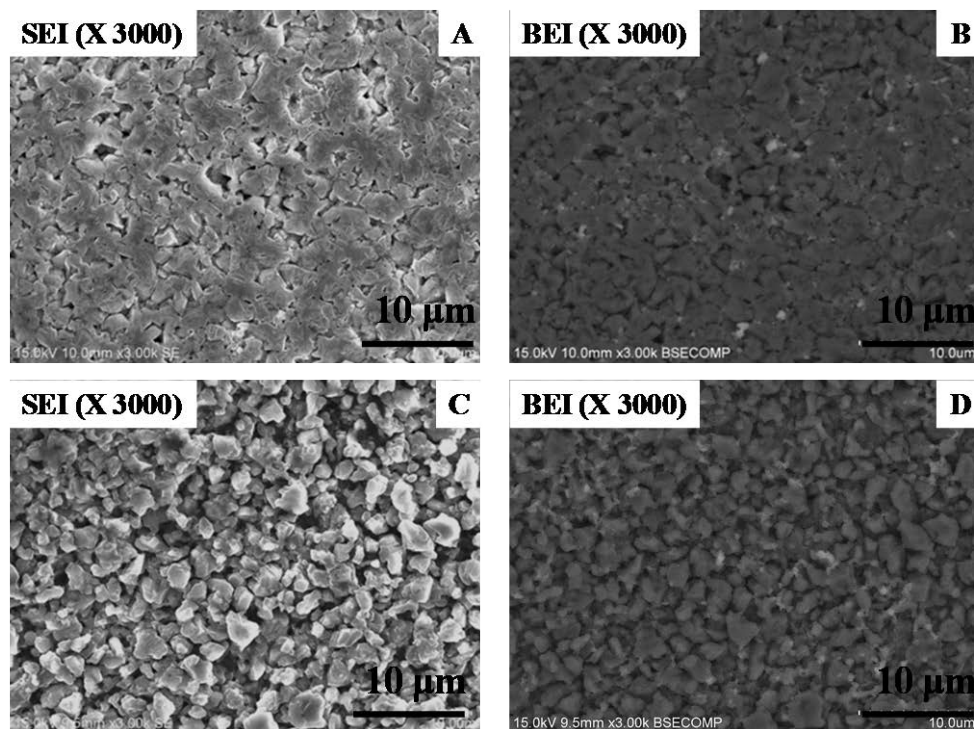
Fig. 6.7. Microstructure images of the 2-4 μm cBN 90 wt% + (Co43-V17-Al40) 10 wt% composite with Al/(BN + Al) value of 4.25 wt% after treated in strong acid for 24 hours. (A) SEM-SEI of the polished surface, and (B) BEI image of A area. (C) SEM-SEI of the acid leached as-sintered surface, and (D) BEI image of C area.

6.4. Conclusions

Polycrsytalline cBN-Co-V-Al composites with homogenous microstructure were sintered at 5.6 GPa and 1600 °C for 30 minutes. The highest Vickers hardness of 39.9 GPa was achieved by sintering the 0.5-2 μm cBN 80 wt% + (Co60-V23-Al17) 20 wt% composite with the Al/(BN + Al) value of 4.0 wt%. It was confirmed that the addition of V into the metal catalyst increasing the ratio of the cBN-cBN direct bonding in the compact. Increasing the Al content in Co-V-Al metal catalyst will increase the creation of AlN and therefore decreasing the hardness of the cBN compact.

References

[1] J. Angseryd, M. Elfwing, E. Olsson and H. -O. Andrén, Intl. J. Ref. Metals Hard Mater. 27 (2009) 249.

[2] R. H. Wentorf Jr. and W. A. Rocco, US patent 3743489 (1973) 1-6.

[3] N. Pretorius, Ind. Diamond Rev. 2/06 (2006) 33.

[4] A. Eko, O. Fukunaga and N. Ohtake, Diamond Relat. Mater. 40 (2013) 1.

[5] A. Eko, O. Fukunaga and N. Ohtake, Intl. J. Ref. Metals Hard Mater. 41 (2013) 73.

[6] O. Fukunaga, Y. S. Ko, M. Konoue, N. Ohashi and T. Tsurumi, Diamond Relat. Mater. **8** (1999) 2036.

[7] Y. Li, S. Li, R. Lv, J. Qin, J. Zhang, J. Wang, F. Wang, Z. Kou and D. He, J. Mater. Res. 23 (2008) 2366.

[8] X. Z. Rong and O. Fukunaga, Sintering of Cubic Boron Nitride with added Aluminum at High Pressure and High Temperatures, in: M. Homma (ed.) Advanced Materials '93, I/B, Elsevier Science B.V. (1994)1455.

[9] O. Fukunaga, S. Takeuchi and T. Taniguchi, Diamond Relat. Mater. 20 (2011) 752-755

[10] R. Lv, J. Liu, Y. Li, S. Li, Z. Kou and D. He, Diamond Relat. Mater. 17 (2008) 2062-2066

[11] A. McKie, J. Winze, I. Sigalas, M. Herrmann, L. Weiler, J. Ro¨del and N. Can, Ceramics International 37 (2011) 1.

Chapter 7 Cutting performance of the polycrystalline cubic BN compact sintered with Co-V-Al sintering media

7.1. Introduction

Cubic boron nitride (cBN) has the highest hardness and thermal conductivity among all materials except for diamond, and also has low reactivity with ferrous materials [1]. Cutting tools manufacturer developed polycrystalline cubic boron nitride (PCBN) by sintering CBN with ceramic binding materials, and contributed to the shift in the machining method of hardened steels from grinding to cutting. Furthermore, they contributed to the productivity improvement and cost reduction in the finishing and semi-finishing of ferrous materials such as cast iron and ferrous powder metal (PM) with high content PCBN tools [2-4].

Gray cast iron is widely used for engine blocks, brakes and so on, due to its low cost and excellent moldability. Carbide and ceramic cutting tools are conventionally used for machining gray cast iron that features easy to cut properties. However, due to the growing demand for high speed, high efficiency and high precision cutting and long life tools, CBN cutting tools are replacing conventional tools [5].

Ferrous PM materials is applied to automotive function parts, such as transmissions, because it can be formed into complex and nearing-completion shapes with the progress of the near net shape technology. In the machining of PM parts, high precision cutting is required for high quality automotive parts. However, the machinability of these parts has been degraded because of the increased hardness of their materials [6]. Therefore, the demand for PCBN cutting tools that enable high-efficiency machining and long tool life has increased.

In this chapter, high content PCBN compact with Co-V-Al alloy base sintering media as described in chapter 6 was sintered. As the high content PCBN with its high toughness is better suited for the machining of cast iron and ferrous PM [2], their cutting performance on the cast iron and ductile cast iron and was evaluated.

7.2. Experimental method
7.2.1 Sample preparation

The starting materials were 0.5-2 and 2-4 μm cBN powders from Showa Denko type BN-F. Co, V, Al metal powders (Rare Metallic, 99.9%) were used as the metal catalysts. The metal catalyst was prepared by mixing each metal powder before finally re-mix it with cBN powders, which were then pressed to form a green compact. Each of green compact was then layered on the tungsten carbide (WC-16 wt%Co) disk having

thickness of 2.5 mm before put it in the Zr can for the HPHT treatment. The amount of the pre-mixed powder compacted over the tungsten carbide disk was adjust so that the cBN compact layer will be around 1.0 mm after sintering. The cBN-metal compositions used for the cutting tools were, 2-4 μm cBN 80 wt% + (Co60-V25-Al15) 20 wt% and 0.5-2 μm cBN 80 wt% + (Co60-V23-Al17) wt%.

The HPHT sintering condition was 5.6 GPa and the temperature 1600 °C with 30 min reaction time. Under the high-pressure condition, the samples were kept at 770 °C for 10 min before raised again to final designated temperature. After keeping for 30 min. at designed temperature, current supply to the heater was slowly decreased for about 1 hour back to room temperature to avoid cracking in the sintered samples before the press load was decreased slowly.

After the HPHT sintering process, the recovered samples were then ground on both cBN layer and the opposite side of carbide layer using surface grinding machine before it was cut into an equilateral triangle with the length of 4.5 mm using wire EDM machine. The cut pieces were then brazed with the active silver brazing filler metals (Tokyo Braze type TB-608T, chemical comp.: Ag-28Cu-2Ti) over the ISO shaped carbide cutting tip of CNMA120408 and then finally lapped to their final dimension.
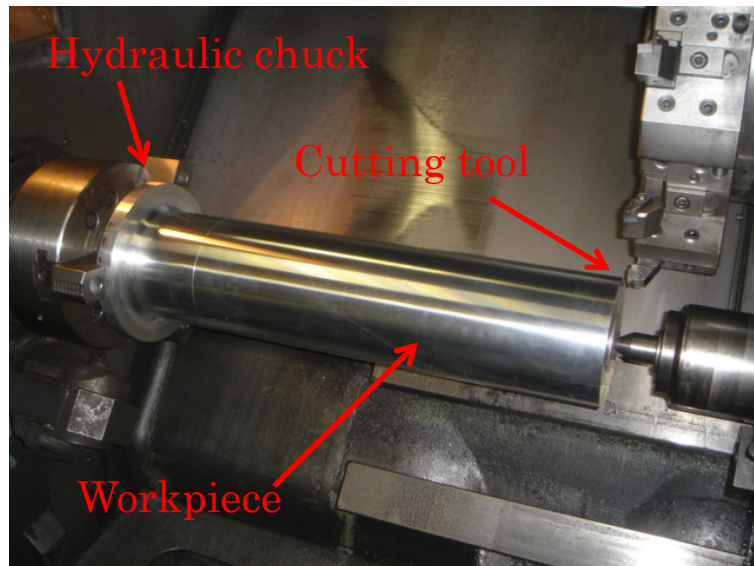
7.2.2 Cutting test

Fig. 7.1. Ready to cut FCD700 mounted on the NC lathe.

The wear resistance of the sintered cBN compact was evaluated on the gray cast iron of FC300 and the ductile cast iron of FCD700. The cutting test was carried out under

continuous turning on the outer diameter of the workpiece. Figure 7.1 showed the mounted workpiece (FCD700) on the lathe machine along with the ready to run cutting tip.

Table 7.1 Workpieces and cutting conditions

Workpiece (size)	Cutting conditions			
	Cutting speed, Vc (m/min)	Depth of cut, ap (mm)	Feed rate, fn (mm/rev)	water soluble coolant (1.4% concentration)
FC300 (φ160 × 600)	350	1.5	0.3	wet
	800	0.2	0.13	wet
FCD700 (φ170 × 600)	400	0.15	0.07	wet

A NC lathe machine was used to perform the cutting test. In referring to the recommend cutting test condition of the high content commercially available PCBN compact on the gray cast iron [7], the test conditions for the FC300 were as follows; cutting speed: 350 m/min., depth of cut: 1.5 mm, feed rate: 0.3 mm/rev. for roughing and 800 m/min., depth of cut: 0.2 mm, feed rate: 0.13 mm/rev. for finishing. While for the finishing of FCD700, the conditions were as follows; cutting speed: 400 m/min., depth of cut: 0.15 mm, feed rate: 0.07 mm/rev. The coolant was used in all cutting test. Table 7.1 shows the summarized the entire cutting conditions in this study. The tool holder is DCLNL2525M12 with the ISO tip of CNMA120408. Flank wear as illustrated in Fig. 7.2 was measured and a cutting edge was observed.
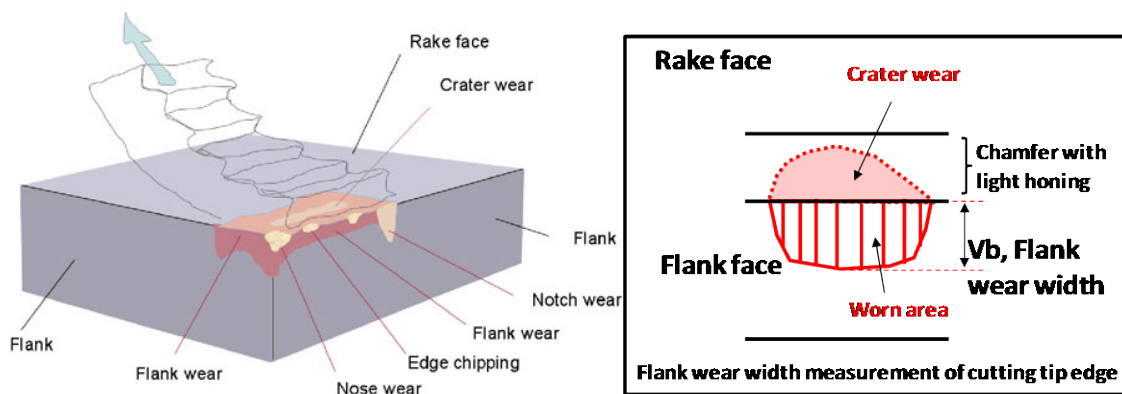

Fig. 7.2 Schematic diagram of the cutting tip edge

Commercially available tungsten carbide (Mitsubishi Carbide, TF15, 10 wt%Co) cutting tip and high content PCBN (90 vol.%) sintered with Co-W-Al alloy sintering media from Sumitomo Hard Metal named BN700 [6] was used as a comparison.

7.3. Result and discussion.
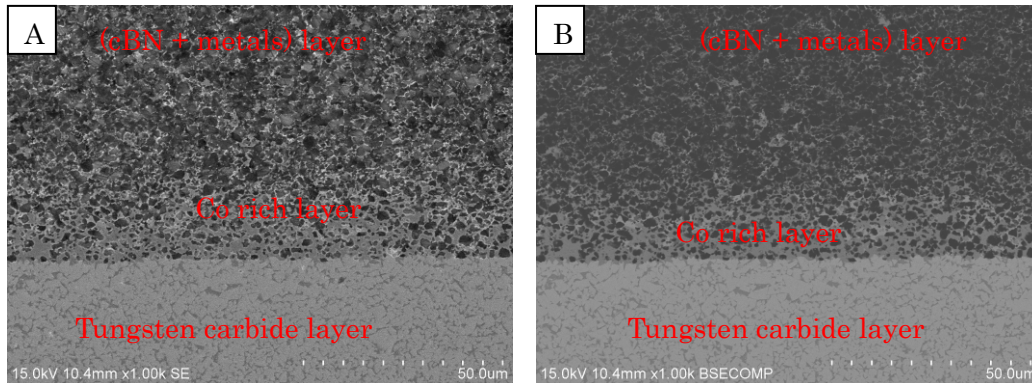
7.3.1 Microstructure of the cBN-carbide interface

Fig. 7.3. SEM images of cBN-carbide interface. A is the SEI and B is the BEI.

The common problem in sintering the polycrystalline cBN compact over the carbide disk is an occurrence of the crack along the cBN-carbide interface due to the shrinkage of cBN layer during the sintering process especially when it was quenched. Such problem could be avoided by decreasing the temperature and pressure slowly. Figure 7.3 showed the SEM images at the cBN-carbide interface from the 2-4 μm PCBN compact. As shown in these images, it was confirmed that there is no crack at the cBN-carbide interface. The appearance of the metal-rich layer just above the carbide was also confirmed. The appearance of such metal-rich layer is thought to be a result of the Co diffusion from the carbide disk into the cBN layer during sintering process. While the details were not been closely studied, it was thought that the diffusion of the Co around the cBN-carbide interface area might prevent the cracking as the metal-rich layer work as the functionally gradient material.

Figure 7.4 showed the dimension of ISO tip CNMA120408 and the overall images of the cutting tip. The cBN part and the brazed layer are shown in Fig. 7.5. Here, it could be confirmed that there is no crack in the cBN layer or at the interface of cBN and carbide disk that might be occurred during the brazing process. The sporadical light/white spots on the flank and rake face of the cBN tip are the nodules of metal alloy as confirmed by SEM observation. Such nodules indicated that the mixing process of the cBN and the metal alloy was not completely homogenous.
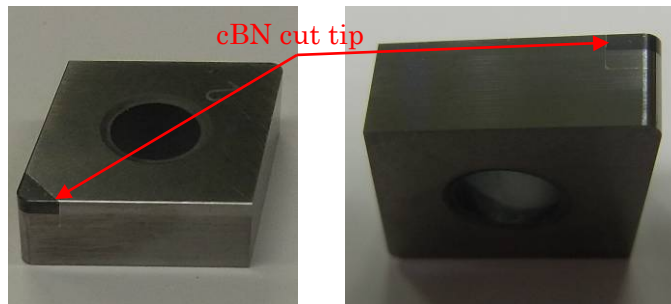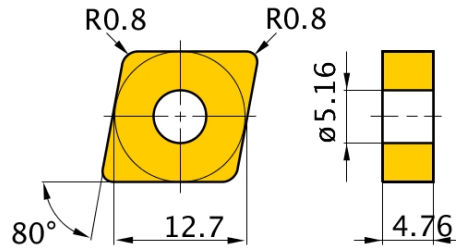
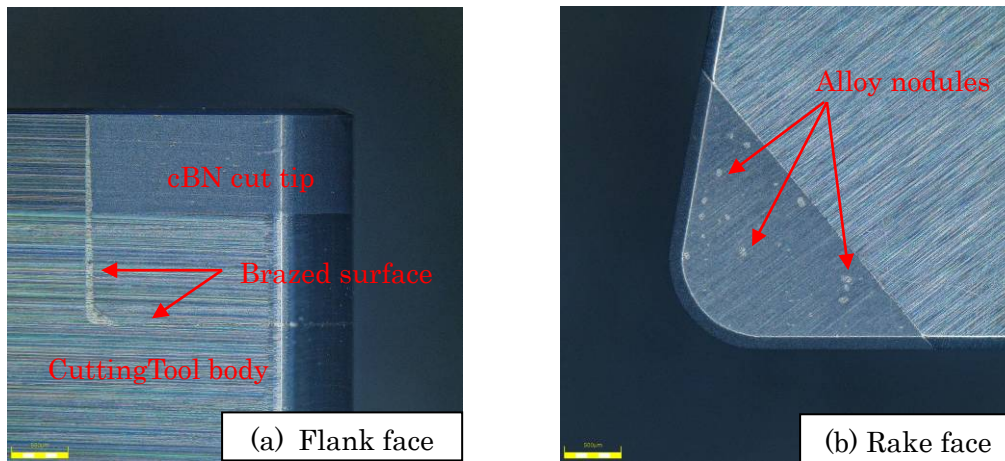Fig. 7.4. Design and appearance of PCBN cutting tip (CNMA120408).

Fig. 7.5. Flank face and the rake face of the PCBN cutting tip.

7.3.2 Microstructure of the polycrystalline cBN compact

Figure 7.6 showed the microstructure of the PCBN compacts used in these study along with Fig. 7.6 (a) showed the microstructure of 0.5-2 μm PCBN compact, Fig. 7.6 (b) showed the microstructure of 2-4 μm PCBN compact while Fig. 7.6 (c) showed the microstructure of BN700 which has the average grain size of 2-4 μm.

(a) 0.5-2 μm PCBN

Alloy nodules

(b) 2-4 μm PCBN

(c) BN700
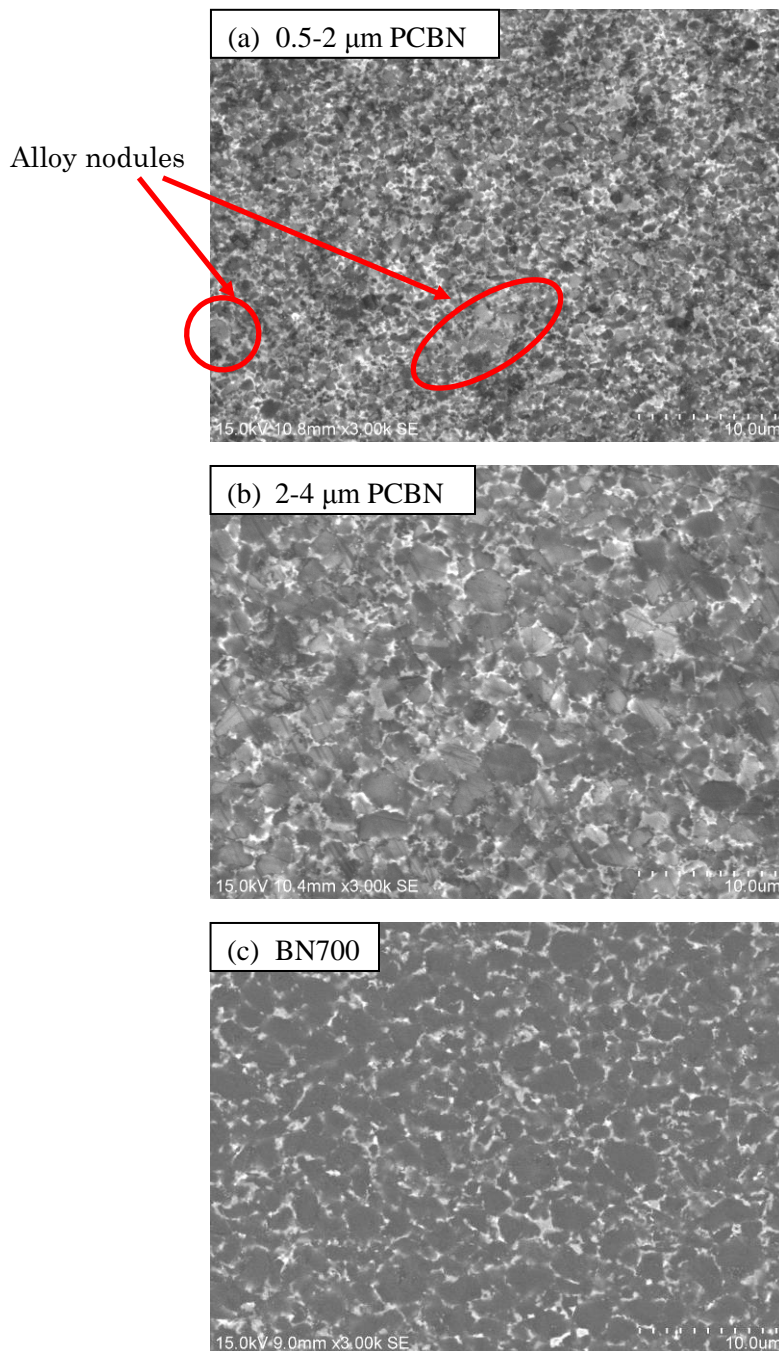
Fig. 7.6. Microstructure of the PCBN used in the cutting test.

7.3.3 PCBN compact cutting performance

7.3.3.1 Cutting performance on rough turning of FC300

At first, the rough turning on the gray cast iron FC300 was performed. While the high speed machining of gray cast iron could be performed at the speed of 1000 m/min under

dry condition [8], the test was performed at the speed of 350 m/min as there is no literature or experience with this (Co-V-Al)-cBN compact. During the rough turning, the depth of cut was set at 1.5 mm and the feed rate at 0.3 mm/rev.
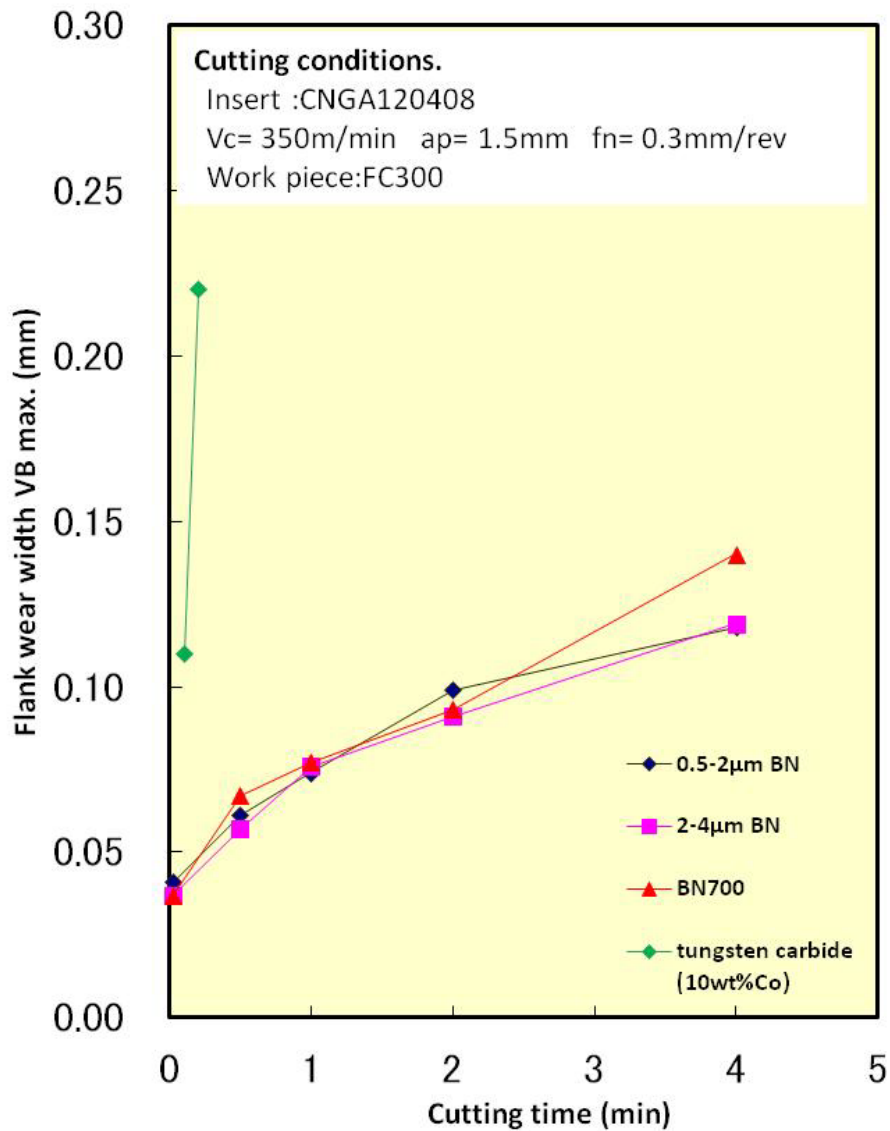
Fig. 7.7. Flank wear width measurement result after rough turning of FC300.

Figure 7.7 shows the evaluation results of FC300 gray cast iron machining with the cutting time of 4 min or 1.4 km cutting length. The flank wear width measurement results showed that (Co-V-Al)-cBN compact has enough bonding strength to be used a cutting tool of the gray cast iron. There were no tip breakages occurred from both 0.5-2 μm PCBN and 2-4 μm PCBN cutting tip. In term of the wear resistance, the difference between 0.5-2 μm PCBN and 2-4 μm PCBN could not be confirmed.

Comparing with BN700, the commercially available high content cBN compact which is sintered using Co-W-Al, it was also confirmed that the increasement or the gradient of the flank wear width of this newly developed (Co-V-Al)-cBN compact is relatively similar. As we stop the cutting test after 1.4 km cutting length, further evaluation is still needed to reconfirm the wear resistance of this PCBN. In general, commercially available high content PCBN could be used in this kind of rough turning of gray cast iron for about 4 km cutting length. On the other hand, the worn on the tungsten carbide tip was rapidly developed. The evaluation of tungsten carbide tip was stopped after 0.2 min of cutting time.

The optical photographs of the tip-edge to observe the development of the wear on the tip were showed in Fig. 7.8. It can be seen from these photos that metal adhesions from the workpiece were developed at the tip-edge during the cutting test.
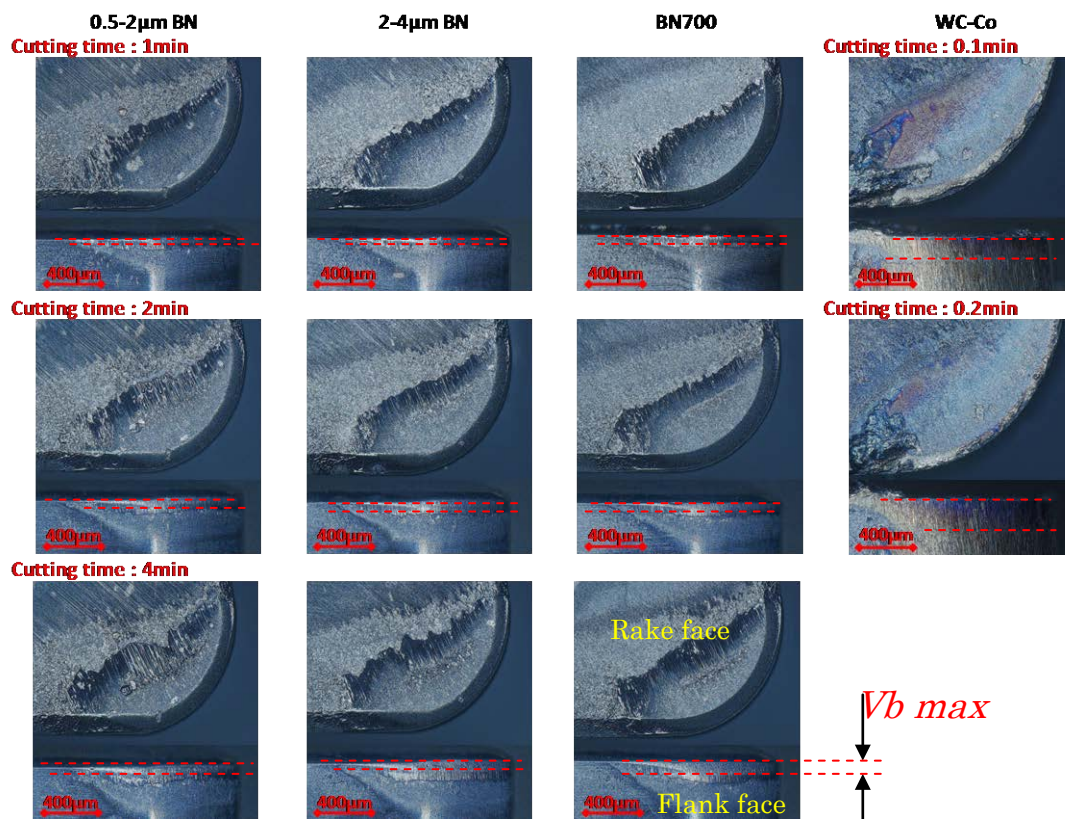

Fig. 7.8. Tip-edge of the PCBN cutting tools after rough turning of FC300. The upper image is the rake face and the lower one is the flank face

7.3.3.2 Cutting performance on finishing of FC300

One of the advantages PCBN compact is its ability to perform the finishing process as an alternate to the grinding process. By replacing the grinding process with the turning or milling process, the production line might be simplified and the production cost could be reduced. Here, an evaluation of the finishing performance of newly developed 2-4 μm PCBN cutting tip was conducted in comparison with the BN700 on the gray cast iron FC300. The cutting test conditions were as follows; 800 m/min., depth of cut: 0.2 mm, feed rate: 0.13 mm/rev. Compare with the above roughing process, the cutting speed was about double and the feed rate was about half with depth of cut was about 1/8.
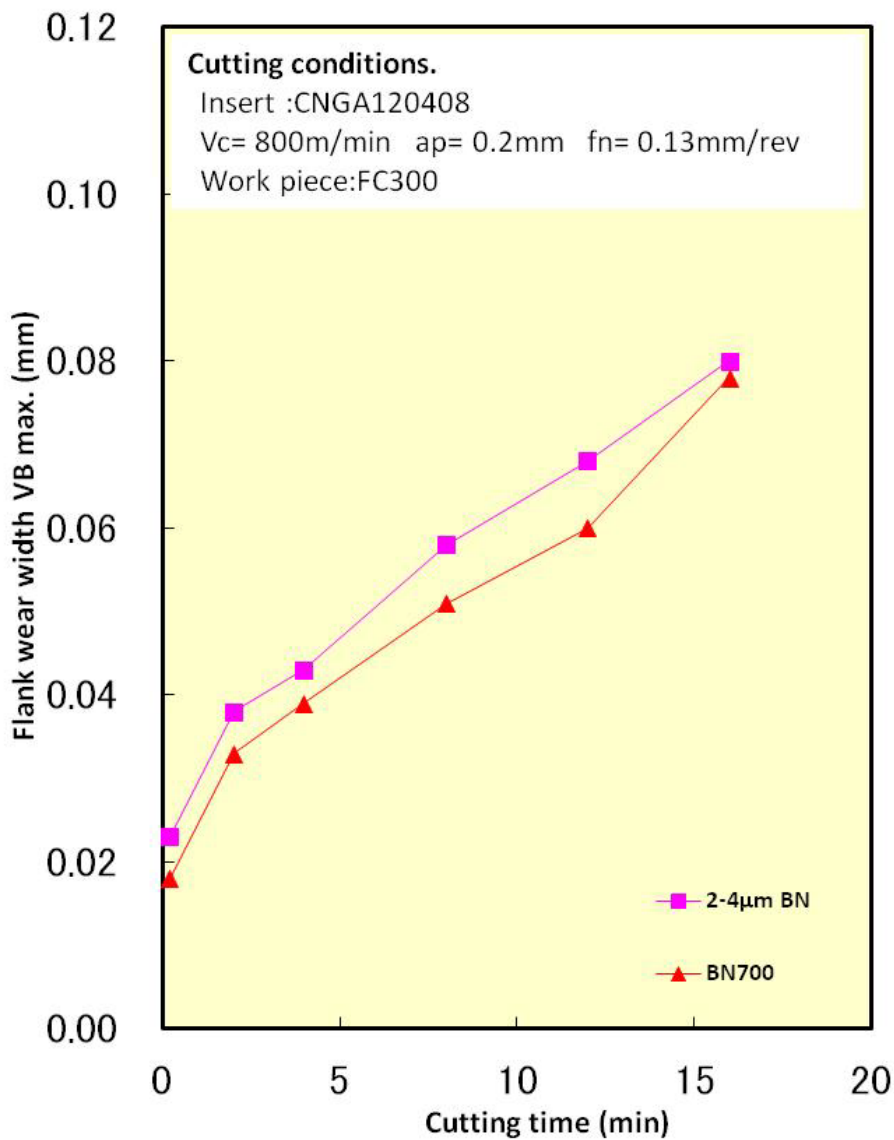

Fig. 7.9. Flank wear width measurement result after finishing of FC300.

Figure 7.9 showed the flank wear width of the 2-4μm PCBN sintered with Co-V-Al and the BN700 (Co-W-Al). The total cutting time was 16 min. or 12.8 km cutting length. In this finishing process of FC300 we confirmed that the degree of the wear from the PCBN sintered with Co-V-Al was relatively the same with the one of BN700. As it was confirmed from the optical photograph of the tip-edge shown in Fig 7.10, there was no chipping or breakage occurred during the operation. The strong cBN-cBN direct bonding as studied and observed in the previous chapter is thought to be the key of this high wear resistance of the PCBN compact sintered with Co-V-Al. Further wear resistance evaluation under the completely dry high speed (100m/min) cutting condition on the cast iron should be performed to confirm the heat resistance of these cBN-cBN direct bonding microstructure.
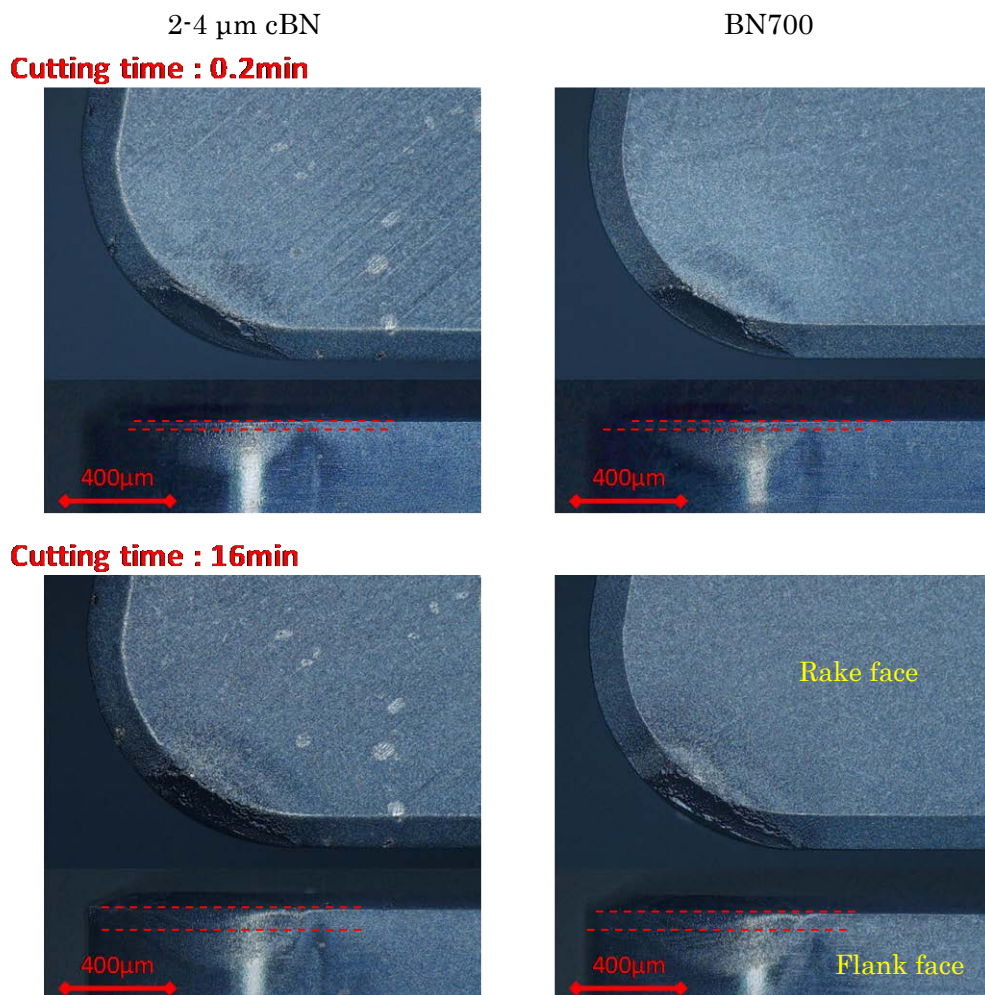

Fig. 7.10. Tip-edge of the PCBN cutting tools after finishing of FC300.
The upper side is the rake face and the lower side is the flank face.

7.3.3.3 Cutting performance on finishing of FCD700

The cutting performance of the PCBN sintered with Co-V-Al was also evaluated by finishing process of ductile cast iron FCD700. The cutting conditions was chosen from the recommend cutting conditions of ductile cast iron as published on the PCBN cutting tools manufacturer catalogue [9]. The cutting test conditions were as follows; cutting speed: 400 m/min., depth of cut: 0.15 mm, feed rate: 0.07 mm/rev. In this test, both 0.5-2 μm PCBN and 2-4 μm PCBN was evaluated in comparison with the BN700. The test was conducted until the cutting time reach 10 min. or 4 km cutting length.

Figure 7.11 showed the measurement result of the flank wear width developed at the tip-edge during the cutting test against the cutting time. As seen in this figure, the wear resistance of the (Co-V-Al)-cBN sintered compact is in the same degree with the one sintered with Co-W-Al.A normal smooth wear without any chipping or breakage developed in the tip-edge could also be confirmed from the Fig. 7.12.
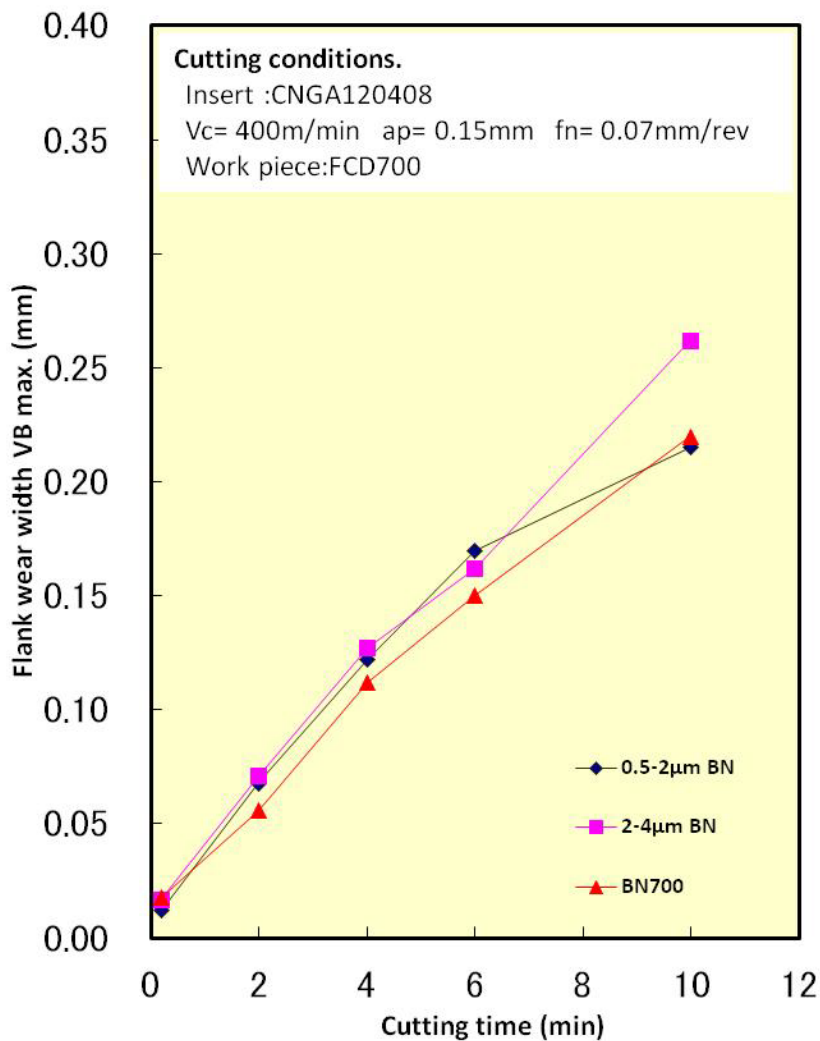

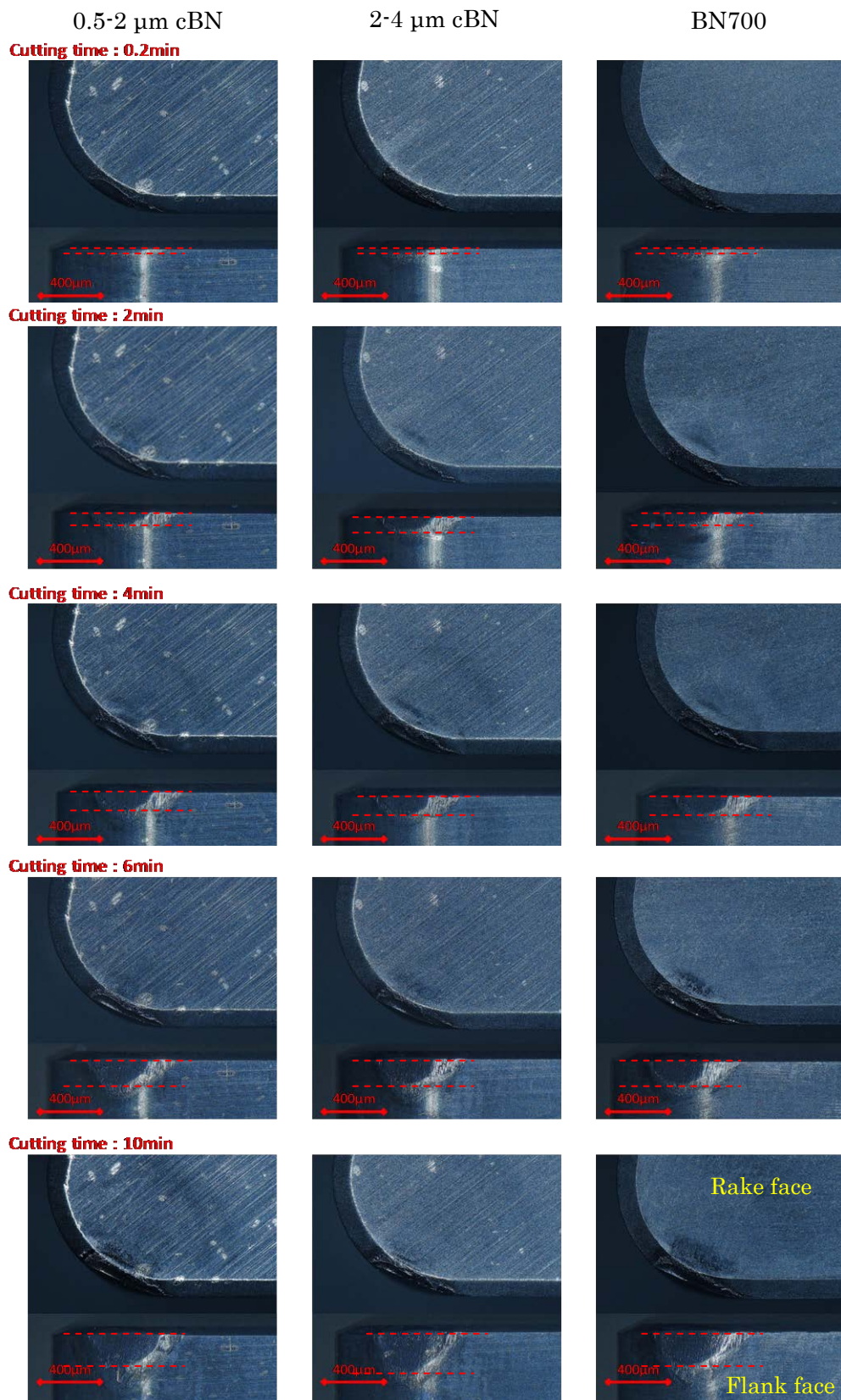Fig. 7.11. Flank wear width measurement result after finishing of FCD700.

Fig. 7.12. Tip-edge of the PCBN cutting tools after finishing of FCD700.

Take a look at the flank wear width after 10 min. of cutting, the 0.5-2 μm fine grained PCBN compact showed better wear resistance compare with the 2-4 μm PCBN. In the finishing process where the feed rate and the depth of cut is relatively small, the breakage of the tip-edge is rare and the failure mode of the cutting tip would be mainly come from the normal wear, PCBN with higher hardness should perform better. To confirm such smooth wear on the tip-edge, an observation by SEM was performed. The results of the SEM observation of the tip-edge after 10 min of cutting were shown in Fig. 7.13. From these images it could be seen that the worn surface is smooth and there is no remarkable cBN grain fell out from the worn surface. Still, further evaluation in difference conditions to confirm the advantage of this fine grained PCBN.
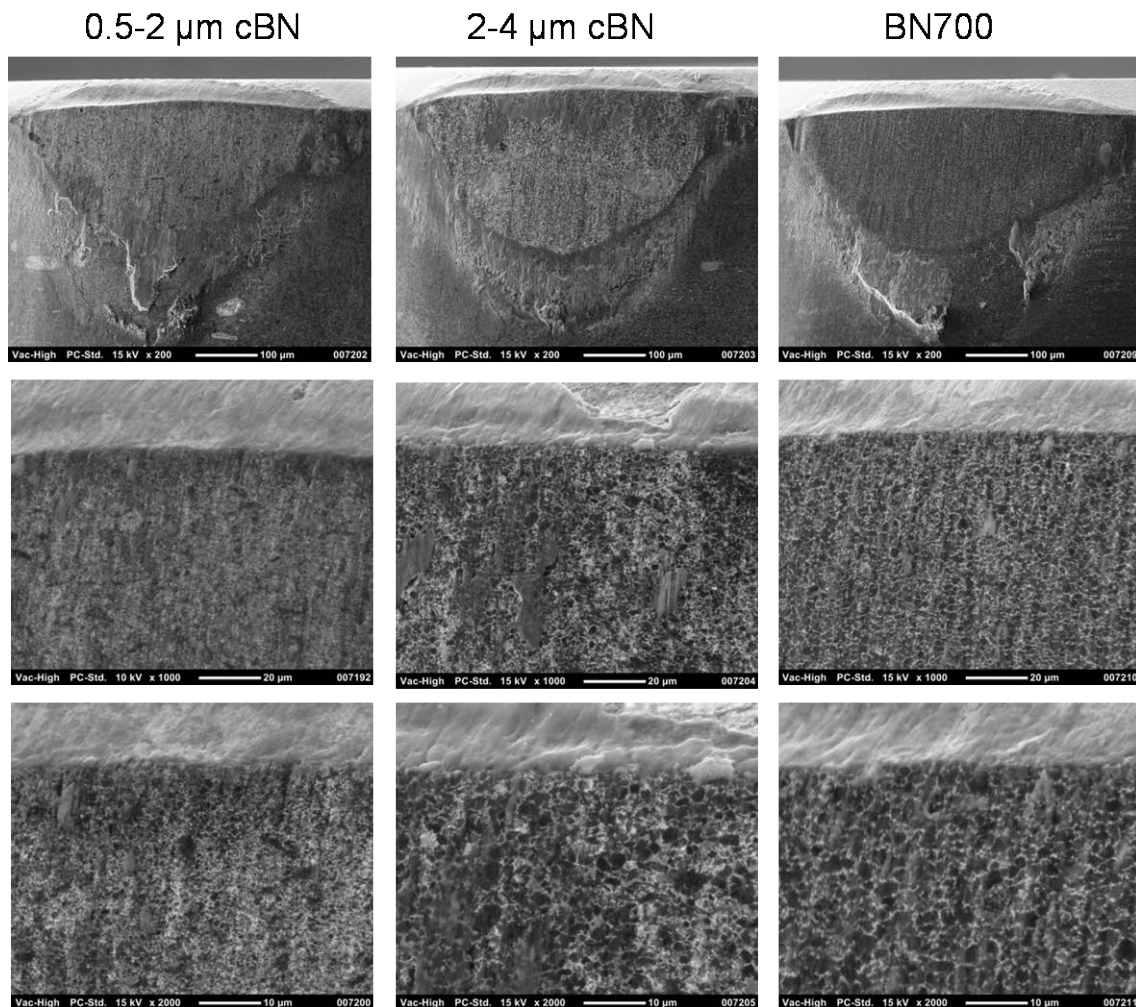

Fig. 7.13. SEM images of the flank face of the cutting tips and their magnified tip-edges after 10 min cutting of FCD700.

7.4. Conclusions

In this chapter, PCBN cutting tools was made from the compact sintered with Co-V-Al as studied in the previous chapter. The sample was sintered over the tungsten carbide. It was confirmed that there is no crack on the interface of the cBN and the carbide during the HPHT and the brazing process.

Cutting performance of the PCBN cutting tip were performed on roughing and finishing of the FC300 gray cast iron and FCD700 ductile cast iron in comparison with commercially available high content PCBN cutting tip sintered with Co-W-Al. It was confirmed that PCBN sintered with Co-V-Al showed the same degree of wear resistance comparing with tested commercial product. Co-V-Al could be used as a candidate of the sintering media for the high content PCBN cutting tool.

Further study to get the best balance of hardness and toughness required as the commercial product are still needed. Changing the composition of the sintering alloy and the cBN grain size combination along with changing the HPHT condition might be useful in tuning the mechanical properties of the sintered PCBN.

References

[1] Hofs¨ass and C. Ronning, in 2nd Internat. Conf. Beam Processing of Advanced Materials, J. Singh, S. M. Copley, and J. Mazumder (eds.), ASM Int., Materials Park (1996) 29.

[2] J. Angseryd, M. Elfwing, E. Olsson and H. -O. Andrén, Intl. J. Ref. Metals Hard Mater. 27 (2009) 249

[3] V. Richter and M. Fripan in: PCBN cutting tools in a competitive market, Proceedings of EURO PM2006 (2006) 115.

[4] P. J. Heath, in: Ultrahard Tool Materials, J. R. Davis (ed) A.S.M. Handbook, 9th ed., Vol. 16, 105.

[5] M. Fleming and A. Wickman, Industrial Diamond Rev. 2/06 (2006) 26.

[6] M. Ota, Sumitomo Electric Technical Review 165 (2004) 81.

[7] Mitsubishi Carbide General Catalog - CBN PCD Inserts (2013) 12.

[8] T. Obikawa, J. Jpn. Soc. Precision Eng., 69/10 (2003) 1397.

[9] Kennametal, Superhard Materials • PCBN and PCD (2012) B132

Chapter 8 Summary and conclusion

8.1. Summaries

 This research was intended to control the cBN morphology and the grain size during synthesis process using the transition metal as the catalyst. Based on the assumption that the addition of Mo, Cr, V into the Fe, Ni, Co alloy is effective to increase nitrogen solubility in the solvent system, we described alloy solvent system as a combination of boron soluble elements, (Fe, Ni and Co), elements of increase nitrogen solubility, (Mo, Mn, Ta, Cr, Nb and V) and Al. Various (Fe, Ni, Co)-(Cr, Mo, V)-Al solvent composition to determine the cBN growth region along with its grain size and crystal was employed. The application of these metal solvents system as the sintering media in the cBN sintering process was also studied. The mechanical properties of the sintered polycrystalline cBN compact were measured and the cutting performance on the cast iron was evaluated.

The Results of this study could be summarized as follows;

Chapter 1:

 An introduction of already well-studied basic properties of cBN, BN phase and equilibrium system was reviewed. The previous researches on the cBN synthesis method by direct conversion and catalyst system including boron nitrogen compounds of alkali, alkali-earth elements and the binary alloy of transition metals with Al were introduced. The sintering methods and the applications of cBN cutting tools especially in the machining process in the automotive industry was also reviewed.

 While there are so many reports on the cBN synthesis and sintering process, few report that focus in studying the morphology and the controlling of the cBN microstructure during synthesis process. The present research aims and methods in microstructure control of the cBN synthesis and their application in sintering process using (Fe, Ni, Co)-(Cr, Mo, V)-Al were proposed.

Chapter 2:

 The details of the HPHT experiment apparatus of FB25B belt press including the pressure and temperature calibration method was introduced. The sample analysis methods including SEM, EPMA and EBSD of the synthesized cBN and the mechanical

properties evaluation including hardness measurement and the cutting test on the cast iron of the sintered cBN compact were explained in this chapter.

Chapter 3:

Pressure and temperature region of cubic boron nitride growth using (Fe,Ni)-Cr-Al, Co-(Cr,Mo)-Al solvent was confirmed in pressure range of about 4-6 GPa and temperature range between 1200 and 1700 °C. The minimum pressure of cubic boron nitride formation were at about 4-4.1 GPa for both (Fe, Ni)-Cr-Al and Co-(Cr, Mo)-Al solvent. Based upon the results of growth pressure temperature region, morphology of cubic boron nitride crystals affected by the reaction pressure and also composition of the solvents was examined.

Chapter 4:

To control the grain size of the cBN crystals, Mo or V were used as a substitute of Cr in the base alloy. The pressure-temperature region of the cBN formation under Co-(Cr, Mo)-Al and Co-(Cr, V)-Al systems were determined at pressure between 4 to 6 GPa and temperature up to 1700 °C. It was confirmed that cBN was obtained at pressures above 4.4 GPa and temperatures above 1290 °C. The grain size of cBN synthesized using Co-(Cr, V)-Al solvent was relatively finer comparing with the ones synthesized with Co-Cr-(Mo)-Al alloy solvent. Under the Co-(Cr, V)-Al alloy solvent system where both Cr and V exist, the grain size of the synthesized cBN could be controlled by changing the composition of Cr and V in the solvent.

Chapter 5:

Cubic boron nitride (cBN)-metal composites were synthesized from hexagonal boron nitride (hBN) using Co-Cr-Al, Co-V-Al and Co-Cr-V-Al as infiltration solvents under high pressure and high temperature conditions (5.6 GPa and 1700 °C for 30 min.). It was confirmed that the grain growth of cBN could be suppressed by adding a small amount of V to the Co-Cr-Al solvent. It was also showed that V could be used as an additive in the metal solvent during the infiltration sintering process of fine grains cBN compact, where the microstructure homogeneity and the cBN abnormal grain growth are the important issues.

Chapter 6:

Polycrystalline cBN-Co-V-Al composites with homogenous microstructure were sintered at 5.6 GPa and 1600 °C for 30 minutes. The highest Vickers hardness of 39.9 GPa was achieved by sintering the 0.5-2 μm cBN 80 wt% + (Co60-V23-Al17) 20 wt% composite with the Al/(BN + Al) value of 4.0 wt%. It was confirmed that the addition of V into the metal catalyst increasing the ratio of the cBN-cBN direct bonding in the compact. Increasing the Al content in Co-V-Al metal catalyst will increase the creation of AlN and therefore decreasing the hardness of the cBN compact.

Chapter 7:

Polycrystalline cBN cutting tools was made from the compact sintered with Co-V-Al as sintering media. The sample was sintered over the tungsten carbide. It was confirmed that there is no crack on the interface of the cBN and the carbide during the HPHT and the brazing process. Cutting performance of the PCBN cutting tip were performed on roughing and finishing of the FC300 gray cast iron and FCD700 ductile cast iron in comparison with commercially available high content PcBN cutting tip sintered with Co-W-Al. It was confirmed that PcBN sintered with Co-V-Al showed the same degree of wear resistance comparing with tested commercial product. Co-V-Al could be used as a candidate of the sintering media for the high content PcBN cutting tool.

8.2. Conclusion

The summarized P-T region of cBN growth under various (Fe, Co, Ni)-(Cr, Mo, V)-Al system was shown in Fig. 8.1. Minimum pressures of cBN formation under (Fe, Ni)-Cr-Al, Co-(Cr, Mo)-Al and Co-V-Al solvents was confirmed at about 4.1 GPa. The minimum pressure of cBN formation was almost similar to that in the traditional alkali or alkali-earth B-N solvents. As comparison with previously reported synthesis solvents, the P-T region under Co-Mo-Al, Co-Al and Li_3N system were also plotted.

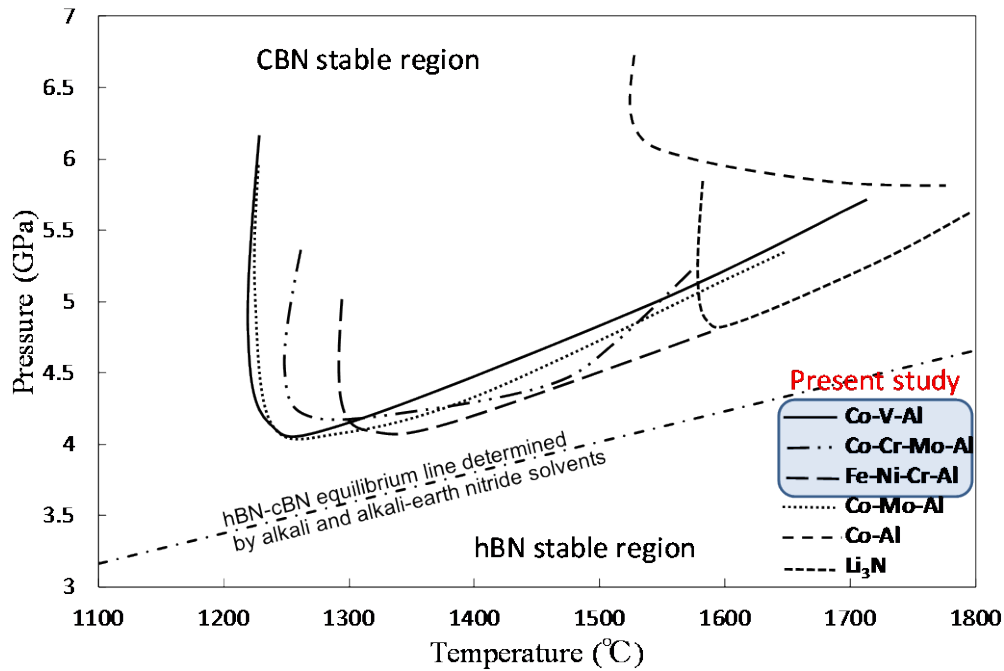Fig. 8.1. P-T region of cBN growth confirmed under (Fe, Co, Ni)-(Cr, Mo, V)-Al solvent sytem.

The variation of alloy composition provides various morphology and grain size of cBN crystals. Boron and nitrogen solubility can be changed continuously by the variation of (Fe, Co, Ni)-(Cr, Mo, V)-Al system. Accordingly, crystal growth parameters such as solubility, diffusion constant of B and N in the alloy could be controlled. The results of the variety of cBN morphology employed the (Fe, Ni, Co)-(Cr, Mo, V)-Al solvent was presented. The crystal size and morphology of the cBN were different due to P-T condition and content of the solvents employed in the experiment.

Figure 8.2 shows the simplified conclusions of the synthesis method confirmed in this study. As seen in this figure, the cBN grain size and morphology could be changed by the use of different metal solvent.

The series of solvent system from Co-Mo-Al to Co-(Cr, Mo)-Al and Co-(Cr, V)-Al were reflected continuously increasing of nitrogen solubility in the alloys. The solubility of nitrogen into the Co-Mo-Al alloy was the smallest and it increase with increase of Cr content in Co-(Cr, Mo)-Al system and further increase of nitrogen solubility in the Co-(Cr, V)-Al was realized with increase the content of vanadium. The grain size of

cBN was decreased with increasing nitrogen solubility of the alloy system and small agglomerate crystals were appeared in the Co-(Cr, V)-Al system.
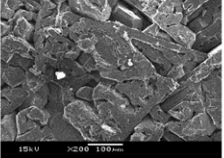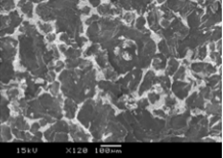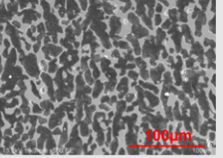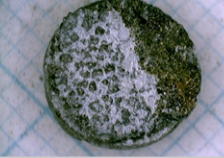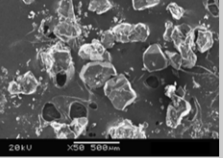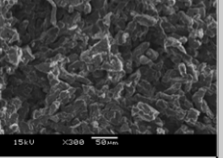
Solvent system	(Fe, Co, Ni)-Cr-Mo-Al	(Fe, Co, Ni)-Cr-Al	(Fe, Co, Ni)-Cr-V-Al	(Fe, Co, Ni)-V-Al
Minimum P-T conditions	4.1 GPa, 1300 °C	4 GPa, 1320 °C	4.2 GPa, 1300 °C	4.4 GPa, 1290 °C
Nitrogen solubility	Lower ⟷		Higher	
4.5±0.1 GPa	Plate-like 100 μm 4.5 GPa 1400 °C 1 h	Irregular 150 μm 4.4 Gpa 1465 °C 1 h		Irregular 20 μm 4.6 Gpa 1400 °C 1 h
4.2 GPa	Facetted 500 μm 4.2GPa 1320 °C 0.5 h	Facetted 300 μm 4.2GPa 1370 °C 1 h	Irregular 30 μm 4.2GPa 1330 °C 1 h	
Morphology	Euhedral ⟷		Irregular	

Fig. 8.2. cBN grain size/morphology control under similar P-T conditions using different metal solvent composition studied in this research.

These results indicated possible application of metallic solvent in the production of cBN abrasive grains. The morphology of cBN crystals is important information to the practice of cBN abrasives. The application of the alloy solvents with various combination of alloy composition could open the new field in cBN synthesis technology.

Secondly, as the metal solvent for cBN synthesis and the metal catalyst for cBN sintering are in general the same, it was showed that metal alloy solvent or catalysts which are able to suppress the cBN grain growth during cBN synthesis such as V is useful in producing the cBN compact with a homogenous microstructure during the infiltration sintering method.

112

High content polycrystalline cBN compact was also sintered with Co-V-Al metal catalyst. It was confirmed that as the nitrogen solubility in the metal catalyst increased by the addition of vanadium, the dissolution–precipitation process of the cBN grains in the molten metal catalyst during sintering process became more active. Hence, enhancing the cBN-cBN direct bonding and resulting the increasement of the hardness in PCBN compacts sintered compacts. The high content PCBN compact with the hardness as high as 39.9 GPa was achieved. Finally high volume content polycrystalline cBN cutting tools was made with Co-V-Al as the sintering media and their cutting performance was evaluated on the gray cast iron of FC300 and the ductile cast iron of FCD700 as a work material. It was showed that the PCBN sintered with Co-V-Al has the same degree of wear resistance comparing with tested commercial product. Co-V-Al could be used as a candidate of the sintering media for the high content PcBN cutting tool. Table 8.1 summarized the already reported polycrystalline cBN sintering methods in comparison with sintering method studied in this research.

Table 8.1. Polycrystalline cBN sintering method conducted in this study in comparison with already reported sintering methods

	cBN-cBN direct bonding sintering methods	Sintering condition	Hardness (Hv)	Application as cutting tool (commercial product)
Previous Studies	Direct conversion	6.5 GPa, 1800 $^{\circ}$C	50-60 GPa	No
	Mg-B-N, Solvent system	5.5 GPa, 1400 $^{\circ}$C	50-60 GPa	No
	Co-W(WC)–Al Solvent system	6 GPa, 1600 $^{\circ}$C	40 GPa	Yes
Present study	Co-V-Al solvent system	5.6 GPa, 1600 $^{\circ}$C (need further study)	40 GPa	Need further study

8.3. Possible future work

As the transition metals are the well-known sintering agent of diamond sintering process, the use of the transition metals along with Al might also be useful in the sintering process of diamond-cBN composite, especially the diamond-cBN composite with the fine grain where the abnormal grain growth is the main issue.

Figure 8.3 showed an example of the interface between diamond and WC-Co from diamond composite with the grain size of 0.5-1.5 μm. As we can see here, the growth of WC occurred in the interface. The growth of the diamond grain was also could be seen from the image.
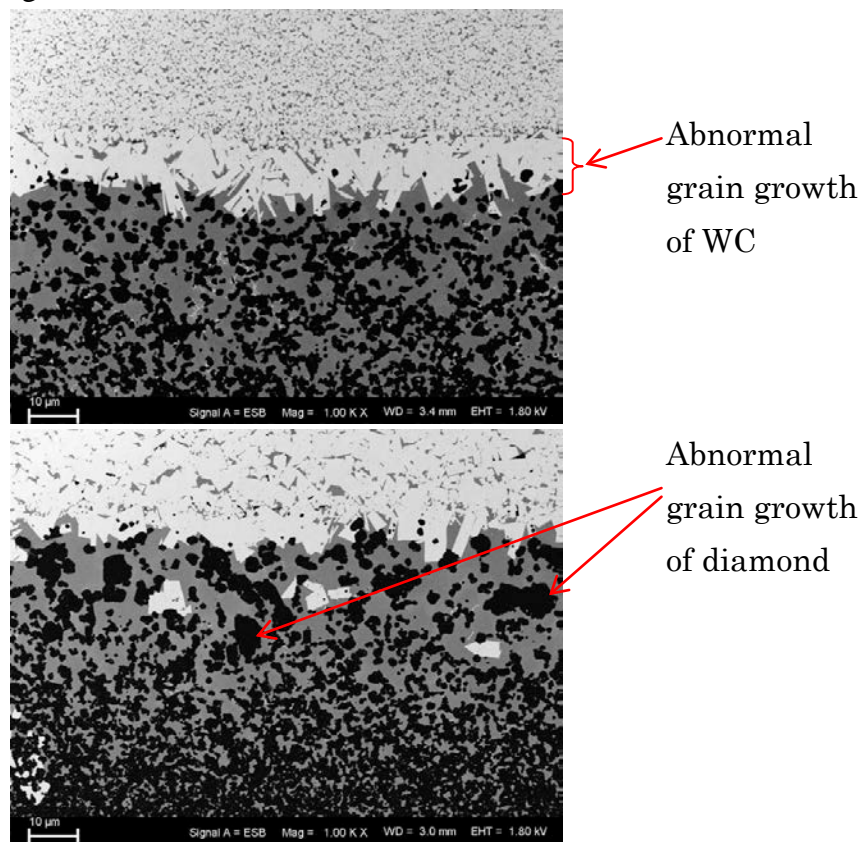

Fig. 8.3. WC and diamond grain growth at the diamond-carbide interface during sintering process of 0.5-1.5 μm fine grain diamond compact.

As another example, Fig. 8.4 showed the optical photograph of abnormal grain growth during fine grain diamond sintering process. The abnormal grain growth of the diamond could be observed at the interface of the diamond layer and the carbide.
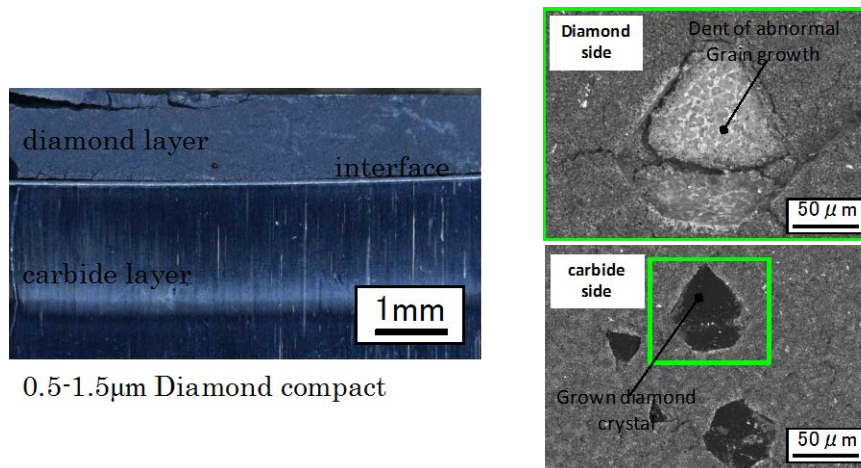

Fig. 8.4. Abnormal grain growth of 0.5-1.5μm diamond at the carbide-diamond interface.

To avoid such abnormal grain growth in the sintering process, various approaches such as adding the small amount of cBN or carbide (WC, TaC, TiC) into the diamond layer has been published.

Diamond sintered compact are widely used in the machining of non-ferrous material such as Al alloy. The diamond-cBN sintered compact might be useful in the environment where the chemical affinity of the cutting tools is required. The multi layers of diamond-cBN composite with various compositions might also be used as functionally graded materials in avoiding the breakage of the tools during the cutting or drilling operation.

To take a look at the ability of the metal alloy studied in this research on the synthesis and sintering process of the diamond-cBN composite, first, a preliminary experiment on the diamond synthesis was performed using Fe10Ni56-Cr20V10-Al4 at 6 GPa, 1470 °C, 0.5 h. with graphite powder as the starting material. Figure 8.5 showed the XRD result of the experiment. It was confirmed here that (Fe, Ni)-(Cr, V)-Al also has an ability to transform graphite into diamond.
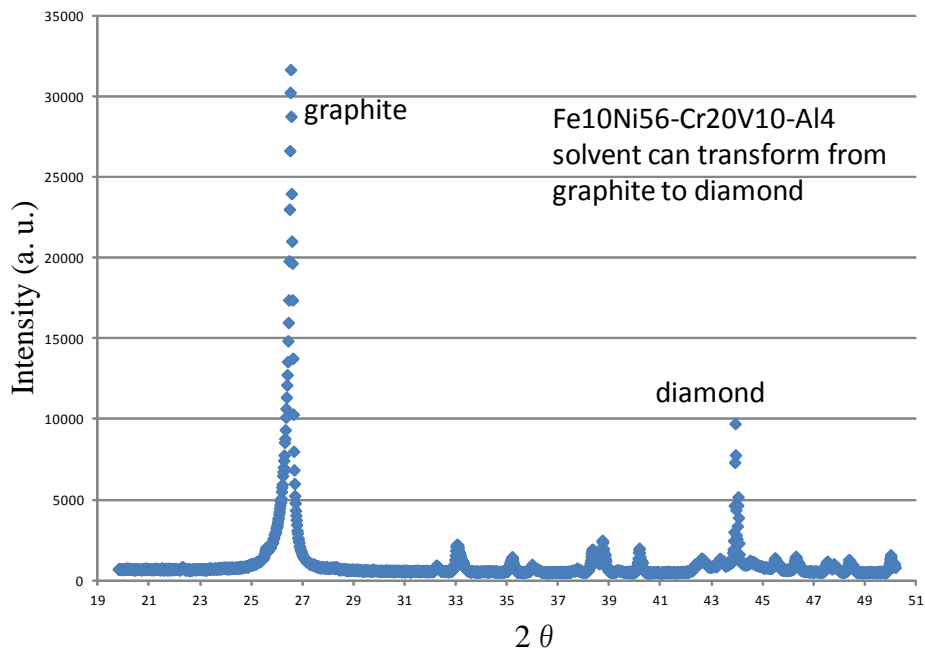
Fig. 8.5. Graphite-diamond transformation using Fe10Ni56-Cr20V10-Al4 solvent system. Synthesis conditions were 6GPa, 1470 °C, 0.5 h.

Preliminary experiments was also performed on the diamond-cBN composite sintering process. Figure 8.6 showed the SEM-BSE images of the interface of the (cBN+diamond)-carbide interface of the diamond-cBN compact. As comparison an interface of the (WC+diamond)-carbide interface was also shown in the same figure. In this experiments, we used (0.5-1.5 μm diamond 65 vol% + 2-4 μm cBN 35 vol% + (Co63Cr20V13Al4 wt%) 10 vol%) as the composition of the diamond-cBN composite and used (0.5-1.5 μm diamond 65 vol% + 2-4 μm WC 35 vol% + (Co63Cr20V13Al4 wt%) 10 vol%) as a comparison.
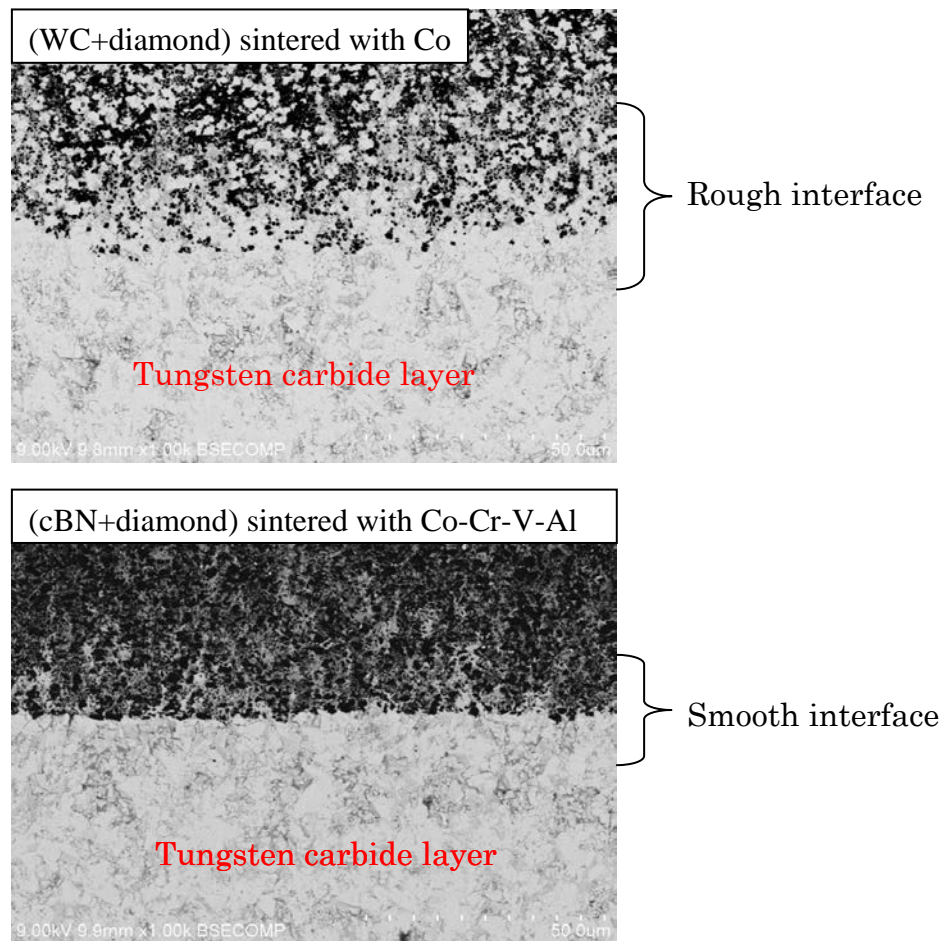
Fig. 8.6. SEM-BSE images of the (WC+diamond) and (cBN+diamond) compact sintered at 5.8 GPa, 1550 ℃ for 0.5 h.

As seen in the figure, transition metal solvent might be used in control the grain growth of the sintered cBN-diamond compact. Further study needs to look at the details of this kind of sintered compact.

Acknowledgments

I would like to express my gratitude to all those who gave me the possibility to complete this thesis.

First and foremost I offer my sincerest gratitude to my supervisor, Professor Naoto Ohtake, who has supported me throughout my thesis with his patience and knowledge while allowing me the room to work in my own way.

I am grateful to members of my thesis reading committee, Professor Kazuo Shinozaki, Professor Hitoshi Tokura, Professor Jeffrey S. Cross and Associate Professor Hiroki Akasaka for spending their time on careful reading of my thesis as well as for their valuable comments.

I am deeply indebted to Emeritus Professor Osamu Fukunaga whose help, stimulating suggestions and encouragement helped me in all the time of research for and writing of this thesis.

I want to thank Mitsubishi Materials Corp. for giving me permission to commence this thesis in the first instance, to do the necessary research work and to use experiments and analysis data. I am thankful to all of my colleagues in Thin Film and Coating Dept. of Central Research Institute, Mitsubishi Materials Corp. for supported me in my research work. I want to thank them for all their help, support, interest and valuable hints.

It is a pleasure to thank all the people working and studying in the Manufacturing Science & Technology Lab. of Dept. Mechanical Eng. and Sci., Tokyo Institute of Technology for their kind help during my enrollment.

These acknowledgments would not be complete without thanking my family for their constant support and care.